universität wien

DIPLOMARBEIT

Characterization of novel porins from *Protochlamydia amoebophila* UWE25

angestrebter akademischer Grad

Magistra der Naturwissenschaften (Mag. rer.nat.)

an der Fakultät für Lebenswissenschaften der Universität Wien

Verfasserin:	Alexandra Hörmann
Matrikel-Nummer:	0405370
Studienrichtung /Studienzweig (lt. Studienblatt):	A441, Diplomstudium Genetik/Mikrobiologie
Betreuerin / Betreuer:	Matthias Horn

Wien, im Februar 2010

Table of contents

1 Introduction

1.1 Chlamydiae – a paradigm of obligate intracellular lifestyle

The phylum *Chlamydiae* represents an independent major lineage within the domain *Bacteria*. For a long time members of this phylum were believed to belong to a single family, namely the *Chlamydiaceae*, in the order *Chlamydiales*. The *Chlamydiaceae*, also known as "clinical chlamydiae", comprise well-established representatives of animal and human pathogens, like *Chlamydia trachomatis* or *Chlamydophila pneumaniae*. *C. trachomatis* is the most frequently sexually transmitted bacterial human pathogen, causing infections that can lead to possible infertility and also to blindness after infection of the eye (Mabey and Fraser-Hurt, 2003; Peipert, 2003).

The discovery of chlamydia-like bacteria in the 1990s marked the beginning of changes in the order *Chlamydiales*, as it turned out that diversity and occurrence in the environment had been highly underestimated (Horn and Wagner, 2004). The discovery of these "environmental chlamydiae" (Horn and Wagner, 2001), also known as "novel chlamydiae" (Corsaro and Greub, 2006), led to an eminent expansion of the diversity of the order *Chlamydiales* based on 16S rRNA sequence analysis. In addition to the *Chlamydiaceae*, the families *Parachlamydiaceae*, *Waddliaceae* and *Simkaniaceae* were discovered (Everett *et al.*, 1999; Rurangirwa *et al.*, 1999) and are now together with the families *Rhabdochlamydiaceae* ((Kostanjsek *et al.*, 2004; Corsaro *et al.*, 2007), *Piscichlamydiaceae* (Draghi *et al.*, 2004), *Clavochlamydiaceae* (Karlsen *et al.*, 2008) and *Criblamydiaceae* (Thomas *et al.*, 2006) representing the order *Chlamydiales* (Figure 1).

Members of the *Chlamydiae* can be considered as obligate intracellular endosymbionts, implying chlamydial growth and replication only in an intracellular environment. So far, *Chlamydiae* could neither be isolated nor cultivated in cell-free media (Fritsche *et al.*, 2000).

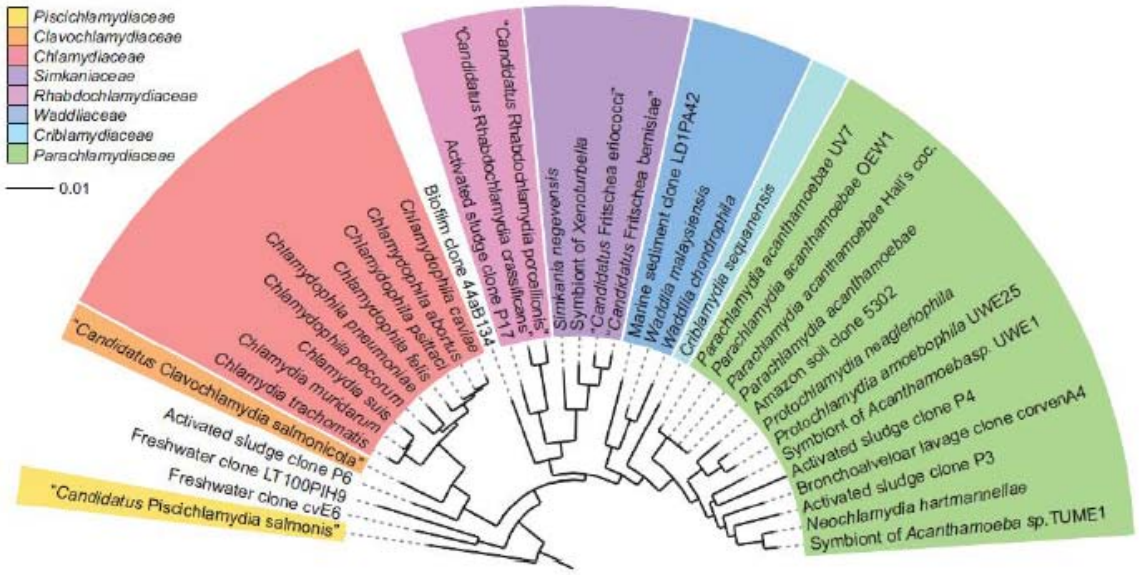

Figure 1. The recently discovered diversity of the order *Chlamydiales* is shown in a phylogenetic tree, based on comparative 16S rRNA analysis (Horn, 2008).

1.1.1 The chlamydial developmental cycle

Chlamydial growth is associated with a characteristic biphasic developmental cycle (Abdelrahman and Belland, 2005) first described in 1932 (Bedson, 1932). The current knowledge of the developmental cycle of environmental chlamydiae is restricted to studies focusing on *Parachlamydia acanthamoebae* and *Simkania negevensis* (Greub and Raoult, 2002; Kahane *et al.*, 2002). New insights into the developmental cycle of *Protochlamydia amoebophila* UWE25 (*P. amoebophila* UWE25) were obtained recently (König, 2008).

During an active infection two distinct developmental stages can be distinguished, whereby the stage of elementary bodies (EB) alternates with the stage of reticulate bodies (RB). EBs are well adapted to the survival in extracellular environments by an osmotically unusually stable cell envelope (Hatch, 1996). While EBs represent the metabolically inert but infectious form, involved in attachment to and endocytosis by the host cell, metabolically active but not infectious RBs multiply inside the host. As an exception, infectivity has been reported for RBs of *Simkania negevensis* (Kahane *et al.*, 2002).

Moreover, the existence of crescent bodies (CB) as an additional infective developmental stage has been suggested for *Parachlamydia acanthamoebae* (Figure 2) associated with prolonged incubation time (Greub and Raoult, 2002).

The developmental cycle proceeds within a membrane-enclosed compartment, the so-called "inclusion" (Scidmore-Carlson and Hackstadt, 2000), where EBs first differentiate into RBs, which then start to undergo binary fission. Several rounds of replication are followed by re-differentiation of RBs back to EBs, and finally the release of progeny takes place in order to infect new host cells (Abdelrahman and Belland, 2005) (Figure 2/E). Chlamydial exit is mainly associated with host cell lysis (Todd and Storz, 1975) but another mode of chlamydial release has been discussed. This way of chlamydial exit is called extrusion, where an intact host cell and parts of the inclusion are left behind (Hybiske and Stephens, 2007).

Environmental chlamydiae are able to establish a symbiosis with their host cell and maintain a stable host-parasite ratio in favourable environmental conditions (Amann *et al.*, 1997; Horn *et al.*, 2000). *In vitro* observations of pathogenic chlamydiae also suggest an alternative life cycle, known as persistence which is characterized by an atypical third developmental form (Hogan *et al.*, 2004). Persistence has been described for the *Chlamydiaceae* by the absence of growth and the reduction of infectious forms (Beatty *et al.*, 1994) leading to temporarily latent chlamydial infections (Hogan *et al.*, 2004).

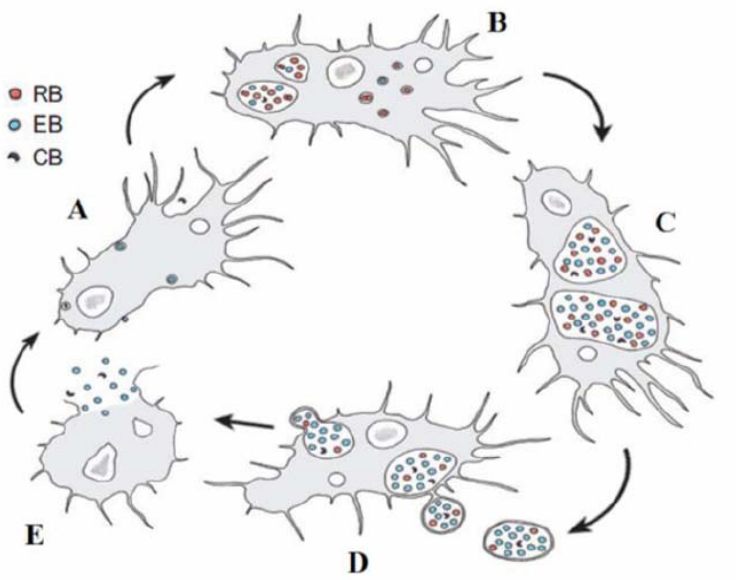

Figure 2. Schematic view of the unique biphasic lifecycle of chlamydiae. After invasion of a host cell by infectious EBs (blue), EBs differentiate to metabolically active RBs (red), followed by several rounds of binary fission. After re-differentiation from RBs to EBs, infectious progeny is released to start a new infection. Modified from Horn, 2008.

1.2 Symbiosis between chlamydia-like bacteria and amoebae

"The living together of unlike organisms" - this definition of the term "symbiosis" by Anton de Bary in 1879 does not consider the effects resulting from this intimate association, thereby including mutualism and commensalism as well as parasitism (de Bary, 1879). Chlamydia-like bacteria that have been identified so far were discovered in a wide variety of habitats. They occur as symbionts in various eukaryotic hosts, like in insects (Thao *et al.*, 2003), terrestrial isopods (Kostanjsek *et al.*, 2004), mammals (Rurangirwa *et al.*, 1999; Chua *et al.*, 2005), fish (Draghi *et al.*, 2004; Karlsen *et al.*, 2008) or the marine worm *Xenoturbella* (Israelsson, 2007) as well as in free-living amoebae (Amann *et al.*, 1997; Fritsche *et al.*, 2000; Horn *et al.*, 2000).

Free living amoebae are ubiquitous protozoa and beside their own pathogenic potential, they also have clinical relevance as reservoirs and vectors for bacterial pathogens (Horn and Wagner, 2004). About 25% of isolated *Acanthamoeba* species harbor bacterial endosymbionts which are stably integrated in the cytoplasm (Fritsche *et al.*, 1993). Fritsche *et al.* could further show that about 5% of these studied *Acanthamoeba* isolates were harboring intracellular chlamydia-like bacteria (Fritsche *et al.*, 2000). Since some bacteria have apparently developed strategies to survive and to multiply inside amoeba hosts, they are also referred to as "trojan horses of the microbial world" (Barker and Brown, 1994).

1.3 Protochlamydia amoebophila *UWE25 - a symbiont of* Acanthamoeba castellanii *Neff*

One representative of the *Parachlamydiaceae* is the amoeba endosymbiont *Protochlamydia amoebophila* UWE25 (E25). *P. amoebophila* was discovered as an obligate symbiont of an *Acanthamoeb*a sp. soil isolate (Fritsche *et al.*, 1993). It is able to maintain a stable symbiotic interaction with various *Acanthamoeba* sp. isolates including the widely used strain *Acanthamoeba castellanii* Neff.

In 2004, the genome sequence of *P. amoebophila* was published, representing the first available genome of a chlamydia-like bacterium, and markedly facilitated all attempts of genetic comparison of chlamydiae (Horn and Wagner, 2004).

The genome sequence of *P. amoebophila* contains 2.4 Mb, which is nearly twice as large as the known genomes of clinical chlamydiae (Stephens *et al.*, 1998; Kalman *et al.*, 1999; Read *et al.*, 2000; Shirai *et al.*, 2000; Read *et al.*, 2003). Comparative genome analysis revealed great differences between pathogenic and environmental chlamydiae (Horn and Wagner, 2004). The genome of *P. amoebophila* was found to harbor reduced central metabolic and biosynthetic pathways, comparable to genomes of clinical chlamydiae and other obligate intracellular bacteria, but differs in encoding the complete tricarboxylic acid cycle. 938 out of the 2031 predicted genes show significant homologies to the corresponding genes in other chlamydial genomes. Finally a core gene set of 711 genes, shared by all members of the chlamydiae, could be defined (Horn and Wagner, 2004).

Evolutionary history reveals a last common ancestor of pathogenic chlamydiae and this member of the environmental chlamydiae, which has lived about 700 million years ago. It is hypothesized that this ancestor was already adapted to intracellular live in order to survive within early eukaryotes (Horn and Wagner, 2004). Recent studies suggest another unexpected but fundamental role of this early ancestor in the evolution of plastids. Plant genomes were found to contain genes of chlamydial origin and on the other hand a high number of plant- and cyanobacteria-like genes were identified in chlamydial genomes. This implicates an involvement of chlamydiae during the process of establishing a stable interaction between ancient plants and its cyanobacterial symbionts (Huang and Gogarten, 2007; Moustafa *et al.*, 2008).

1.4 Chlamydia-like bacteria - emerging human pathogens?

While members of the *Chlamydiaceae* are parasites for humans and animals, the pathogenic potential of chlamydia-like organisms remains unclear. Evidently, they are using ubiquitous free-living amoebae as environmental reservoirs without being harmful to their protozoan hosts.

Protozoa may be sources of emerging pathogenic bacteria, since this symbiosis offers a way of protection against the harsh conditions of the extracellular environment and also possibly enhances their infectivity in mammals by benefiting from the structural and biochemical conservation of cellular processes in eukaryotes. Thus, chlamydia-like bacteria may develop strategies to survive within humans and animals (Harb *et al.*, 2000).

Some studies have already suggested to categorize these recently discovered chlamydia-like bacteria as emerging human pathogens, since invasion of human cells and the subsequent multiplication within were observed (Greub *et al.*, 2003; Corsaro and Greub, 2006; Baud *et al.*, 2007). In addition, 16S rRNA analysis assumed an association of chlamydia-like bacteria with respiratory tract infections (Haider *et al.*, 2008). To date, abortion in cattle (Ruhl *et al.*, 2009) and epitheliocystis in fish (Draghi *et al.*, 2004; Karlsen *et al.*, 2008) have already been linked to infections caused by chlamydia-like bacteria.

1.5 *The chlamydial cell envelope* – Chlamydiaceae *vs.* P. amoebophila

As chlamydiae belong to the Gram-negative bacteria, their cell envelope is characterized by an inner and an outer membrane separated by a periplasmic space. Whereas other Gram-negative bacteria additionally possess a layer of peptidoglycan, its presence in chlamydiae is still discussed controversially (McCoy and Maurelli, 2006). According to genome analyses, the presence of a truncated pathway for the synthesis of peptidoglycan could be assigned, but the detection of N-acetylmuramic acid, a key constituent of peptidoglycan, has failed so far. Since cysteine-rich proteins are present in the outer membrane of *P. amoebophila*, they are considered to be responsible for cell wall stability in chlamydiae and further regarded as the functional equivalent of peptidoglycan (Hatch, 1996).

1.5.1 Porins as outer membrane components

Porins are important components of the outer membrane of Gram-negative bacteria, making it largely permeable, whereas the inner membrane represents the major permeability barrier (Welte *et al.*, 1995). These pore-forming components are water-filled channels and composed of beta-sheets linked by beta-turns, forming a beta-barrel structure that crosses the cellular membrane (Nikaido, 2003).

Porins are regarded as unspecific transporters and unlike other membrane transport proteins they are large enough to allow passive diffusion of molecules ranging from 600 to 5000 Da, showing a transport rate proportional to the concentration gradient (Welte *et al.*, 1995)

1.5.2 The outer membrane of the *Chlamydiaceae*

Components of the outer membrane are of particular importance, since they play a role during attachment to the host cell and the transport of nutrients and other substances across the cell envelope (Stephens *et al.*, 2001).

In the *Chlamydiaceae*, the most abundant component of the outer membrane is the major outer membrane protein (MOMP; 39 kDa) (Caldwell *et al.*, 1981). In the EB cell envelope the cysteine-rich proteins OmcB (60 kDa) and OmcA (12 kDa) are extensively cross-linked by disulfide bridges. These proteins are considered to provide rigidity to the cell wall of EBs and to render osmotical stability, compensating the lack of peptidoglycan. Reduction of these disulfide bridges is characteristic for the process of transformation of EBs to osmotically fragile RBs, which then undergo intracellular division (Hatch, 1996). This mechanism is reversed by cross-linking of cysteines during conversion from RBs to EBs, either spontaneously by host cell lysis (Hatch *et al.*, 1986) or by an enzymatic reaction (Newhall, 1987), but the exact mechanism is not known.

Localization and identity of both major cysteine-rich proteins were studied by testing sarcosyl solubility of outer membrane proteins of clinical chlamydiae (Everett and Hatch, 1995). Sarcosyl is a weak anionic detergent and removes cytoplasmic membrane proteins from integral outer membrane proteins (Filip *et al.*, 1973). This technique was adapted to chlamydial studies by Caldwell *et al.* and Hatch *et al.* in order to identify chlamydial outer membrane proteins insoluble in sarcosyl (Caldwell *et al.*, 1981; Hatch *et al.*, 1981). Studies demonstrated that the small cysteine-rich protein OmcA is insoluble in sarcosyl, therefore associated to the outer membrane and firmly anchored in the inner leaflet of the outer membrane (Hatch, 1996). The large cysteine-rich protein OmcB was first considered to be a no integrated outer membrane protein (Everett and Hatch, 1995). Though, its involvement into EB stability could be demonstrated, as it is considered to form a stabilizing lattice in the periplasm by inter- and intramolecular disulfide bridges (Caldwell *et al.*, 1981; Mygind *et al.*, 1998). However, there is evidence for regarding OmcB as a true outer membrane component of *C. trachomatis* and *C. pneumonia*, since involvement of this protein in heparin-binding on the surface of eukaryotic cells was affirmed (Stephens *et al.*, 2001; Fadel and Eley, 2007; Moelleken and Hegemann, 2008). Therefore, OmcB is considered to occur as an outer membrane component as well as in the periplasmic space (Figure 3) (Heinz, 2008).

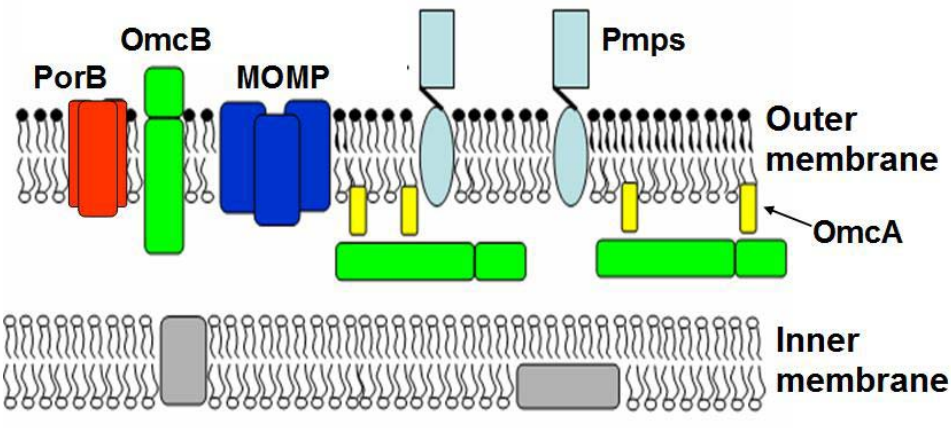

Figure 3. Schematic representation of the outer membrane of the *Chlamydiaceae*. The major outer membrane protein (MOMP) in blue is responsible for the transport of substrates across the outer membrane. The localization of OmcB either in the outer membrane or in the periplasm is shown in green (Heinz, 2008).

OmcA, OmcB as well as MOMP are the essential subunits of the chlamydial outer membrane complex (COMC). Additionally, members of the polymorphic outer membrane protein (POMP) family, a family of autotransporters, are components of the outer membrane of pathogenic chlamydiae (Henderson and Lam, 2001). These proteins feature an unusually high polymorphism, which might be an explanation for tissue specificity of different *C. trachomatis* disease groups (Stothard *et al.*, 2003; Gomes *et al.*, 2006). Some members of the POMP family were shown to contribute to the attachment to host cells (Wehrl *et al.*, 2004) as well as to expansion of the chlamydial inclusion (Jorgensen and Valdivia, 2008).

1.5.2.1 The major outer membrane protein

MOMP is the dominant component of the outer membrane of clinical chlamydiae making up about 60% of the chlamydial outer membrane (Caldwell *et al.*, 1981). The secondary structure is composed of 16 beta-sheets forming a barrel-like structure, a typical feature of bacterial porins (Sun *et al.*, 2007). This barrel structure consists of five well conserved transmembrane domains, connected by four variable surface exposed loops (Stephens *et al.*, 1987; Baehr *et al.*, 1988; Yuan *et al.*, 1989).

The structure of the MOMP was analyzed by Sodium dodecyl sulfate polyacrylamide gel electrophoresis (SDS-PAGE). Hatch *et al.* demonstrated the formation of MOMP trimers in EBs, whereas the monomeric form of MOMP dominated in RBs (Hatch *et al.*, 1984).

First, disulfide bridges were thought to be the stabilizing agents in this trimeric structure. However, more recent studies suggested that disulfide bonds are present but not required for stability of MOMP trimers (Findlay *et al.*, 2005; Sun *et al.*, 2007).

Several studies tried to verify the proposed function of MOMP as a porin (Caldwell *et al.*, 1981; Bavoil *et al.*, 1984; Koehler *et al.*, 1992; Findlay *et al.*, 2005). The first approach by Bavoil *et al.* used preparations of COMC in liposome swelling assays for functional analysis, where pore-forming activity seemed to be regulated by disulfide bonds. The authors demonstrated that channel activity was up-regulated under reducing conditions which lead to breaking-up of disulfide bridges (Bavoil *et al.*, 1984). These findings were consistent with the observation of different tasks of MOMP during the developmental cycle. MOMP operates as a stabilizing agent in EBs, but it functions as a transporter in RBs, where disulfide-bridges are absent (Hatch *et al.*, 1984). Various studies confirmed the pore-forming activity of MOMP by lipid bilayer measurements and liposome swelling assays, using purified native and recombinant MOMP (Wyllie *et al.*, 1998; Findlay *et al.*, 2005; Sun *et al.*, 2007), however, opening of the pore by a simple reduction mechanism could not be shown for these preparations.

Surface-exposed outer membrane proteins encounter direct surveillance of the immune system. Hence, the four variable surface-exposed domains of MOMP are considered to be responsible for hiding from immunological reactions by high sequence variability (Stephens *et al.*, 1988). Different antibodies targeting these variable regions can be applied for serovar typing in *C. trachomatis* (Wang *et al.*, 1985; Yuan *et al.*, 1989).

MOMP can be regarded as a strong antigen and a potentially good vaccine candidate, but the development of a successful general vaccine has failed so far. Only partial protection is given if the vaccine is based on recombinant and therefore non-native MOMP (Pal *et al.*, 1997). Vaccines containing native MOMP have been shown to be protective against chlamydial diseases (Tan *et al.*, 1990; Pal *et al.*, 1997), but in either case high variation in the surface-exposed parts of MOMP-sequences complicates the preparation of a general vaccine.

The porin function of MOMP creates problems during large scale overexpression for vaccine development and further analyses due to its lethal effects by pore-forming activity (Koehler *et al.*, 1992).

Various studies focused on cloning and overexpression of MOMP in *E. coli* but always encountered toxicity of MOMP for the host cells (Koehler *et al.*, 1992; Findlay *et al.*, 2005). It was hardly possible to obtain a stable clone due to the formed holes in the outer membrane (Koehler *et al.*, 1992). Successful overexpression of MOMP could be finally achieved and even correct processing and incorporation into the outer membrane was observed, which was closely associated with lethal effects on *E. coli* cells (Findlay *et al.*, 2005).

1.5.3 Expression analysis of outer membrane components of clinical chlamydiae during an infectious cycle

Genomic transcriptional profiling of components of the outer membrane of clinical chlamydiae suggested specific transcriptional patterns during the developmental cycle (Belland *et al.*, 2003; Maurer *et al.*, 2007).

Outer membrane components, like OmcA and OmcB, are associated with stability and cross-linking of the outer membrane and play an important role during the differentiation from RBs to EBs at late stages of the developmental cycle (Hatch, 1996). Thus, up-regulation of these outer membrane components at late stages of the cycle characterizes those as members of the late gene cluster (Belland *et al.*, 2003). Also *ompA*, encoding MOMP of *C. trachomatis*, was identified as a member of the late gene cluster (Gomes *et al.*, 2005). A further differentiation into “tardy” genes, which are up-regulated even after the “late” genes, distinguishes EB specific mRNA from late genes, encoding EB proteins. Tardy genes are typically associated with EB specific mRNA, including *omcB* as an exception, since it encodes an EB protein (Maurer *et al.*, 2007).

1.5.4 The outer membrane of *P. amoebophila*

Little is known about the composition and the actual components of the cell envelope of environmental chlamydiae. With the help of the first available genome sequence for *P. amoebophila* in 2004 (Horn *et al.*, 2004), first insights into the outer membrane of chlamydiae not belonging to the *Chlamydiaceae* were possible. As expected, a homologue of the large cysteine-rich protein OmcB, pc0616, was identified and also a homologue of OmcA, pc0617, was detected due to its position in the genome and the high amount of cysteines in its sequence (Heinz, 2008).

Interestingly, no homologues of MOMP, PorB and members of the POMP family were found in *P. amoebophila*, implying significant differences to the outer membrane of clinical chlamydiae (Heinz, 2008).

Analyses of outer membrane fractions of *P. amoebophila* approved the *in silico* data by combining 1D and 2D gel electrophoresis with mass spectrometry. Experimental analyses identified 38 outer membrane proteins in total. The protein pc0978 was found as frequently in outer membrane fractions as the cysteine-rich protein pc0616 and also contains a high number of cysteines. Hence, it might represent an additional component of the COMC being responsible for outer membrane stability (Heinz, 2008).

In addition, four proteins sharing an amino acid sequence identity of 22-28% were classified as a novel putative porin family. Strikingly, these proteins have no homologues in other organisms except for the close relative *Parachlamydia acanthamoebae*. Two representatives of this putative porin family, pc1489 and pc1077, were present in high amounts in all outer membrane fractions (Heinz, 2008). It is suggested that these two proteins, along with pc0616, constitute the chlamydial outer membrane complex COMC, like OmcA, OmcB and MOMP in the *Chlamydiaceae* (Bavoil *et al.*, 1984). Secondary structures for pc1489 and pc1077 predict the formation of beta-barrels and, therefore, the potential function as porins. Since both were proposed to encode signal peptides, pc1489 and pc1077 are thought to be the functional replacement of MOMP in *P. amoebophila*.

Previous studies concentrating on the characterization of pc1489 have already visualized the localization of this porin candidate in the outer membrane of *P. amoebophila* by specific antibodies. Moreover, lipid-bilayer measurements proved the hypothesized function as porin by clearly demonstrating pore-forming features (Aistleitner, 2009).

Interestingly, the function of the two other members of the new porin family, pc0870 and pc1860, cannot be predicted as easily. For pc0870 a signal peptide but no beta-barrel structure was predicted, whereas pc1860 contains signatures of beta-barrel structures as well as of lipoproteins (Heinz, 2008). To date, it is still not clear whether they feature porin function.

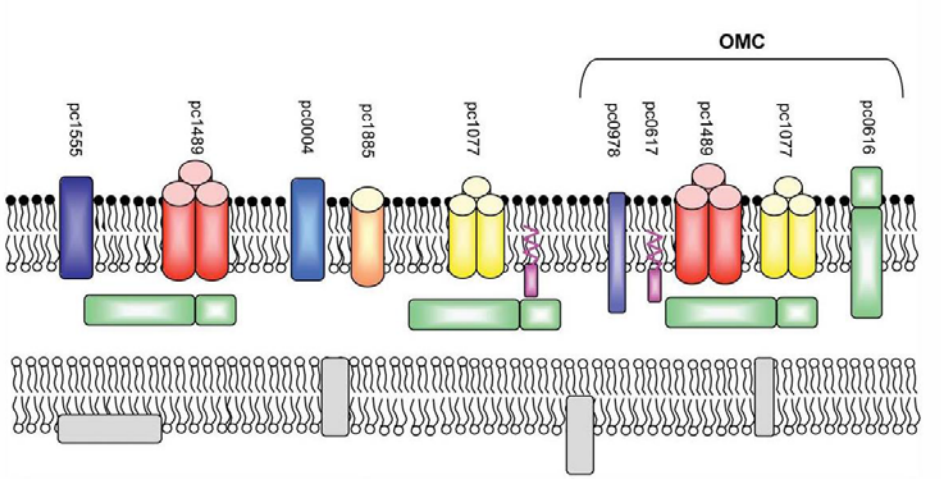

Figure 4. Schematic representation of the outer membrane of *P. amoebophila*. No homologue of MOMP could be found, whereas several other outer membrane components could be identified including a novel putative porin family (e.g. pc1489 – red, pc1077 – yellow) (Heinz, 2008).

1.6 Chlamydial heat shock proteins

Heat shock proteins (HSPs), also known as chaperones, form a family of closely related proteins, being distributed in the cytoplasm of many different organisms. HSPs from widely different sources show a remarkable structural similarity of about 40% or even higher (Amberger *et al.*, 1997; Karunakaran *et al.*, 2003). The chlamydial heat shock proteins Hsp60 and Hsp70, also known as DnaK, show marked homology with bacterial and mammalian HSPs.

In general, HSPs get drastically up-regulated in response to high temperatures in order to act as stabilizing agents and to prevent the aggregation of stress-denatured proteins (Lindquist and Craig, 1988). HSPs are able to distinguish native from partially unfolded proteins and help the latter to reassemble its original structure. An efficient folding into the native structure of denatured proteins *in vivo* is achieved by several binding and releasing steps by HSPs (Hendrick and Hartl, 1993; Bukau and Horwich, 1998).

Chlamydial heat shock proteins are considered to be involved in human diseases (Taylor *et al.*, 1990; Wick *et al.*, 1995; LaVerda *et al.*, 1999; Pan *et al.*, 1999). Since Hsp60 is widely distributed among bacteria and parasites, nearly all human-beings develop antibodies against it as a general reaction of the immune system. Chlamydial Hsp60 displays 48% homology with the human Hsp60, thus, molecular mimicry may contribute to autoimmune inflammatory damage during a chronic chlamydial infection (Brunham and Peeling, 1994).

1.7 Aims of this study

Outer membrane proteins are considered to be key players in initial steps of host cell invasion. Recent studies identified components of the *P. amoebophila* outer membrane by an *in silico* approach and promised to improve our knowledge about the structure and actual function of these important structural components.

Based on the prediction of a novel putative porin family in *P. amoebophil* this work mainly focused on initial studies concerning the localization and function of the four putative porins pc0870, pc1077, pc1489 and pc1860.
Studies dealing with MOMP of clinical chlamydiae suggested *E. coli* as a suitable system for overexpression of proteins. Hence, the aim of the present study was to achieve a heterologous expression of each of the four putative porins in *E. coli*. In parallel, viability assays should contribute to a functional characterization, since correctly processed porins feature pore-forming activity with toxic effects for *E. coli* cells.

An additional goal was to produce antibodies against purified porins in order to visualize the proposed localization in the outer membrane, supporting the theory of an outer membrane protein and allowing assumptions on function and importance in symbiont-host interactions. Nevertheless, a definite confirmation of the function as a porin would only be achieved by lipid-bilayer measurements.

In a second project, we wanted to track the transcriptional pattern of the porin pc1489 during a developmental cycle to provide insights into the expression profile of an important outer membrane protein of environmental chlamydiae. Comparable studies with representatives of pathogenic chlamydiae were used as a basis.

Apart from that, we aimed to use a cytoplasmic protein of *P. amoebophila* for the generation of an internal standard antibody for immunofluorescence experiments. Hence, DnaK and EF-TU of *P. amoebophila* should be overexpressed using *E. coli* as an expression system, followed by protein purification and antibody production. As DnaK and EF-TU are located in the cytoplasm, specific antibodies against them are considered to visualize permeability of the outer membrane while using other antibodies simultaneously.

This work was conducted as a basis for follow-up studies for further characterization of the outer membrane of the increasingly diverse *Chlamydiae*, leading to a better understanding of the mechanisms of initial steps of host cell invasion.

2 Material and Methods

2.1 Software

Table 1. Software used in this study

Software	URL/Company	Reference
Basic Local Alignment Search Tool (BLAST)	http://www.ncbi.nlm.nih.gov/BLAST/	(Altschul *et al.*, 1990)
Clone Manager	Scientific & Educational Software	
Expasy Proteomic Tools	http://www.expasy.ch/tools/dna.html	(Gasteiger *et al.*, 2003)
Finch TV	Geospiza Inc., Lincoln, NE, USA	
iCycler, Optical System Software, Version 3.1	Bio-Rad Laboratories GmbH, Munich, Germany	
Microsoft Office 2007	Microsoft Corporation, Redmond, WA, USA	
PIR - Pairwise Alignment	http://pir.georgetown.edu/pirwww/search/pairwise.shtml	(Barker *et al.*, 1998)
Primer3	http://biotools.umassmed.edu/bioapps/primer3_www.cgi	(Rozen and Skaletsky, 2000)
Primer3plus	http://www.bioinformatics.nl/cgi-bin/primer3plus/primer3plus.cgi	(Untergasser *et al.*, 2007)
Reverse Complement	http://www.bioinformatics.org/sms/rev_comp.html	(Stothard, 2000)
SignalP 3.0 Server	http://www.cbs.dtu.dk/services/SignalP/	(Nielsen *et al.*, 1997)

2.2 Technical equipment

Table 2. **Technical equipment used in this study**

Equipment	Company
AL-2000 dual pump	World Precision Instruments, Sarasoto, FL, USA
Agarose gel electrophoresis apparature Sub–Cell GT	Bio-Rad Laboratories GmbH, Munich, Germany
CCD camera AxioCam HRc	Carl Zeiss MicroImaging GmbH, Jena, Germany
Centrifuges: Centrifuge 5840 R Mikro 22 R Optima™ L-100 XP ultracentrifuge Rotina 35 R	 Eppendorf AG, Hamburg, Germany Andreas Hettich GmbH & Co. KG, Tuttlingen, Germany Beckman Coulter, Inc., Paolo Alto, CA, USA Andreas Hettich GmbH & Co. KG, Tuttlingen, Germany
Concentrator 5301	Eppendorf AG, Hamburg, Germany
Electroporator Micro Pulser™	Bio-Rad Laboratories GmbH, Munich, Germany

Fast Prep® FP120	BIO 101, Inc., Vista, CA, USA
Devices for gelelectrophoresis: Electrophoresis cell (Sub-Cell GT) Electrophoresis power supply (PowerPac Basic) Gel-documentation system	 Bio-Rad Laboratories GmbH, Munich, Germany Bio-Rad Laboratories GmbH, Munich, Germany Biostep, Jahnsdorf, Germany
iCycler Thermal cycler	Bio-Rad Laboratories GmbH, Munich, Germany
Mastercycler gradient	Eppendorf AG, Hamburg, Germany
Microbiological incubator KB 115	Binder GmbH, Tuttlingen, Germany
Laminar flow hood, model 1.8	Holten, Jouan Nordic, Allerod, Denmark
Magnetic stirrer RCT basic	IKA® Werke GmbH & Co. KG, Staufen, Germany
Microscopes: Inverse microscope Axiovert 25 Epifluorescence microscope Axioplan 2 imaging Confocal laser scanning microscope LSM 510 Meta	 Carl Zeiss MicroImaging GmbH, Jena, Germany Carl Zeiss MicroImaging GmbH, Jena, Germany Carl Zeiss MicroImaging GmbH, Jena, Germany
Mixing Block MB-102	Biozym Scientific GmbH, Hessisch Oldendorf, Germany
NanoDrop® ND-1000 UV/Vis spectrophotometer	NanoDrop Technologies Inc., Wilmington, DE, USA
Neubauer counting chamber	Paul Marienfeld GmbH & Co KG, Lauda-Königshofen, Germany
Platform Shaker Innova 2300	New Brunswick Co., Inc., Madison NJ, USA
pH meter inoLab pH Level 1	Wissenschaftlich technische Werkstätten (WTW) GmbH & Co. KG, Weilheim, Germany
Scales: OHAUS® Analytical Plus balance Sartorius BL 3100	 Ohaus Corporation, Pine Brook, NJ, USA Sartorius AG, Göttingen, Germany
ScannerEpson Expression 1680 Pro	Epson Deutschland GmbH, Meerbusch, Germany
Sonicator Bandelin Sonoplus HD2070	Bandelin electronic GmbH & Co. KG, Berlin, Germany
Sonotrode Bandelin Sonoplus UW 2070	Bandelin electronic GmbH & Co. KG, Berlin, Germany
Spectral photometer SmartSpec™ 3000	Bio-Rad Laboratories GmbH, Munich, Germany
Sub-Cell GT UV-Transparent Gel Tray (15 x 15 cm)	Bio-Rad Laboratories GmbH, Munich, Germany
Trans-Blot® SD Semi-Dry Electrophoretic Transfer Cell	Bio-Rad Laboratories GmbH, Munich, Germany
Thermostatic circulator MultiTemp™ III	GE Healthcare Bio-Sciences AB, Uppsala, Sweden
Transilluminator	Biostep GmbH, Jahnsdorf, Germany
Ultrasonic Cleaner SC100T	VWR International bvba/sprl, Leuven, Belgium
UV sterilizing PCR workstation	PeqLab Biotechnologie GmbH, Erlangen, Germany
Vacuum pump	Millipore GmbH, Vienna, Austria
Water baths: DC10 GFL® type 1004	 Thermo Haake GmbH, Karlsruhe, Germany Gesellschaft für Labortechnik GmbH, Burgwedel, Germany

Water purification system MILLI-Q® biocel	Millipore GmbH, Vienna, Austria
Watervapour high pressure autoclaves: Varioclav® 135 S H+P Varioclav® 25 T H+P	H+P Labortechnik GmbH, Oberschleißheim, Germany

2.3 Expendable items

Table 3. Expendable items used in this study

Expendable item	Company
25cm^2 Tissue culture flasks	Asahi Techno Glass Corporation, Iwaki Glass Co., Ltd., Funabashi-City, Japan
500cm^2 Tissue culture flasks	Nunc, Roskilde, Denmark
96-well microtiter plate	MJ Research, Waltham, MA, USa
Cellulose acetate membrane filters (0.45 µm pore size, 25 mm diameter)	Sartorius AG, Göttingen, Germany
Cover glasses 24 x 60 mm	Paul Marienfeld GmbH & Co. KG, Lauda-Königshofen, Germany
Cryostock caps, Viabank ™	Medical Wire & Equipment, Carsham, UK
Electroporation cuvette (0.2 cm)	Bio-Rad Laboratories GmbH, Munich, Germany
Glass beads (0.75-1.0 mm)	Carl Roth GmbH & Co. KG, Karlsruhe, Germany
Greiner tubes (15 ml, 50 ml)	Greiner Bio-One GmbH, Frickenhausen, Germany
Isopore™ polycarbonate membrane filters (0.22 µm pore size, 25 mm diameter, black)	Millipore GmbH, Vienna, Austria
Lysing Matrix A	MP Biomedicals, Brussels, Belgium
Microscope slides (76 x 26 mm)	Carl Roth GmbH & Co. KG, Karlsruhe, Germany
Microscope slides, 10 well	Paul Marienfeld GmbH & Co. KG, Lauda-Königshofen, Germany
Multiwell dishes, polystyrene (24 wells)	Nunc, Roskilde, Denmark
Needles Sterican® (ø 0.45 x 25 mm, ø 0.90 x 40 mm), single use, sterile	B.Braun Melsungen AG, Melsungen, Germany
Nitrocellulose filter (0.025 µm pore size)	Millipore GmbH, Vienna, Austria
PCR tubes (0.2 ml)	Biozym Scientific GmbH, Hessisch Oldendorf, Germany
Pipette Tipps (various sizes)	Carl Roth GmbH & Co. KG, Karlsruhe, Germany
Plastic cuvettes	Greiner Bio-One GmbH, Frickenhausen, Germany
Plastic pipettes (10 ml, 2 ml), single use, sterile	Barloworld Scientific Ltd., Staffordshire, UK
Polyvinylidene fluoride membrane (Hydrobond P)	GE Healthcare Bio-Sciences AB, Uppsala, Sweden
Reaction tube (1.5 ml)	GenXpress Service & Vertriebs GmbH, Wiener Neudorf, Austria

Reaction tube (2 ml)	Greiner Bio-One GmbH, Frickenhausen, Germany
Round coverslips (12 mm diameter)	Carl Roth GmbH & Co. KG, Karlsruhe, Germany
Screw caps Cryobank™	Mast Diagnostika Lab. Präparate GmbH, Reinfeld, Germany
Syringe (1 ml) Inject® - F 1ml, single use, sterile	B.Braun Melsungen AG, Melsungen, Germany
Syringe (5 ml) Omnifix® single use, sterile	B.Braun Melsungen AG, Melsungen, Germany
Syringe (50 ml) Omnifix® single use, sterile	B.Braun Melsungen AG, Melsungen, Germany
Syringe filter, single use, sterile, 0.20µm pore size	Asahi Techno Glass Corporation, Iwaki Glass Co., Ltd., Funabashi-City, Japan
Syringe filter, single use, sterile, 0.45µm pore size	Asahi Techno Glass Corporation, Iwaki Glass Co., Ltd., Funabashi-City, Japan
Syringe filter, single use, sterile, 1.20µm pore size	Sartorius AG, Goettingen, Germany
Thermostable foil	MJ Research, Waltham, MA, USA
Ultracentrifuge tubes	Beckham Coulter, Inc., Paolo Alto, CA, USA
Whatman® Chromatography Paper 3MM Chr	Whatman International Ltd., Maidstone, UK
ZelluTrans, Dialyseschlauch	Carl Roth GmbH & Co. KG, Karlsruhe, Germany

2.4 Kits and ready-to-use solutions

Table 4. **Kits used in this study**

Kit	**Company**
2-D Quant Kit	GE Healthcare Bio-Sciences AB, Uppsala, Sweden
Amersham HisTrap HP Columns	GE Healthcare Bio-Sciences AB, Uppsala, Sweden
BCA Protein Assay Kit	Thermo Scientific Pierce Protein Research Products, Waltham, Massachusetts, USA
DNeasy Blood & Tissue Kit	QIAgen, Hilden, Germany
Hi Trap™ IgY Purification HP Column	GE Healthcare Bio-Sciences AB, Uppsala, Sweden
Platinum® SYBR® Green qPCR SuperMix-UDG	Invitrogen, Carlsbad, CA, USA
Qiaquick PCR Purification Kit	QIAgen, Hilden, Germany
Qiaprep Spin Miniprep Kit	QIAgen, Hilden, Germany
RevertAid First Strand cDNA Synthesis Kit	Fermentas Inc., Hanover, MD, USA
TOPO® XL PCR Cloning Kit	Invitrogen, Carlsbad, CA, USA
Western Lightning Chemiluminescence Plus Kit	Perkin Elmer, Waltham, Massachusetts, USA

Table 5. Ready-to-use-solutions used in this study

Ready-to-use-solutions	Company
Gene Ruler™ 1kb DNA ladder	Fermentas Inc., Hanover, MD, USA
Gene Ruler™ 100bp DNA ladder	Fermentas Inc., Hanover, MD, USA
PageRuler™ Prestained Protein Ladder improved	Fermentas Inc., Hanover, MD, USA
PageRuler™ Unstained Protein Ladder	Fermentas Inc., Hanover, MD, USA
RiboRuler™ RNA Ladder, High Range	Fermentas Inc., Hanover, MD, USA
2x RNA Loading Dye	Fermentas Inc., Hanover, MD, USA
Spectra™ Multicolor Broad Range Protein Ladder	Fermentas Inc., Hanover, MD, USA

2.5 Chemicals

Table 6. Chemicals used in this study

Chemical	Company
4´,6-diamidino-2-phenylindole (DAPI)	Laktan Chemikalien und Laborgeräte GmbH, Graz, Austria
Acetonitrile	Sigma-Aldrich Chemie GmbH, Steinheim, Germany
Acetic acid	Carl Roth GmbH & Co. KG, Karlsruhe, Germany
Agar	Fluka Chemie AG, Buchs, Switzerland
LE Agarose	Biozym Scientific GmbH, Hessisch Oldendorf, Germany
Ammonium bicarbonate	Fluka Chemie AG, Buchs, Switzerland
Ammonium persulfate (APS)	GE Healthcare Bio-Sciences AB, Uppsala, Sweden
Ampicillin	Sigma-Aldrich Chemie GmbH, Steinheim, Germany
Boric acid	Carl Roth GmbH & Co. KG, Karlsruhe, Germany
Bovine serum albumin (BSA)	Carl Roth GmbH & Co. KG, Karlsruhe, Germany
Bromphenol blue	Sigma-Aldrich Chemie GmbH, Steinheim, Germany
Calcium chloride dihydrate	Carl Roth GmbH & Co. KG, Karlsruhe, Germany
Chloramphenicol	Sigma-Aldrich Chemie GmbH, Steinheim, Germany
Citifluor AF1	Agar Scientific Ltd., Stansted, UK
Coomassie brillant blue G-250	Carl Roth GmbH & Co. KG, Karlsruhe, Germany
Di-ethyl-pyrocarbonat (DEPC)	Sigma-Aldrich Chemie GmbH, Steinheim, Germany
Di-methylsulfoxid (DMSO)	Fluka Chemie AG, Buchs, Switzerland
Disodiumhydrogenphosphate dihydrate (Na_2HPO_4 x $2H_20$)	Carl Roth GmbH & Co. KG, Karlsruhe, Germany
Dithiothreitol (DTT)	Fluka Chemie AG, Buchs, Switzerland

Ethanol absolute	AustrAlco Österreichische Alkoholhandels GmbH, Spillern, Austria
Ethidium bromide (EtBr)	Fluka Chemie AG, Buchs, Switzerland
Ethylenediamine-tetraaceticacid (EDTA)	Carl Roth GmbH & Co. KG, Karlsruhe, Germany
Ferrous ammonium sulfate hexahydrate	Sigma-Aldrich Chemie GmbH, Steinheim, Germany
Ficoll® 400	Sigma-Aldrich Chemie GmbH, Steinheim, Germany
Formaldehyde (37% (w/w))	Carl Roth GmbH & Co. KG, Karlsruhe, Germany
Glucose	Carl Roth GmbH & Co. KG, Karlsruhe, Germany
Glycogen	Applied Biosystems/Ambion, Austin, TX, USA
Glycerol (87% (w/v))	Carl Roth GmbH & Co. KG, Karlsruhe, Germany
Glycine	Carl Roth GmbH & Co. KG, Karlsruhe, Germany
HEPES	Carl Roth GmbH & Co. KG, Karlsruhe, Germany
Hydrochloric acid (HCl) (37% (w/w))	Carl Roth GmbH & Co. KG, Karlsruhe, Germany
Hydrogen peroxide (H_2O_2), 30%	Carl Roth GmbH & Co. KG, Karlsruhe, Germany
Imidazol	Carl Roth GmbH & Co. KG, Karlsruhe, Germany
Iodacetamide	GE Healthcare Bio-Sciences AB, Uppsala, Sweden
Isopropanol (2-propanol)	Carl Roth GmbH & Co. KG, Karlsruhe, Germany
Isopropyl-β-D-thiogalactopyranoside (IPTG)	Sigma-Aldrich Chemie GmbH, Steinhausen, Germany
Kanamycin	Sigma-Aldrich Chemie GmbH, Steinhausen, Germany
Magnesium chloride hexahydrate	Carl Roth GmbH & Co. KG, Karlsruhe, Germany
Magnesium sulfate heptahydrate	Merck GmbH, Vienna, Austria
Methanol	Carl Roth GmbH & Co. KG, Karlsruhe, Germany
Milk powder	Carl Roth GmbH & Co. KG, Karlsruhe, Germany
Mowiol 4-88	Sigma-Aldrich Chemie GmbH, Steinheim, Germany
N,N,N´,N´-tetramethylethane-1,2-diamine (TEMED)	Fluka Chemie AG, Buchs, Switzerland
Potassium chloride (KCl)	Merck GmbH, Vienna, Austria
Paraformaldehyde (PFA)	Sigma-Aldrich Chemie GmbH, Steinheim, Germany
Proteose peptone	Oxoid Ltd., Hampshire, England
Roti®-Chloroform/I	Carl Roth GmbH & Co. KG, Karlsruhe, Germany
Rotiphorese® NF-Acrylamide/ Bisacrylamide-solution 30 % (29:1)	Carl Roth GmbH & Co. KG, Karlsruhe, Germany
Sodium chloride (NaCl)	Carl Roth GmbH & Co. KG, Karlsruhe, Germany
Sodium dihydrogen phosphate	Mallinckrodt Baker B.V., Deventer, Holland
Sodium dodecly sulfate (SDS)	Carl Roth GmbH & Co. KG, Karlsruhe, Germany
Sodium hydroxide (NaOH)	Carl Roth GmbH & Co. KG, Karlsruhe, Germany
Sucrose	Merck GmbH, Vienna, Austria
SYBR® Green II Nucleic Acid Gel Stain	Lonza Rockland, Inc., Rockland, ME, USA
Trifluoretic acid	Fluka Chemie AG, Buchs, Switzerland
Trishydroxymethylaminomethane (Tris-HCl)	Carl Roth GmbH & Co. KG, Karlsruhe, Germany
Trizol	Invitrogen, Lofer, Austria

Trypticase Soy Broth	Oxoid Ltd., Hampshire, England
Trypsin gold powder	Promega Corporation, Madison, USA
Tween™ 20	Sigma-Aldrich Chemie GmbH, Steinheim, Germany
Urea	USB Corp., Cleveland, USA
Xylene cyanole FF	Sigma-Aldrich Chemie GmbH, Steinheim, Germany
Yeast extract	Oxoid Ltd., Hampshire, England

2.6 Enzymes

Table 7. Restriction enzymes used in this study

Restriction Enzyme	Restriction site	Company
BamHI	5'-G^G A T C C-3'	Fermentas Inc., Hanover, MD, USA
EcoRI	5'-G^A A T T C-3'	Fermentas Inc., Hanover, MD, USA
KpnI	5'-G G T A C^C-3'	Fermentas Inc., Hanover, MD, USA
NdeI	5'-C A^T A T G-3'	Fermentas Inc., Hanover, MD, USA
NotI	5'-G C^G G C C G C-3'	Fermentas Inc., Hanover, MD, USA
PstI	5'-C T G C A^G-3'	Fermentas Inc., Hanover, MD, USA
SalI	5'-G^T C G A C-3'	Fermentas Inc., Hanover, MD, USA
SmaI	5'-C C C^G G G-3'	Fermentas Inc., Hanover, MD, USA
XhoI	5'-C^T C G A G-3'	Fermentas Inc., Hanover, MD, USA

^…cleavage site
5´, 3´…5’ end, 3’ end of DNA sequence

Table 8. Restriction enzyme buffers

Buffer	Company
Buffer O	Fermentas Inc., Hanover, MD, USA
Buffer Red	Fermentas Inc., Hanover, MD, USA
Buffer Tango	Fermentas Inc., Hanover, MD, USA
10x Ex Taq polymerase Buffer	Fermentas Inc., Hanover, MD, USA

Table 9. Enzymes, except restriction enzymes, used in this study

Enzyme/Enzyme inhibitor	Company
Benzonase	Novagen, Darmstadt, Germany
Complete EDTA free Protease Inhibitor Cocktail	Roche Diagnostics GmbH, Mannheim, Germany
DNaseI	Sigma-Aldrich Chemie GmbH, Steinheim, Germany
High Fidelity PCR Enzyme Mix	Fermentas Inc., Hanover, MD, USA
Lysozyme (human)	Sigma-Aldrich Chemie GmbH, Steinheim, Germany
Ribo Lock™ RNase Inhibitor	Fermentas Inc., Hanover, MD, USA
Taq DNA Polymerase (5U/µl)	Fermentas Inc., Hanover, MD, USA
Trypsin gold (mass spectrometry grade)	Promega Corporation, Madison, WI, USA
T4 DNA Ligase	Fermentas Inc., Hanover, MD, USA
M-MuLV Reverse Transcriptase	Fermentas Inc., Hanover, MD, USA

2.7 Organisms

Table 10. Amoeba strains and endosymbionts used in this study

Host	Endosymbiont	Source	Reference
Acanthamoeba castellanii Neff	none	American Type Culture Collection (ATCC), Manassas, VA, USA	(Neff, 1957)
Acanthamoeba castellanii Neff	*Protochlamydia amoebophila* UWE25	Universitiy of Washington, Seattle, USA	(Fritsche *et al.*, 1998; Collingro *et al.*, 2005)

Both *Acanthamoeba* sp. and *P. amoebophila* are classified as L2 organisms and were handled according to L2 laboratory guidelines.

To provide sterility of the cultures and experiments, all vessels and flasks containing L2 organsims were only opened within a class II safety cabinet, and multi-well plates containing these organisms were sealed with parafilm before removing them from the safety cabinet. Fluid waste containing these organisms was disposed according to the biosafety guidelines for L2 laboratories.

2.8 General primers for polymerase chain reaction (PCR)

Primers were produced by Thermo Fisher Scientific GmbH (Ulm, Germany). Stock solutions were diluted with $Aqua_{bidest.}$ (Mayrhofer Pharmazeutika GmbH & Co. KG, Leonding, Austria) and solutions were stored at -20°C until use.

Table 11. General primers used in this study

Primer name	Target gene/site	Primer sequence** (5´-3´ end)	Annealing temperature	Reference/ Company
M13 R	M13 binding site in lacZ gene of the vector pCR® II TOPO®	CAG GAA ACA GCT ATG AC	60°C	TOPO® XL cloning kit, Invitrogen, Carlsbad, CA, USA
M13 F		GTA AAA CGA CGG CCA G		
pgEX R	3' end of MCS* in pGEX vectors	CCG GGA GCT GCA TGT GTC AGA GG	50°C	GE Healthcare Bio-Sciences AB, Uppsala, Sweden
pgEX F	3' end of glutathione-S-transferase	GGG CTG GCA AGC CAC GTT TGG TG		
pQE R	3' end of MCS in pQE vectors	GTT CTG AGG TCA TTA CTG	50°C	QIAgen, Hilden, Germany (pQE sequencing-primer set)
pQE F	5' end of MCS in pQE vectors	CCC GAA AAG TGC CAC CTG		
T7 R	T7 terminator of pet vectors	GCT AGT TAT TGC TCA GCG G	58°C	New England Biolabs GmbH, Frankfurt, Germany.
T7 F	T7 promoter of pet vectors	TAA TAC GAC TCA CTA TAG GG		
PcR	16S rRNA gene of *Parachla-mydiaceae*, *Waddliaceae*	GTC ATC RGC CYY ACC TTV SRC RYY TCT	58°C	(Horn and Wagner, 2001)
PcF		TCA GAT TGA ATG CTG AC		
PanR	16S rRNA gene of *Chlamydiales*	GTC ATC RGC CYY ACC TTV SRC RYY TCT	65°C	(Corsaro *et al.*, 2002)
PanF		CGT GGA TGA GGC ATG CRA GTC G		
1492R	16S rRNA gene of *Bacteria*, but not *Chlamydiales*	GGY TAC CTT GTT ACG ACT T	52°C	(Lane, 1991)
27F		AGA GTT TGA TYM TGG C		

*MCS: multiple cloning site
**According to the Nomenclature Committee of the International Union of Biochemistry (NC-IUB) the unspecified bases are represented as follows: R=G or A, Y=T or C, M=A or C, V=Gor C or A, S=G or C, N=G or C or A or T

2.9 General media, buffers and solutions

Buffers, media and solutions were produced using double distilled and filtered water (H_2O_{dd}). For adjustment of the pH sodium hydroxide (NaOH) and hydrochloric acid (HCl) were used.

All media and buffers described here were sterilized for 20 min at 121°C and 1013 x 10^5 Pa using a watervapour-high pressure autoclave. Substances and solutions that are unstable at high temperatures like antibiotics were filter-sterilized (0.22 µm pore size) and added after autoclaving.
If not stated otherwise, media and buffers were stored at room temperature until further usage.

2.9.1 Media for cultivation of organisms

2.9.1.1 Media for cultivation of amoebae

- **Trypticase Soy Broth with Yeast Extract (TSY)**

Trypticase Soy Broth	30 g
Yeast extract	10 g
H_2O_{dd}	ad 1000 ml
pH 7.3	

- **Peptone-Yeast-Glucose-medium (PYG)**

Peptone	20 g
Glucose	18 g
Yeast extract	2 g
Sodiumcitrate	1 g
$MgSO_4$ x 7 H_2O	980 mg
Na_2HPO_4 x 7 H_2O	355 mg
KH_2PO_4	340 mg
$Fe(NH_4)_2(SO_4)_2$ x 6 H_2O	20 mg
H_2O_{dd}	ad 1000 ml
pH 6.5	

2.9.1.2 Media for cultivation of Escherichia coli (E. coli)

- **Luria Bertani medium (LB medium)**

Tryptone	10 g
Yeast extract	5 g
NaCl	5 g
H_2O_{dd}	ad 1000 ml
pH 7.0-7.5	

- **Terrific Broth medium (TB medium)**

Solution A

Tryptone	12 g
Yeast extract	24 g
Glycerol	4 ml
H_2O_{dd}	ad 1000 ml

Solution B

KH_2PO_4	2.31 g
K_2HPO_4	12.54 g
H_2O_{dd}	ad 1000 ml

Before use 1 volume of solution B was added to 9 volumes of solution A.

- **dYT - medium**

Tryptone	16 g
Yeast extract	10 g
NaCl	l5 g
H_2O_{dd}	ad 1000 ml

- **SOC medium**

Tryptone	20 g
Yeast extract	0.5 g
NaCl	0.58 g
KCl	0.19 g
$MgCl_2$	0.95 g
$MgSO_4$	1.20 g
Glucose	3.60 g
H_2O_{dd}	ad 1000 ml

For solid media 15 g/l agar were added before autoclaving.

2.9.2 Antibiotic solutions and solution for induction of heterologous expression

For solid media antibiotic stock solutions were added to the autoclaved media at ~50°C. Solid media containing antibiotics were stored at 4°C until further use.
Antibiotics were added to liquid media right before usage.

- **Ampicillin stock solution (Amp)** 100 mg/ml
  Amp was dissolved in 50% EtOH and stored at -20°C.
  Amp was added to media to reach a final concentration of 100 µg/ml.

- **Kanamycin stock solution (Kan)** 100 mg/ml
  Kan was dissolved in H_2O_{dd} and stored at -20°C.
  Kan was added to media to reach a final concentration of 100 µg/ml.

- **Chloramphenicol stock solution (Cam)** 25 mg/ml
  Cam was dissolved in 100% $EtOH_{abs}$ and stored at -20°C.
  Cam was added to media to reach a final concentration of 125 µg/mL

- **1M IPTG stock solution**

  Isopropyl-β-D-thiogalactopyranosid (IPTG) 238.3 mg/ml

  IPTG was dissolved in H_2O_{dd}, filter-sterilized by passing through a 0.2 µm filter and stored at -20°C.

  The IPTG stock solution was added to an actively growing *E. coli* culture to reach a final concentration of 1mM.

2.9.3 General buffers and solutions

- **10x Page's Amoebic Saline (PAS)**

NaCl	1.20 g
$MgSO_4$ x $7H_20$	0.04 g
$CaCl_2$ x H_20	0.04 g
NaH_2PO_4 x $2H_20$	1.78 g
KH_2PO_4	1.36 g
H_2O_{dd}	ad 1000 ml

- **PBS stock solution**

Solution 1: 35.6 g/l Na_2HPO_4

Solution 2: 27.6 g/l NaH_2PO_4

pH of solution 1 was adjusted to 7.2-7.4 by adding solution 2.

- **10x PBS**

Na_2HPO_4	26.8 g
NaH_2PO_4	13.8 g
NaCl	81.6 g
H_2O_{dd}	ad 1000 ml

- **1x PBS**

PBS stock solution	50 ml
NaCl	7.6 g
H_2O_{dd}	ad 1000 ml

- **Sucrose-Phosphate-Glutamate (SPG) buffer**

Sucrose	75 g
KH_2PO_4	0.52 g
Na_2HPO_4 x 2 H_20	2.30 g
Glutamc acid	0.75 g
H_2O_{dd}	ad l000 ml

- **4% paraformaldehyde (PFA) solution**

1x PBS	25 ml
Paraformaldehyd (37% w/v)	2.7 ml

2.9.4 Buffers and solutions for gel electrophoresis

- **10x TBE**

Tris-HCl	162 g
Boric acid	27.5 g
EDTA	9.3 g
H_2O_{dd}	ad 1000 ml

pH 8.3 – 8.7

- **1x TBE**

10 x TBE	100 ml
H_2O_{dd}	ad 1000 ml

- **Loading buffer**

Ficoll	2.5 g
Bromphenol blue	0.05 g
Xylencyanol	0.05 g
EDTA	0.15 g
H_2O_{dd}	ad 10 ml

2.9.5 Ethidium bromide solution

- Ethidium bromide stock solution:
  10 mg/ml Ethidium bromide (EtBr) in H_2O_{dd}

- Ethidium bromide staining solution:
  Ethidium bromide stock solution diluted 1:10000 in H_2O_{dd}

2.10 Cultivation and maintenance of amoeba cultures

Solutions

PYG medium

TSY medium

Procedure

Acanthamoeba castellanii Neff, either harboring *P. amoebophila* or without endosymbionts, were grown axenically in liquid TSY or PYG medium in 10 ml and 150 ml flasks at 20°C. Amoebic growth was observed by using an inverse microscope, screening for potential contaminations in parallel.

Medium was exchanged if high rates of encystation or detachment of the trophozoites from the culture flasks got visible. Also well grown cultures with densely attached trophozoites were subjected to shaking off and subsequent medium exchange in order to maintain amoebae at the stage of growing. Medium was replaced by pouring the old medium out into a glass bottle, followed by adding the same standardized volume of fresh medium. The remaining amoebae were allowed to recover and grow again to a stage of densely attachement.

New or poorly grown cultures were inoculated with respective cells from well-grown cultures. For this purpose, a 10 ml culture flask was shaken vigorously and 1-2 ml of the cell suspension were transferred to the target culture flasks by disposable single-use pipettes.

2.11 Harvesting and quantification of amoebae

Depending on the number of amoebae needed for an experiment, the number of culture flasks to be harvested was estimated. One small well-grown culture yielded about 1.5 x 10^6 cells whereas a large one resulted in a yield of about 1 x 10^7 amoebae.

Culture flasks were shaken rigorously in order to detach amoebae from the surface, suspensions were poured out into 50 ml Greiner tubes and cultures were supplied with fresh medium. The cell suspension was centrifuged at 7323x g for 5 minutes and the supernatants were discarded. Pellets were resuspended in 1 ml 1x PAS, pooled and another centrifugation step (7323x g, 5 min) was carried out.

Cell concentrations of harvested amoebae were determined using a Neubauer counting chamber. For this purpose amoebal suspensions were diluted in 1x PAS either 1:10 or 1:100, depending on the harvested culture. These dilutions were subsequently pipetted into the two chambers of the Neubauer counting chamber. Cells were immediately subjected to counting with the help of an inverse phase contrast microscope.

The cell concentration per ml was calculated as follows:

$$\frac{\text{Cells}}{\text{ml}} = \frac{\text{Number of all cells counted x D}}{\text{Number of fields counted x Depth of chamber}}$$

Dilution factor (D) = 100

Depth of chamber = 0.1 mm

2.12 Screening of Acanthamoeba castellanii Neff cultures by 4', 6-Diamidino-2-phenylindol (DAPI) staining

Regularly, the amoeba cultures had to be screened for contaminations. One possibility to detect extracellular bacteria or other chlamydiae was DAPI staining.

Solutions

DAPI

1x PAS

4% PFA

Procedure

DAPI was prepared at a dilution of 1:10000 and stored at 4°C in the dark until further use. 1 ml of an amoeba culture was harvested by centrifugation and the resulting pellet was washed once with 1x PAS. Subsequently, the pellet was resuspended in 200 µl 1x PAS and 20 µl of this suspension were applied to one well of a microscope slide. Amoebae were allowed to attach for 30 min, afterwards the liquid was removed carefully and 10 µl of 4 % PFA were added for the fixation of the cells. After incubation for 10 min at RT, the fixative was removed and the wells were washed with 10 µl H_20_{dd}. Then, 10 µl of the DAPI-solution were added onto each well and slides were incubated for 7 min in the dark. The DAPI-solution was removed and wells were washed with 20 µl H_20_{dd}. Slides were dried at RT in the dark and prepared for microscopic analysis by embedding them in Citifluor.

2.13 Partial purification of EBs

Pellets after partial purification were expected to contain mostly elementary bodies of *P. amoebophila,* since reticulate bodies are thought to get destroyed during the procedure of partial purification.

Solutions

SPG-Buffer

1x PAS

Procedure

Well grown amoebae cultures infected with *P. amoebophila* were harvested (2.11). The pellets were washed once with 1x PAS, subsequently resuspended in 1x PAS and finally pooled. To disrupt cell membranes of amoebae, they were first frozen at -20°C followed by thawing at 45°C. This freeze-and-thaw step was repeated once leading to a release of intracellular bacteria. For further lysis of the cells, 5 ml glass beads were added to the suspension and vortexed for 3 min to achieve a mechanical lysis of amoebae cells and RBs.

The suspension was centrifuged at 300x g for 10 min at 4°C in order to get rid of the glass beads and amoebal cell debris. The supernatant was then transferred through a 1.2 µm filter to an ultracentrifuge tube and 1x PAS was added to a final volume of 10 ml.

After centrifugation at 35700x g for 40 min at 4°C, the pellet was resuspended in about 10 ml precooled SPG buffer, followed by a final ultracentrifugation step (35700x g, 40 min, 4°C). The pellet containing partial-purified bacteria was resuspended in 3 ml SPG and the suspension was passaged through a 0.45 mm needle several times in order to break up clusters of bacteria.
Finally, SPG buffer was added to the *P. amoebophila* suspension to a total volume of 7 ml and 1 ml aliquots were stored at -80°C.

2.14 Quantification of purified P. amoebophila *cells*

Solutions

1x PBS (filter-sterilized)

DAPI

Procedure

After partial purification *P. amoebophila* suspensions were quantified by filtration of particles (>0.22 µm diameter) onto a membrane, followed by DAPI staining.

After thawing at 37°C, 1 µl of purified *P. amoebophila* EBs was diluted with 5 ml 1x PBS and suspensions were stored on ice until use. In the meantime, the filter device was flame-sterilized and assembled using a black 0.22 µm polycarbonate membrane filter and a 0.45 µm cellulose acetate membrane support underneath the filter. To rinse the funnel 5 ml filter-sterilized 1x PBS were filtered by applying a vacuum pump running at 250 millimeter of mercury. Next, the bacterial suspension was filtered, followed by another rinsing step to remove all bacteria from the funnel. Subsequently, 150 µl of DAPI solution were added on top of the filter and the filter was incubated for 5 min in the dark. By applying the vaccum pump, the DAPI solution was removed and the filter was washed with 1x PBS.
Finally, the membrane was placed on a microscope slide and embedded in Citifluor for further analysis with an epifluorescence microscope.

The number of DAPI signals within a 10 x 10 grid was counted using the 100x objective. Only clearly coccoid DAPI signals were considered to be *P. amoebophila* cells.

The cell number/ml was calculated as follows:

$$\text{cells/ml} = \frac{\text{number of counted cells}}{\text{number of fields}} \times \text{M} \times \text{DF}$$

M…Microscope factor = 11264

DF… Dilution factor = 1000

2.15 *Infectious cycle of* P. amoebophila *in* A. castellanii *Neff*

Solutions

TSY

1x PAS (filter-sterilized)

1x PBS (filter-sterilized)

4% PFA

Methanol

Procedure

A 150 ml culture of *A. castellanii* Neff was harvested and amoebae were counted using a Neubauer counting chamber (2.11). The suspension was pelleted by centrifugation and resuspended in the volume of TSY needed to obtain the required number of cells/ml.

The following steps were performed in duplicates. 10^6 amoebae in 3 ml TSY were seeded in each well of a 6-well plate and samples were incubated for 1 or 2 hours at 20°C to allow attachment of amoebae. Partially purified *P. amoebophila* EBs were thawed at 37°C and directly placed on ice. Amoebae were infected with EBs at a theoretical multiplicity of infection (MOI) of 10 by adding a defined amount of EB suspension to each well. Amoebae from one well were not infected and used as a negative control. The plates were put on a shaking platform in order to equally distribute the EBs, then, plates were centrifuged at 600x g for 15 min at 20°C to stimulate the uptake of bacteria. The end of centrifugation was regarded as time point 0 hours post infection (h p.i.). Immediately afterwards, amoebae from time point 0 h p.i. were harvested by resuspension and centrifugation in a Greiner tube at 3900x g for 10 min at 20°C. In parallel, 15 µl of amoeba suspension from 0 h p.i. were incubated on one well of a 10-well microscopic slide for 20 min and finally fixed with methanol for 10 min at RT.

The medium from the other wells was exchanged to remove excess EBs that were not attached to amoebae and the infected cultures and the negative control were grown at 20°C. Ameobae were harvested 24, 48 and 96 h p.i., whereby the uninfected control was harvested at the last time point 96 h p.i.. Again, 15 µl aliquots of each time point were incubated on 10-well microscopic slides and fixed with methanol for further analysis.
Cell pellets from each time point were stored at -20°C.

2.16 Cultivation and maintenance of recombinant E. coli *strains*

Solutions

LB medium
LB agar plates
Amp stock solution
Kan stock solution
Cam stock solution

Procedure

For culturing recombinant *E. coli* cells either liquid medium or plates with solid medium were used. To avoid the growth of cells without plasmid the appropriate antibiotic stock solution was added, depending on the resistance gene on the vector.
Cells subjected for cultivation in liquid media were picked under sterile conditions from a single colony, inoculated in 5 ml of LB + antibiotics and incubated at 37°C on an orbital shaker over night (o/n) at 200 rpm. The *E. coli* cultures were used for isolation of plasmid DNA or for further overexpression experminents.

Larger cell volumes were cultured in Erlenmeyer flasks containing the designated volume of medium. The medium was inoculated with an o/n culture of the desired *E. coli* strain at a ratio of 1:20 and incubated at 37°C on an orbital shaker until the desired cell density was reached.

Short time maintenance was achieved by transferring single clones to a masterplate. This plate was incubated o/n at 37°C and stored at 4°C until further use. For long time maintenance cryostocks of single clones were prepared according to the following procedure:

800 µl of o/n culture were transferred into 2 ml screw caps containing a special cryostock solution and hollow plastic spheres for the attachment of the cells. The caps were inverted about 10 times, the supernatant was removed and the caps were frozen at -80°C. To grow cells from this stock one sphere could be removed from the cap and placed into fresh LB medium.

2.17 Measurements of the optical density (OD) of E. coli cell cultures

The growth of *E. coli* cultures was tracked by measurements of the optical density. Cultures were removed from the rocking platform and 500 µl were filled into a cuvette for photometric measurements at a wavelength of 600 nm using a spectral photometer.

2.18 Sample preparation from E. coli cell cultures

E. coli cell pellets were obtained by centrifugation of an *E. coli* culture at 7323x g for 10 min. The obtained pellet was resuspended in an appropriate amount of 4x SDS-PAGE loading buffer, depending on the size of the pellet. Samples were heated to 95°C for 5 min in order to break up the cells. 1 µl of Benzonase was added to the samples and digestion of nucleic acids was performed for 1 h at 4°C. Samples were stored at -20°C until further use.

2.19 Preparation of electrocompetent E. coli strains

Solutions

dYT medium

10% glycerine

Procedure

All solutions as well as the necessary instruments und tubes had to be precooled to 4°C in advance. All steps were carried out in the 4°C room and all centrifugation steps had to be conducted at 4°C.

750 ml dYT medium were inoculated with an over-night culture containing the desired *E. coli* strain at a ratio of 1:1000. Cells were grown at 37°C on a shaking platform and the optical density at a wavelength of 600 nm was measured in regular intervals until the cultures reached an OD_{600} of ~ 0.6. Cells were placed on ice to cool them and were harvested by centrifugation (7323x g, 15 min, 4°C).

Each cell pellet was washed with 50 ml ice-cold H_2O_{dd}, resuspended in 50 ml 10% glycerine and again centrifuged. The supernatant was removed and the pellets were resuspended in an equal volume of 10% glycerine solution, aliquoted à 100µl in screw caps and immediately stored at -80°C until further use.

2.20 Methods for DNA isolation

2.20.1 Isolation of total DNA from amoeba cultures

10 ml of an amoeba culture were harvested in order to isolate DNA from the resulting pellet. DNA isolation was accomplished by using the DNeasy Blood & Tissue Kit according to the manufacturer´s instructions following the protocol for Gram-negative bacteria.

Finally, the concentration of isolated DNA dissolved in $H2O_{dd}$ was determined by using a Nano Drop® device (2.24.2) and could be subsequently used as template in PCR.

2.20.2 Isolation of plasmid DNA from recombinant *E. coli* strains

Solutions

LB medium

Kan/Amp/Cam stock-solution

Procedure

5 ml LB medium were mixed with 5µl antibiotic stock solution, and recombinant *E. coli* cells were inoculated and cultivated as described in 2.16.

Finally, plasmids were isolated with the QIAprep® Spin Miniprep Kit following the manufacturer`s instructions and analyzed quantitatively by Nanodrop measurements. Plasmids were sequenced to verify correct inserts prior to restriction experiments.

2.21 Simultaneous isolation of RNA from amoebae and their bacterial endosymbionts

Solutions

$H_2O_{dd/DEPC}$

0.1 Vol% Diethylpyrocarbonat (DEPC) was dissolved in 1 l H_2O_{dd} by stirring, incubated at RT o/n and finally autoclaved.

In general all aqueous solutions used for RNA treatment were prepared with DEPC-treated H_2O_{dd} in order to inactivate RNases.

Trizol

Chloroform

Isopropyl alcohol

75% $EtOH_{DEPC}$

Procedure

Phenol was used for the extraction of RNA, hence all steps including Phenol were carried out under the hood.

For the isolation of RNA, 3 ml of amoebal culture were harvested at 7323x g for 10 min at 20°C. After removing the supernatant carefully, the pellet was resuspended in 750 µl Trizol by pipetting up and down about 30 times. The cells were disrupted using a bead beater at an intensity of 4.5 for 30 sec and the disrupted cell suspenison was then centrifuged at 12000x g for 5 min. The supernatant was incubated at RT for 5 min followed by the addition of 200 µl chloroform per 750 µl Trizol. This solution was shaken vigorously by hand for 15 sec, incubated at RT for 5 min and finally centrifuged at 12000x g for 15 min at 4°C. The aqueous supernatant was taken off carefully, avoiding a carryover of chloroform. The supernatant was then mixed with 500 µl isopropyl alcohol per 750 µl volume and incubated at RT for 10 min.

After another centrifugation step (12000x g, 10 min, 4°C) the resulting gel-like RNA-pellet was washed with 1 ml 75% EtOH and centrifuged once more for 5 min at 7000x g at 4°C. The RNA pellet was air-dried for 10 min, and finally dissolved in 30 µl RNase free $H_2O_{dd/DEPC}$.

The isolated RNA was then quantified photometrically (2.24.2) and could either be stored at -80°C or treated directly with DNase.

2.22 DNase treatment of isolated RNA

In order to ensure that the isolated RNA was free of DNA, DNase digestion was carried out.

Solutions

Deoxyribonuclease I amplification grade 2 Units/µl

10x DNase reaction buffer

RNase inhibitor

$H_2O_{dd/DEPC}$

3M Natrium acetat, pH 5.2

Glycogen

70% $EtOH_{DEPC}$

100% EtOH

Procedure

The DNase digestion reaction had to be prepared according to the following standard procedure considering the use of 1 Unit DNase per 2µg RNA. As DNase is susceptible to any physical stress, the digestion reaction was never vortexed.

DNase digestion mixture:

RNA	30 µl
10x reaction buffer	5 µl
DNase	x
RNase inhibitor	2.5 µl
$H_2O_{dd/DEPC}$	ad 50 µl

This reaction was incubated for 1 h at RT, then 5 µl stop solution were added and the reaction was heat inactivated for 10 min at 70°C.

2.23 Ethanol precipitation of isolated RNA

After DNase digestion, RNA had to be precipitated by using Ethanol. $H_2O_{dd/DEPC}$ was added to the reaction mix to a final volume of 200 µl, next 20 µl 3M sodium acetat were added and RNA samples were additionally treated with 20 µl glycogen. 600 µl 100% EtOH were used for precipitation at -20°C o/n.

Finally, the reaction mixture was centrifuged at 12000x g for 15 min at 4°C. The resulting pellet was washed with 70% $EtOH_{DEPC}$ and once more centrifuged. RNA precipitation was completed by air-drying the pellet for 10 min and resolving in 30 µl $H_2O_{dd/DEPC.}$ The RNA was measured photometrically and the quality of the RNA samples was checked as described in 2.28.1.

2.24 Qualitative and quantitative analysis of nucleic acids

2.24.1 Qualitative analysis of nucleic acids using agarose gel electrophoresis

For qualitative analysis of nucleic acids, horizontal agarose gel electrophoresis was used. This technique offers the possibility to separate nucleic acids according to their size by migration through an agarose gel under the influence of an electric field.

Solutions

1x TBE
Loading buffer
DNA ladder
EtBr staining solution

Procedure

Agarose gels with concentrations of 1-2.5 % were obtained by mixing 1.5 g – 3.75 g agarose with 150 ml of 1x TBE and melting it in a microwave. The solution was poured into a gel–tray with applied combs. After polymerization, the gel-carriage was inserted into an electrophoresis apparature filled with 1x TBE, the combs were removed and nucleic acid solutions, mixed 1:1 with loading buffer, were pipetted into the pockets of the gel. By applying a voltage of 80 - 100 V for 60 - 90 min, depending on the type of analysis, nucleic acids got separated according to their fragment size.

After separation the gels were incubated in ethidium bromide staining solution for 30 min and nucleic acids were visualized with UV-transillumination (λ = 312 nm). Band patterns were recorded and digitalised with a gel–documentation system.

2.24.2 Quantitative, photometric analysis of nucleic acids

Concentration and purity of nucleic acids were determined using a NanoDrop® ND-1000 spectralphotometer. For this purpose 1.5 µl nucleic acid solution were pipetted onto the end of the fibre optic cable of the NanoDrop® device. Measurments were performed at λ = 260 nm according to the manufacturer's instructions.

2.25 In silico *design of new PCR primers for the amplification of target genes*

Specific PCR primers targeting the respective start- and end-sequences of genes of *P. amoebophila* UWE25 were constructed by using the Clone Manager software. The primers inserted two different restriction sites at the 3'- and 5'-end of the PCR products (Table 13 and Table 14) for cloning of the amplified genes into an expression vector. If necessary, the reverse primers were designed to insert a 6x Histidine tag at the 5`end for purification. The used restriction sites were also present in the vector of choice for further cloning experiments.
All primers described in this study were obtained from Thermo Electron GmbH (Ulm, Germany). All PCR amplifications were carried out using the iCycler or the Mastercycler gradient PCR cycler.

2.25.1 Detection of the leader sequence of the porins of *P. amoebophila*

For the *in silico* design of new PCR primers it was necessary to identify the leader sequence of the porins using the software SignalP3. These primers should amplify the porins without leader sequence during a PCR reaction; therefore the most probable cutting sites were identified by using the methods "neutral networks" and "hidden Markov models".

Furthermore, the *E. coli* OmpT protease leader sequence was integrated during primer design: CGGGCGAAACTCCTAGGAATAGTCCTGACAACCCCTATCGCGATCAGCTCTTTTGCGTCGAC (Novagen, Darmstadt, Germany – pet12a)

Table 12. **SignalP3 prediction for the leader sequences of the 4 putative porins**

Porin	cut between amino acid
pc0870	21 + 22
pc1077	20 + 21
pc1489	20 + 21
pc1860	22 + 23

2.26 Primers used for amplification of target genes

Table 13. **Specific primers for the amplification of porins**

Primer name*	Target molecule	Primer sequence (5´-3´ end)	Comments**	Restriction site for	For cloning into
pet0870R	pc0870	CGG GTA CTC GAG AAT CCC AAA TCC AAT ATC	HPLC Ta=58°C	XhoI	pet21b
pet0870F		CGG GTA GAA TTC ATG AAA AAA GTT TGT TGC GTT		EcoRI	
pet1077R	pc1077	CGG GTA CTC GAG GAA TGC CAT TCC TAC ATC		XhoI	
pet1077F		CGG GTA GTC GAC ATG CGC AAA ATC CTT TTG ACA		SalI	
pet1489R	pc1489	CGG GTA CTC GAG GAA TTG TTT TCC AAA TGT		XhoI	
pet1489F		CGG GTA GTC GAC ATG CGA AAG TTG ATA ACC TTC		SalI	
pet1860R	pc1860	CGG GTA CTC GAG GAA AGA ATG GGA TAA TGC		XhoI	
pet1860F		CGG GTA GAA TTC ATG TTT AGA TCT CTG GTC GCT		EcoRI	
pet0870R_2	pc0870	CGG GTA GGA TCC GTG GTG GTG GTG GTG GTG CCC AAA TCC AAT ATC	PAGE Ta=58°C	BamHI	pet16b
pet0870F_2		CGG GTA CAT ATG AAA AAA GTT TGT TGC GTT	HPLC Ta=58°C	NdeI	
pet1077R_2	pc1077	CGG GTA GGA TCC GTG GTG GTG GTG GTG GTG GAA TGC CAT TCC TAC ATC	PAGE Ta=58°C	BamHI	
pet1077F_2		CGG GTA CAT ATG CGC AAA ATC CTT TTG ACA ATT	HPLC Ta=58°C	NdeI	
pet1489R_2	pc1489	CGG GTA CTC GAG GTG GTG GTG GTG GTG GTG GAA TTG TTT TCC AAA TGT	PAGE Ta=58°C	XhoI	
pet1489F_2		CGG GTA CTC GAG CGA AAG TTG ATA ACC TTC	HPLC Ta=58°C	XhoI	

pet1860R_2	pc1860	CGG GTA GGA TCC GTG GTG GTG GTG GTG GTG GAA AGA ATG GGA TAA TGC	PAGE Ta=58°C	BamHI	pet16b
pet1860F_2		CGG GTA CAT ATG TTT AGA TCT CTG GTC GCT	HPLC Ta=58°C	NdeI	
qe0870R	pc0870	CGG GTA CTG CAG GTG GTG GTG GTG GTG GTG TAC CCG AAT CCC AAA TCC AAT ATC	PAGE Ta=58°C	PstI	pQE-30
qe0870F		CGG GTA GGT ACC AAA AAA GTT TGT TGC GTT	HPLC Ta=58°C	KpnI	
qe1077R	pc1077	CGG GTA CTG CAG GTG GTG GTG GTG GTG GTG TAC CCG GAA TGC CAT TCC TAC ATC	PAGE Ta=58°C	PstI	
qe1077F		CGG GTA GGT ACC CGC AAA ATC CTT TTG ACA	HPLC Ta=58°C	KpnI	
qe1489R	pc1489	CGG GTA CTG CAG GTG GTG GTG GTG GTG GTG TAC CCG GAA TTG TTT TCC AAA TGT	PAGE Ta=58°C	PstI	
qe1489F		CGG GTA GGT ACC CGA AAG TTG ATA ACC TTC	HPLC Ta=58°C	KpnI	
qe1860R	pc1860	CGG GTA CTG CAG GTG GTG GTG GTG GTG GTG TAC CCG GAA AGA ATG GGA TAA TGC	PAGE Ta=58°C	PstI	
qe1860F		CGG GTA GGT ACC TTT AGA TCT CTG GTC GCT	HPLC Ta=58°C	KpnI	
gx0870F	pc0870	CGG GTA GAA TTC A AAA AAA GTT TGT TGC GTT	HPLC Ta=58°C	EcoRI	pgEX-4T-3
gx1077R	pc1077	CGG GTA GC GGCC GC GAA TGC CAT TCC TAC ATC		NotI	
gx1489F	pc1489	CGG GTA CCC GGG AA CGA AAG TTG ATA ACC TTC		SmaI	
gx1860F	pc1860	CGG GTA GAA TTC A TTT AGA TCT CTG GTC GCT		EcoRI	
noL0870R	pc0870	CGG GTA CTG CAG AAT CCC AAA TCC AAT ATC		PstI	pQE-30
noL0870F		CGG GTA GGT ACC GAA CTA TTA AGT TTT GAT		KpnI	
noL1077R	pc1077	CGG GTA CTG CAG GAA TGC CAT TCC TAC ATC		PstI	
noL1077F		CGG GTA GGT ACC TTT TGG CCT GAA GCA ACA		KpnI	
omp1860R	pc1860	CGG GTA CTG CAG GTG GTG GTG GTG GTG GTG TAC CCG GAA AGA ATG GGA TAA TGC	PAGE Ta=58°C	PstI	
omp1860F		CGG GTA GGT ACC CGG GCG AAA CTC CTA GGA ATA GTC CTG ACA ACC CCT ATC GCG ATC AGC TCT TTT GCG TCG AC AAG TTG TCA ACA AAG TGT GGA		KpnI	

*noL: resulting amplicon without leader sequence

omp: resulting amplicon with OmpT leader sequence

**Ta: annealing temperature

HPLC: High Performance Liquid Chromatography, technique for primer purification, purity of the oligonucleotide >80%

PAGE: Polyacrylamid gel electrophoresis, technique for primer purification, suitable for the purification of very long oligonucleotides

Table 14. Specific primers for the amplification of cytoplasmic proteins

Primer name	Target molecule	Primer sequence (5´-3´ end)	Comments*	Restriction site for	For cloning into
qe0595R	pc0595	CGG GTA CTG CAG TTT AAG GAT TTC GGA AAC	HPLC Ta=58°C	PstI	pQE-30
qe0595F		CGG GTA CCC GGG A GCT AAA GAA ACT TTT CAG		SmaI	
qe1499R	pc1499	CGG GTA CTG CAG TGG TTT TTT ATC ATC CAA		PstI	
qe1499F		CGG GTA CCC GGG A AGC CAA AGT CAA ACA AAA		SmaI	
gx0595R	pc0595	CGG GTA CTC GAG TTT AAG GAT TTC GGA AAC		XhoI	pgEX-4T-3
gx0595F		CGG GTA CCC GGG AA GCT AAA GAA ACT TTT CAG		SmaI	
gx1499R	pc1499	CGG GTA CTC GAG TGG TTT TTT ATC ATC CAA		XhoI	
gx1499F		CGG GTA CCC GGG AA AGC CAA AGT CAA ACA AAA		SmaI	

*Ta: annealing temperature

HPLC: High Performance Liquid Chromatography, technique for primer purification, purity of the oligonucleotide >80%

2.27 In vitro amplification of DNA fragments via PCR

DNA fragments of interest were amplified by PCR using specifically designed primers.
Every PCR reaction starts with a denaturation step to separate the double strands of the DNA from each other, followed by an annealing step, where the primers bind to the DNA template. An ultimate step results in elongation of the primers by a DNA polymerase (Taq). By repeating this cycle several times, millions of copies of one gene can be amplified in a short time.

Table 15. Components for a standard reaction mixture for PCR

Component	Volume/ 50 µl reaction
$MgCl_2$ (25 mM) (Fermentas Inc., Hanover, MD, USA)	4 µl
10 x Taq buffer (with KCl)	5 µl
dNTP – Mix (2 mM each) (Fermentas Inc., Hanover, MD, USA)	5 µl
Forward primer (50 pmol/µl)	1 µl
Reverse primer (50 pmol/µl)	1 µl
Taq DNA Polymerase (5 u/µl)	0.2 µl
$Aqua_{bidest.}$ (Mayrhofer Pharmazeutika GmbH & CoKG, Leonding, Austria)	ad 50 µl
Template	~100 ng

Procedure

$H_2O_{dd.}$, $MgCl_{2,}$ 10x Taq polymerase buffer and tubes needed for PCR were exposed to UV-light for 15 min before preparing the standard reaction mixture in order to avoid contaminations. All pipetting steps, except for the addition of the positive control, were carried out in a UV sterilizing PCR hood.

For easier handling a mastermix for the standard reaction mixture was prepared. Furthermore, each PCR contained a positive and a negative control.

Standard PCR reaction:

PCR step	Temp. (°C)	Time	Number of cycles
Denaturation	95	3 min	1
Denaturation	95	30 sec	35
Annealing	*	30 sec	
Elongation	72	30 sec/ 500 basepairs	
Final elongation	72	7 min	1

*Annealing temperature see Table 13 and Table 14

2.27.1 Gradient PCR

In order to determine the optimal annealing temperatures of the newly designed primer pairs a gradient PCR was performed. Denaturation, elongation and final elongation were conducted as in the standard PCR approach (2.27). A negative control containing no template DNA was run at the lowest annealing temperature in order to check for PCR contaminations.

100 ng DNA were used as template for the amplification.

Temperature gradient of the thermocycler								
Row	A	B	C	D	E	F	G	H
Temperature (°C)	65	64	62.3	59.5	55.7	53	51.1	50

2.27.2 High Fidelity PCR

This PCR approach used the Hi-Fidelity PCR Enzyme Mix for the amplification of genes. This DNA polymerase features proof reading activity for correct copying of the amplified sequence. Thus, frameshifts were minimized and correct expression was expected.

Components and volumes were the same as for standard reactions (Table 15), except using the Hi-Fidelity polymerase. DNA isolated from E25 elementary bodies (2.14) was used as template. The same amplification conditions as for standard PCR were used.

2.28 Reverse Transcription PCR (RT-PCR)

To exclude degradation effects of RNA and contaminations with DNA should, only RNA samples of approved quality were used in RT-PCR.

2.28.1 Methods for testing RNA quality

A 2% agarose gel was prepared using TAE_{DEPC} and gel electrophoresis was performed (2.24.1) in order to separate RNA by size. The samples for electrophoresis were prepared by mixing 1 µl of each isolated RNA sample with 2 µl of RNA loading dye.
Furthermore, the isolated RNA was used as template in PCR in combination with specific primers, designed for quantitative PCR (qPCR) (Table 16). Since no DNA should be contained in the RNA samples, no amplification of gene fragments was expected. PCR products were controlled on a 2% agarose gel.

2.28.2 Reverse transcription

Reverse transcription was performed by using the RevertAid™ First Strand cDNA Kit according to the manufacturer's instructions. 1 µg RNA was applied per reaction and random hexamer primers were used for reverse transcription. A negative control was performed in parallel where no reverse transcriptase was added. During this reaction no creation of cDNA was expected.
The obtained cDNA was stored at -20°C until further use in qPCR as described in the next chapter.

2.29 Quantitative polymerase chain reaction (qPCR)

qPCR was used as a method for transcriptional analysis of the porin pc1489 in comparison to the 16S rRNA gene of *P. amoebophila* during an infectious cycle. Three independent biological replicates of isolated RNA were analyzed (2.15). The third replicate, which was kindly provided by Albert Müller, did not comprise a RNA sample from a non-infected culture.

The Platinum® SYBR® Green qPCR SuperMix-UDG Kit was used for amplification following the manufacturer`s instructions by applying cDNA to the reaction mixture.

Table 16. **Specific primers for qPCR were designed using the online tool Primer3plus**

Primer name	Target molecule	Size of amplicon	Primer sequence (5´-3´ end)	Comments*
q16S_R	16S rRNA gene of *P. amoebophila*	88 bp	TTC CAA CCG TTA TCC CAG AG	HPLC Ta=60°C
q16S_F			GCA AGT CGA ACG AAA CCT C	
q1489_R	pc1489 gene of *P. amoebophila*	143 bp	CAG CCC CAA TTT ACA GAA GC	
q1489_F			TGG AAC CAA AAA GCT CCA TC	

*Ta: annealing temperature

HPLC: High Performance Liquid Chromatography, technique for primer purification, purity of the oligonucleotide >80%

2.29.1 Preparation and calculation of qPCR standards by TOPO™ XL cloning

All qPCR runs had to include internal standards for the quantification of unknown samples. As the 16S rRNA gene and the gene for pc1489 were subjected to detailed transcriptional analysis, standards for these genes had to be included in the whole process.

Plasmids for each involved gene were prepared by TOPO™ XL cloning following the manufacturer`s instructions, and the plasmid copy number was calculated according to the molecular weight (Table 17). A dilution series was produced and the most appropriate dilutions, ranging from 10^9 to 10^2, were chosen as standard in qPCR.

Table 17. Calculation of plasmid copies of the 16S and pc1489 standard plasmids

Gene fragment	Concentration of isolated recombinant TOPO XL	Molecular weight in kilo Daltons (kDa)	TOPO XL plasmid copies per µl
16 S rRNA	451 ng /µl	2988	9.1 E+13
pc1489	323 ng/µl	2952	6.6 E+13

2.29.2 Plate setup for qPCR

All standards for the 16S rRNA gene, the pc1489 gene as well as the unknown cDNA samples from the infectious cycle had to be analyzed on one plate during a single run in order to produce comparable results. Each reaction was performed in duplicates.

	16S 1 10^9	16S 1 10^9		1489 1 10^9	1489 1 10^9		16S 1 0 hpi	16S1 0 hpi	1489 1 0 hpi	1489 1 0 hpi	
	16S 2 10^8	16S 2 10^8		1489 2 10^8	1489 2 10^8		16S 2 24 hpi	16S 2 24 hpi	1489 2 24 hpi	1489 2 24 hpi	
	16S 3 10^7	16S 3 10^7		1489 3 10^7	1489 3 10^7		16S 3 48 hpi	16S 3 48 hpi	1489 3 48 hpi	1489 3 48 hpi	
	16S 4 10^6	16S 4 10^6		1489 4 10^6	1489 4 10^6		16S 4 96 hpi	16S 4 96 hpi	1489 4 96 hpi	1489 4 96 hpi	
	16S 5 10^5	16S 5 10^5		1489 5 10^5	1489 5 10^5		16S 5 neg	16S 5 neg	1489 5 neg	1489 5 neg	
	16S neg1	16S neg2		1489 neg1	1489 neg2		16S 6 -RT	16S 6 -RT	1489 6 -RT	1489 6 -RT	

Figure 5. Plate setup for qPCR used in this study

primers q16S R+F

primers q1489 R+F

no template

10^9 – 10^5: dilution series of standards, 0 h p.i. – 96 h p.i.: unknown samples of infectious cycle

2.29.3 qPCR program

Since primer concentrations and annealing temperatures had to be optimized first, a gradient PCR was performed as described in 2.27.1. Further, the optimal template concentration had to be tested in a qPCR pre-run.
The following qPCR program was designed for transcription analysis, including a melt curve after amplification of the gene fragments. Camera recording and data collection took place during cycle 2.

qPCR program for the primer pairs q16S R+F and q1489 R+F

Cycle	Temperature (°C)	Time	Repeats
1	95	3 min	1
2	95	40 sec	35
	60	30 sec	
	72	30 sec	
3	72	1 min	1
4	95	30 sec	1
5	55	30 sec	1
6	55-95	10 sec	80

Each run included a negative control (NTC) containing H_2O_{dd} as template in the reaction mix. In order to create an additional negative control, single-stranded RNA was used as template in one qPCR reaction. Since this RNA sample has not been treated with reverse transcriptase during RT-PCR, no amplicons were expected after qPCR.
For interpretation and further analysis of the qPCR results the iCycler software was used.

2.30 Purification of PCR products

PCR products were purified in order to remove reaction mix components that could disrupt subsequent DNA measurements, cloning and sequencing. Purification was achieved by using the QIAquick PCR purification Kit according to the manufacturer´s instructions. Elution of DNA was carried out by placing the spin column into a clean reaction tube, adding 30 µl H_2O_{dd} to the center of the membrane and centrifugation for 1 min at maximum speed.

2.31 DNA Sequencing

PCR products were sequenced by Christian Baranyi using an ABI 3130*xl* DNA sequencer and the BigDye Terminator Cycle Sequencing Kit v3.1 (Applied Biosystems). This kit is based on Sanger's chain-termination dideoxynucleotide method for sequencing, leading to termination of DNA synthesis after incorporation of a di-deoxynucleotide (ddNTP). The mix contains deoxynucleotides (dNTPs) as well as ddNTPs linked to different fluorescent dyes. Incorporation of a ddNTP results in termination of DNA synthesis, caused by lacking of the 3'OH-group which is necessary for elongation of the strand by DNA polymerase. DNA-fragments of different sizes are separated electrophoretically and recognized by a laser. The same primers as for standard PCR analysis were used at a concentration of 10 pmol/µl. Proof-reading of the sequences had to be done manually using the FinchTV software and subjected to BLAST search (http://blast.ncbi.nlm.nih.gov/Blast.cgi).

The porin sequences analyzed during this work all consist of a length of about 1000 bp, thus, they all required sequencing from both directions to finally obtain a reliable sequence. After proof-reading of the output data of DNA sequencing the corresponding forward and reverse sequences were put together and translated into the amino acid sequence. The obtained sequence was compared to the original genomic data of the analyzed gene.

2.32 2-Step-Cloning of gene amplificates

2.32.1 Vectors and vector maps

Table 18. **Vectors used in this study**

Plasmid	Manufacturer	Size	Characteristics	Antibiotic resistance	Addition of bases for primer desgin
pet21b	Novagen	5442 basepairs (bp)	10x His-Tag at C-terminus T7 promoter	Ampicillin	+1
pet16b	Novagen	5711 bp	10x His-Tag at N-terminus T7 promoter	Ampicillin	-

pQE-30	Qiagen	3461 bp	6x His-Tag at N-terminus T5 promoter *E. coli* M15 for overexpression	Ampicillin	+1
pgEX-4T-3*	Amersham	4968 bp	Glutathion-S-Transferase (GST)-Tag at N-terminus tac promoter	Ampicillin	+2
TOPO XL	Invitrogen	3519 bp	M13 binding sites	Kanamycin	-

*Gene expression using the vector pgEX-4T-3 leads to a fusion of the N-terminus of the expressed gene with the GST-tag. This GST-tag has a molecular weight of 26 kDa, therefore a band of higher molecular weight had to be expected for the fusion protein (Table 20).

All vetor maps (Figure 6 - Figure 9) were produced by using the software “Clone Manager”. The Ampicillin-resistance gene and the tag are marked with red arrows, the multiple cloning site (MCS) with a blue square. Not all restriction sites were included in the vectors maps.

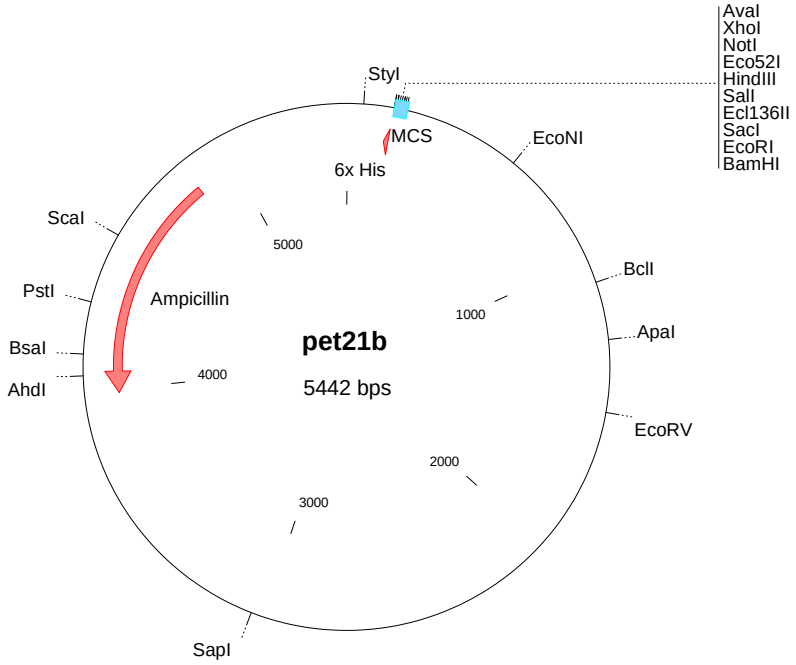

Figure 6. Vector map of the empty expression vector pet21b

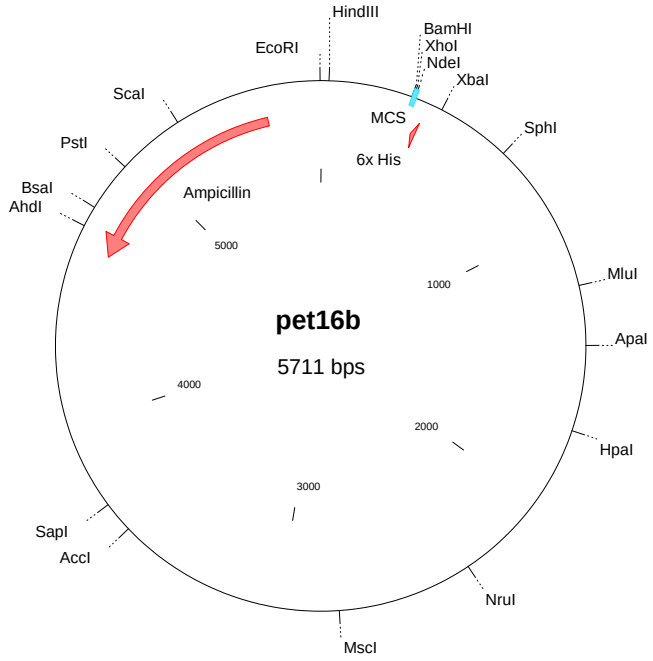

Figure 7. Vector map of the empty expression vetor pet16b

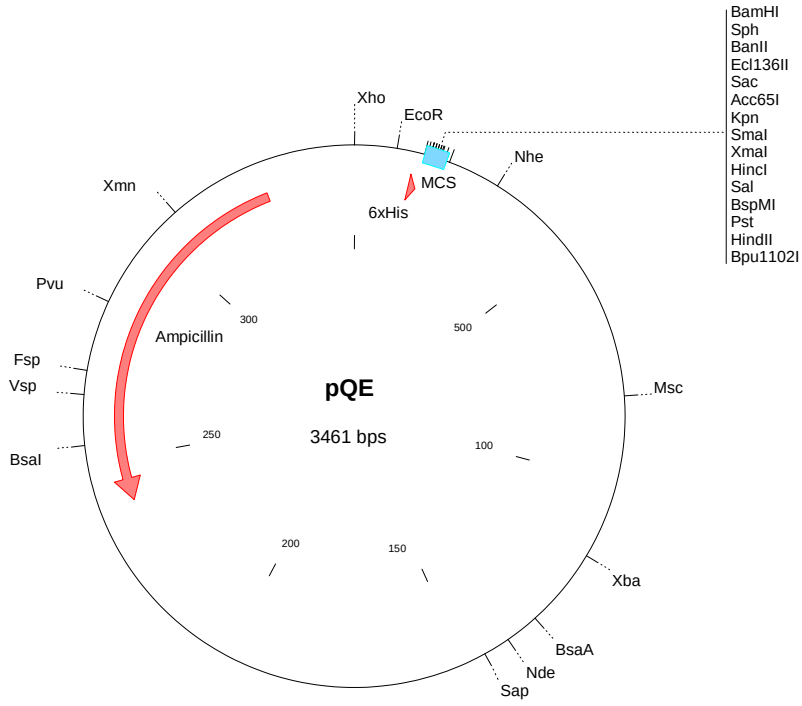

Figure 8. Vector map of the empty expression vector pQE-30

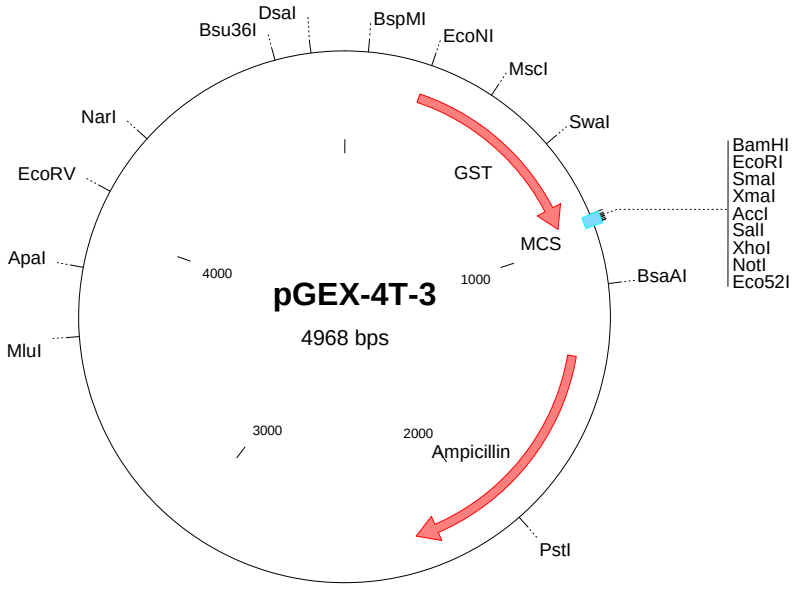

Figure 9. Vector map of the empty expression vector pgEX-4T-3

2.32.2 *E. coli* strains

Table 19. Competent *E. coli* strains used in this study

Strain	Source	Genotype	Reference/ Source	Comment
TOP10	Invitrogen	*F- mcrA _(mrrhsdRMS-mcrBC) Φ80lacZ_M15_lacX74 recA, ara139 _(araleu), 7697 galU galK rpsL (StrR) endA1 nupG*	TOPO® XL cloning kit	chemical competent
BL21 (DE3)	Stratagene	F– *ompT hsdS*B(rB– mB–) *gal dcm* (DE3)	(Studier and Moffatt, 1986)	*
C43 (DE3)	Avidis	F- *dcm ompT gal hsdSB* (rB- mB-) *lon* _DE3	(Miroux and Walker, 1996)	for overexpression of outer membrane proteins *
M15 [pREP4]	Qiagen	derived from *E. coli* K12 - NaIS, StrS, RifS, Thi–,Lac–, Ara+, Gal+, Mtl–, F–, RecA+, Uvr+, Lon+.	(Blattner *et al.*, 1997)	for overexpression of proteins cloned into the vector pQE-30 *
Rosetta (DE3) pLysS	Novagen	F– *ompT hsdS*B(rB– mB–) *gal dcm* (DE3) pLysSRARE2 (CamR)	(Kane, 1995)	encodes rare codons *
XL1blue	Stratagene	*recA1 endA1 gyrA96 thi-1 hsdR17 supE44 relA1 lac [F´ proAB lacIqZΔM15 Tn10 (Tetr)]*	(Bullock, 1987)	for maintenance of recombinant plasmids*

*electrocompetent *E. coli* strain

All *E. coli* strains described in Table 19, except *E. coli* TOP10, were available as electrocompetent cells (Miller and Nickoloff, 1995). The strain XL1blue was used for amplification, preparation and maintenance of vectors and recombinant plasmids. The other strains are common expression strains suitable for heterologous expression of proteins.
All used expression strains feature a protease-deficiency in order to prevent degradation of the heterologously produced proteins. The *E. coli* strain C43 features a dampened overexpression rate favorable for expressing outer membrane proteins.

2.32.3 Preparation of PCR-products

After amplification of the genes of interest using the High Fidelity polymerase and the specific primers (Table 13 and Table 14), reactions were controlled on an agarose gel, pooled and finally purified using the QIAquick PCR Purification Kit.

Table 20. Sequence length and molecular weight of the four members of the putative porin family

Porin	Sequence length (bp)	Protein size (kDa)	Protein fused with GST-tag (kDa)	Leader sequence (bp)	cut between amino acid
pc0870	891	34	60	60	21 + 22
pc1077	1038	39	65	66	20 + 21
pc1489	945	36	62	63	21 + 22
pc1860	978	37	63	60	22 + 23

2.32.4 TOPO™ XL cloning

The purified PCR products were cloned using the TOPO® XL Cloning Kit following the manufacturer`s instructions. Transformed *E. coli* TOP10 cells were grown on LB+Kan plates at 37°C o/n.

2.32.5 Screening for recombinant clones – Insert screening via M13 PCR

The recombinant cells, grown on LB+Kan cells, were screened for the presence of a plasmid containing the desired PCR-product as insert.

For M13-screening 10 to 20 clones of each *E. coli* transformation were picked and screened with the primer pair M13 R+F (Table 11). The primers bind to the flanking regions of the insert site on the vector, therefore allowing amplification of the insert and finally an estimation of the insert size. The reaction mix and the conditions were the same as for standard PCR except the volume of $Aqua_{bidest.}$. Recombinant *E. coli* cells were used as template. Therefore, a colony was picked using a sterile toothpick, stroke out on a masterplate and suspended in 25 µl of PCR water. After adding the PCR reaction mixture the microtiterplate was sealed with a thermostable foil and PCR was started.
PCR products were analyzed on a 1% agarose gel to detected clones with an insert of correct size for further analyses. Selected PCR products were sequenced as described in 2.31.

2.32.6 Double digestion of recombinant plasmids

Plasmids containing a validated insert were digested using the according restriction enzymes and buffers (see Table 7 and Table 8).

Digestion reaction mixture

Vector	2 µg
Buffer, see Table 8	2.5 µl
Enzyme, see Table 7	0.5 µl
H_2O_{dd}	up to 25 µl

The reaction mixture was incubated for 3 hours in a water bath at the appropriate temperature. Afterwards the temperature was shifted to 65°C for 20 min leading to inactivation of the restriction enzyme. Next, the second enzyme was added following the same procedure, including an incubation and an inactivation step.

2.32.7 Double digestion of empty vectors

The empty expression vector was isolated as described in 2.20.2 and digested with the same restriction enzymes as the corresponding PCR product. The same digestion procedure was conducted as for double digestion of recombinant plasmids.

2.32.8 Ligation of empty vectors and target gene amplificates

The PCR-products as well as the vectors were cut with the according restriction enzymes resulting in complementary ends of the vector and the PCR-product. This complementary ends were necessary for ligation and correct insertion direction of the PCR-product into the vector.

Since double digestion produced sticky ends, a ligation reaction using T4-DNA-ligase could be performed. In order to ensure an excess of PCR products compared to the vector, a ratio of 3:1 (insert:vector) was used.

Ligation reaction mixture (20 µl)

5x Ligase Buffer	4 µl
ATP	1 µl
Vector, double digested	x µl
Insert, double digested	x µl
T4 DNA Ligase	1 µl
H_2O_{dd}	up to 20 µl

The reaction was incubated at 4°C o/n.

In order to stop ligation and to get rid of ions, dialysis against H_2O_{dd} was performed for 20 min by using a nitrocellulose filter (pore size 0.025 µm).

2.33 Transformation of electrocompetent E. coli *cells*

One common method for the transformation of plasmid DNA into bacterial cells is electroporation. The bacterial cell membrane gets permeable for charged molecules by a short electric impulse.

Solutions

SOC medium

electrocompetent *E. coli* cells (Table 19)

Procedure

The dialyzed ligation reaction was used for transformation of electrocompetent *E. coli* XL1blue cells. Cells were thawed on ice for 10 min and then 5 µl of the ligation reaction were added. After stiring carefully, the cells were incubated on ice for 30 min, followed by electroporation. The electrical impulse was carried out at the following parameters: voltage of 2.5 kV, capacity of 25 mF, resistance of 200 Ω, with a time for the electric discharge of 4.5 to 5 msec.

After electroporation, 250 µl of SOC medium were added and the suspension was incubated for 1 h at 37°C on an orbital shaker. Finally, 100 and 150 µl of the suspension were plated on LB plates containing the appropriate antibiotics depending on the vector and the *E. coli* strain. The plates were incubated at 37°C o/n.

2.34 Identification of positive clones – Insert screening via T7/ pQE/ pgEX PCR

Screening for positive clones was done as described in 2.32.5, except of using the primer pairs T7/ pQE/ pgEX R+F (Table 11) instead of the M13 primers.

2.35 Heterologous expression of proteins in different E. coli strains

Extraction of sufficient amounts of protein from a homologous system is difficult in general. To address this problem, proteins are expressed in a heterologous expression system, like *E. coli*. Vectors and *E. coli* strains used for the heterologous expression of target genes are listed in Table 18 and Table 19.

Table 21. **Optimal conditions for successful porin overexpression in the vectors pQE-30 and pgEX-4T-3**

pc0870

Vector	***E. coli* strain**	**Leader sequence**	**Tag**
pQE 30	M15	no	His
pgEX	C43	yes	GST

pc1077

Vector	*E. coli* strain	Leader sequence	Tag
pQE 30	M15	no	His
pgEX	C43	yes	GST

pc1489

Vector	*E. coli* strain	Leader sequence	Tag
pgEX	C43	yes	GST

pc1860

Vector	*E. coli* strain	Leader sequence	Tag
pQE 30	M15	OmpT	His
pgEX	C43	yes	GST

Solutions

LB medium

TB medium

IPTG stock solution

Procedure

For protein overexpression, 5 ml of LB medium containing the suitable antibiotics were inoculated with an o/n culture of an *E. coli* expression strain containing the recombinant plasmid. Cells were grown at 37°C on an orbital shaker for 2 hours or until an OD of 0.5-0.6 was reached. Protein expression was induced by adding IPTG to a final concentration of 1 mM in the medium. A negative control without IPTG induction was prepared in parallel and both approaches were incubated on an orbital shaker for 2, 4 or 6 hours at 37°C or 20°C.

1.5 ml of cell suspension were harvested by centrifugation (7323x g, 10 min, 4°C). The cell pellet was either stored at -20°C until further analysis or directly resuspended in 4x SDS-PAGE loading buffer for loading on an SDS-PAGE gel.

For protein purification (2.36) larger amounts of induced cell culture were required. Therefore, cells were grown in 300 ml or 1 l of liquid medium, depending on the rate of the overexpression at small scale.

2.36 Purification of His-tagged proteins

The 6x histidine tag (His-tag) encoded on the vector or the primer and located at the N-terminal part or C-terminus of the expressed protein allows the purification of the expressed protein via immobilized metalaffinity chromatography.

Solutions

Binding buffer (20 mM Imidazol)

25x Protease Inhibitor

Benzonase

Elution buffers A/B/C/D (60 /100/300/500 mM Imidazol)

20% Ethanol

8M Urea

2.36.1 Sample preparation from *E. coli* cell cultures for purification of His-tagged proteins

Protein overexpression in *E. coli* might result in aggregation of inclusion bodies containing the desired protein. Hence pre-experiments with and without urea had to be done prior to the final purification in order to determine if urea had to be included in all the buffers for purification.

For protein purification larger amounts of cell cultures (up to 1 l) were required. Cells were grown in liquid media and overexpression was induced as described above (2.35).
After harvesting of the cells pellets were resuspended in 5-10 ml binding buffer per 1g cell pellet and treated with protease inhibitor to prevent protein degradation. The suspensions were pooled in a 50 ml Greiner tube and sonicated 5 times for 1 min with 0.9 sec pulse and 60-70% power. During sonication, the cell suspension was kept on ice. Volume was adjusted to 10 ml by adding binding buffer and additionally 100 µl protease inhibitor. After centrifugation (7323x g, 30 min, 4°C) the supernatant was used for further analysis.

2.36.2 Purification of His-tagged proteins using Amersham HisTrap HP Columns

This protocol is based on protein binding to a Ni^{2+} matrix via the His-tag of the overexpressed proteins. The Amersham HisTrapHP column was used according to the manufacturer`s instructions.

Protein elution was achieved by the addition of increasing concentrations of imidazole, which features a strong chelating nature and therefore competes with the proteins for binding to the matrix.
Protein purification was performed following the instructions of the manufacturer using 8 M urea if necessary.
Collected fractions were controlled on a SDS-PAGE gel and the fraction containing the highest amount of protein according to the band intensities was chosen.

2.37 Dialysis and precipitation of purified protein fractions

As 8M urea and imidazol could be harmful for animals during antibody generation, the selected protein fractions were dialyzed and finally precipitated.

Solutions

1x PBS
ice-cold acetone

Procedure

Fractions of eluted proteins that had been collected during protein purification were transferred to a dialysis tube for dialysis against 1x PBS. The first 30 min of dialysis were carried out at room temperature on a magnetic stirrer, followed by buffer change and continuing dialysis at 4°C o/n.
Ice-cold acetone was added at a ratio of 4:1 to the dialyzed fractions and proteins were precipitated for at least 6 hours or o/n at -20°C.
Finally, the precipitated proteins were harvested by centrifugation (10621x g for 15 min at 4°C), resuspended in an appropriate amount of 1x PBS and stored at 4°C.

2.38 Quantification of purified proteins with the BCA™ Protein Assay Kit

Protein concentrations were measured using the BCA™ Protein Assay Kit following the manufacturer`s instructions. This Kit is based on the use of bicinchoninic acid (BCA) for the colorimetric detection and quantification of total protein.

It combines the reduction of Cu^{2+} to Cu^{1+} by proteins in an alkaline medium with the colorimetric detection of the cuprous cation (Cu^{1+}). The purple-colored reaction product of this assay is formed by the chelation of two molecules of BCA with one Cu^{1+}.

Procedure

Standards were prepared as suggested by the manufacturer. The protein content of different fractions was determined using the enhanced protocol, implying incubation of protein samples and reagent for 30 min at 60°C according to the manufacturer's instructions. All standards as well as the samples were measured at a wavelength of 562 nm with a spectral photometer. After plotting a standard curve of known protein concentrations, this curve was used to determine the unknown protein concentration of the samples.

All measurements were performed in duplicates using the mean absorbance for the determination of protein concentrations.

2.39 Sample preparation for the identification of proteins by mass spectrometry

In order to guarantee the identity of proteins which were present in the bands of SDS-PAGE gels after His-trap purification, bands of interest were excised from the gel. The samples were prepared and analyzed by linear quadrupole ion trap mass spectrometry (LTQ).

Solutions (all buffers and solutions were prepared right before use)

10% (v/v) and 0.1% (v/v) trifluoroacetic acid (TFA)

50 mM ammonium bicarbonate (ABC)

Acetonitrile (ACN)

Alkylation buffer (10 mg/ml iodacetamide in 50 mM ABC)

Destaining solution (100 µl 50 mM ABC + 80 µl ACN)

Reduction buffer (10 mM DTT in 50 mM ABC)

Trypsin gold working solution:

Trypsin gold was dissolved in 50 mM acetic acid to yield a concentration of 100 ng/µl and aliquots were stored at -80°C. Immediately before use, one aliquot of 10 µl was thawn and diluted by addition of 70 µl ABC-buffer leading to a final concentration of 12.5 ng/µl.

Procedure

All incubation steps were performed on a rocking platform at room temperature (RT), if not stated otherwise.

Bands of interest were excised from Coomassie stained SDS-PAGE gels, transferred to screw caps and either stored at -80°C until further use or processed immediately for mass spectrometry. Gel bands were cut into small pieces, washed three times in 200 µl H_20_{dd} and destained by adding 100 µl destaining solution. This solution was replaced every 15 min, resulting in a completely destained gel. Thereafter, the gel pieces were incubated for 5 min in acetonitrile. ACN was removed and bands were vacuum-dried for 5-10 min at room temperature.

The disulfide bonds of the proteins were reduced by using 200 µl reduction buffer for 30 min at 56°C, followed by incubation in 160 µl ACN for 5 min. ACN was removed and 100 µl iodacetamide were added causing alkylation of the proteins. After 20 min incubation in the dark the samples were washed 3 times with 200 µl ABC, gel bands were dehydrated with 160 µl ACN and vacuum-dried.

20 µl trypsin gold working solution were added to each dried sample and rehydration was carried out for 10 min at 4°C. Afterwards, residual trypsin solution was removed, samples were covered with ABC-buffer and tryptic digestion was performed overnight at 37°C (12-16 h). The reaction was stopped by addition of 2 µl 10% TFA resulting in 1% final TFA concentration.
Peptides were extracted by sonication for 10 min in a cooled sonication waterbath. The peptide solution was transferred to a clean tube and the sonication step was repeated by adding 10 µl 0.1% TFA to the sample. The peptide extracts were pooled and stored at -80°C prior to nano-liquid chromatography matrix-assisted laser desorption-ionization (MALDI) - time of flight (TOF)/TOF (nanoLC-MS/MS) analysis.

2.40 Protein analysis by nanoLC-MS/MS

Chromatographic separation of peptides and measurements were carried out at the Institut für Biochemie und molekulare Zellbiologie der Universität Wien at the Vienna Biocenter by Dr. Dorothea Anrather.

For protein identification MS/MS spectra were matched against a custom designed database with Mascot version 2.2 (Matrix Science, London, UK). This database contained the protein sequences of *P. amoebophila* UWE25 and protein sequences availabe for other environmental chlamydiae. Since protein sequences of the host should also be considered, all availabe protein sequences for *E. coli* were included. Additionally a list of sequences of frequently found contaminants in MS samples, like trypsin, keratins and BSA, was included.

2.41 Lipid bilayer measurements

Lipid-bilayer measurments were performed at the laboratory of Prof. Roland Benz (Germany) according to previous studies (Hunten *et al.*, 2005). After overexpression, purification and precipitation, the samples containing pc1077 and pc0870 were diluted 1:100 in 1 % Genapol.

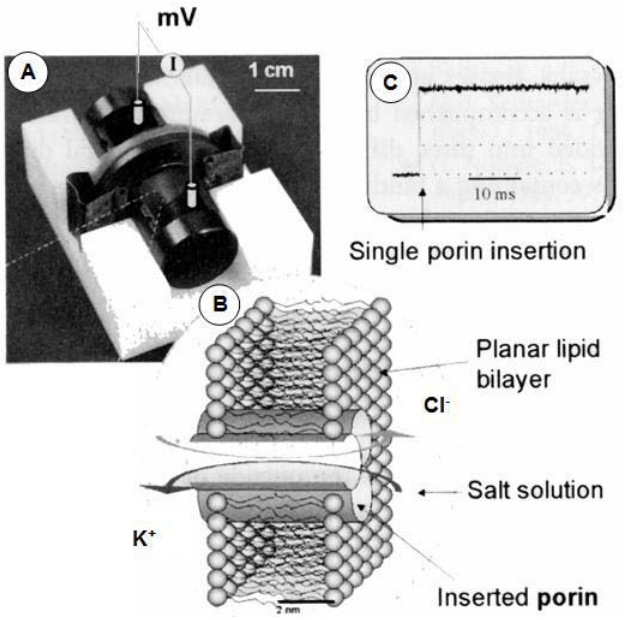

Figure 10. Principle of lipid bilayer measurements. This technique is based on measurements of conductance, which increases if a channel-forming protein is incorporated in an aritificial lipid-bilayer (Fig.9, B and C). The used apparature consists of two chambers (cis- and trans-chamber) which are connected by a small circular hole (Fig.9, A). Across this hole an artificial lipid-bilayer is formed, the protein to be investigated is added and pore-formation in the membrane is measured. Modified from (Benz, 2004).

2.42 Antibody generation against purified proteins

Antibodies were produced by Eurogentec (Seraing, Belgium). Depending on the immunization program and the included animal different amounts of protein were needed for the immunization, including a first immunization and three additional boosts.

Primary antibodies against the protein DnaK were raised in both chicken and guinea pig. Approximately 400 µg of the purified protein were used for the immunization of a chicken and 300 µg for 2 guinea pigs. Primary antibodies against the porin pc1077 were obtained from an immunization program containing 2 rabbits. For this purpose, 800 µg of purified and dialyzed protein were needed in total.

Pre-immune sera and pre-immune egg yolks obtained before the first antigen boost were provided as negative controls. Rabbit and guinea pig sera as well as egg-yolks were collected throughout the program. After the immunization program for the chicken and the rabbits had officially finished, an additional boost was ordered to improve the specificity and concentration of the generated antibodies.

2.43 Purification of antibodies using a HiTrap™ IgY Purification HP column

Solutions

- **Binding Buffer**

NaH_2PO_4	3.12 g
K_2SO_4	87.13 g
H_2O_{dd}	ad 1000 ml
pH 7.5	

- **Elution Buffer**

NaH_2PO_4	3.12 g
H_2O_{dd}	ad 1000 ml
pH 7.5	

- **Cleaning Buffer**

NaH_2PO_4	3.12 g
Isopropanol	300 ml
H_2O_{dd}	ad 1000 ml
pH 7.5	

Procedure

IgY antibodies from the pre-immune egg yolks as well as from the consecutive egg yolk collections were purified with the help of a HiTrap™ IgY Purification HP column according to the manufacturer´s instructions except that just 6 column volumes instead of 10 were used as elution volume in order to get a higher concentration of antibodies in the eluat.

According to the protocol using a pump and 50 ml syringes, the required buffer volumes were filled into a syringe, which was then inserted into a pump and fixed. With the help of a flexible tube and adaptors, the respective buffers were passed through a 1.2 µm and a 0.45 µm filter and loaded onto the column. The adjustments of the pump had to be set according the following parameters: rate: 5 ml/min, diameter of the 50 ml syringe: 27.8 mm.

2.44 Inactivation of antibodies targeting amoeba proteins

Amoebae are ubiquituous, hence a contamination of the sera with antibodies against amoebal proteins was considered. To avoid unspecific background in immunofluorescence experiments due to amoeba antibodies, all obtained sera were inactivated first against amoeba proteins.

2.44.1 Preparation of amoeba lysate

Solutions

FA-block solution

10x PBS	100 ml
Bovine Serum Albumine (BSA)	20 g
H_2O_{dd}	ad 1000 ml

Aliquots can be stored at -20°C until further use. Upon thawing aliquots were stored at 4°C.

Procedure

An *A. castellanii* Neff culture containing no endosymbiont was harvested by centrifugation (5 min, 7323x g) and the pellet was resuspended in 500 µl – 1 ml FA-block solution, depending on the size of the pellet. In order to break up amoeba cells, the suspension was either sonicated 4 times for 30 seconds or treated with two freeze-and-thaw steps (freezing at -20°C/ thawing at 42°C in a water bath). The resulting lysate was stored at -20°C and when needed, thawed at 37°C in a water bath.

2.44.2 Blocking of antibodies

Antibody sera were mixed 1:1 with amoeba cell lysates, vortexed briefly and incubated at 4°C o/n. On the following day the solution was mixed again and incubated for another 30 min at 4°C. Amoeba cell debris which had bound the host-reactive antibodies was removed by centrifugation for 2 min at 6797x g. The supernatant containing the unbound protein-specific antibodies was transferred to a new tube and used for further analysis.

2.45 Fixation of cells

Fixation of the samples is an essential step to preserve the morphology of cells for microscopic examination. The fixative to be used depends on the cell type that should be analyzed.
In this study, cells were fixed either with PFA, which cross-links cell constituents, thereby stabilizing the cells, or with Methanol.

2.45.1 Cell fixation with 4% PFA

Solutions

4% PFA

1x PBS

Procedure

A 24-well plate was prepared by placing round steril cover slips into each well. A well grown 10 ml amoeba culture, either uninfected or harboring chlamydial endosymbionts, was harvested by shaking.

1 ml of cell suspension was pipetted into each well of the 24-well plate and the amoeba cells were allowed to attach to the surface of the cover slip o/n.
On the next day, the medium was aspirated off and each well was washed with 500µl 1x PBS. Then 500 µl 4% PFA were added and cells were fixed for 1 h at RT. After this incubation the fixative was removed, each well was washed once with 1x PBS and fixed cells were stored in 1x PBS up to 2 weeks at 4°C.

2.45.2 Cell fixation with Methanol

Solutions

Methanol

1x PBS

Procedure

The amoebal cells were prepared in the same way as for cell fixation with 4% PFA, with the exception that the cells were fixed for 10 min with methanol.

2.46 Primary and secondary antibodies

The immunofluorescence (IF) technique used is an indirect assay. The antigen-specific primary antibody is not fluorescently labeled but the secondary antibody, which binds to the primary antibody, is conjugated to a fluorescent dye.
The optimal dilutions of the primary antibodies were determined empirically using several dilutions.

Table 22. **Primary antibodies used in this study**

Primary antibody	Antigen	Source of antibody	Dilution	Reference/ Manufacturer
anti -Pam	*P. amoebophila* elementary bodies	rabbit	1 : 2000	(Heinz, 2008)
anti -Pam	*P. amoebophila* elementary bodies	chicken	1 : 2000	(Heinz, 2008)
anti- DnaK	pc1499, overexpressed in *E. coli*	guinea pig	1 : 2000	this study
anti- DnaK	pc1499, overexpressed in *E. coli*	chicken	1 : 1000	

preI DnaK (pre-immune serum)	none	guinea pig	1 : 2000	this study
preI DnaK (pre-immune serum)	none	chicken	1 : 1000	
anti- pc1077	pc1077 without leader sequence	rabbit	immunization program not fnished at the end of this work	
preI pc1077	none	rabbit		
anti- GST	Glutathion-S-Transferase	rabbit	1:10000	Sigma-Aldrich Chemie GmbH, Steinheim, Germany
anti- His	Histidine	mouse	1 : 1000	Novagen, Darmstadt, Germany
anti- Hsp60	Hsp60 of *Chlamydophila caviae* GPIC	guinea pig	1 : 2000	(Yuan *et al.*, 1992)
anti- pc1489	pc1489 purified from EBs	chicken	1 : 2000	(Aistleitner, 2009)

Table 23. Secondary antibodies used in this study

Secondary antibody	Antigen	Modification	Source of antibody	Dilution	Manufacturer
anti- chicken	chicken IgY	Cy3	donkey	1 : 1000	Dianova GmbH, Hamburg, Germany
anti- chicken	chicken IgY	Cy2	donkey	1 : 1000	
anti- chicken	chicken IgY	HRP	goat	1 : 10000	
anti- guinea pig	guinea pig IgG (heavy chains)	Cy3	goat	1 : 1000	
anti- guinea pig	guinea pig IgG (heavy chains)	Cy2	goat	1 : 1000	
anti- guinea pig	guinea pig IgG (heavy chains)	HRP	goat	1 : 10000	
anti- rabbit	rabbit IgG	FITC	goat	1 : 1000	
anti- rabbit	rabbit IgG	Cy5	goat	1 : 10000	
anti- rabbit	rabbit IgG	Cy3	goat	1 : 1000	
anti- rabbit	rabbit IgG	Cy2	goat	1 : 1000	GE Healthcare Bio-Sciences AB, Uppsala, Sweden

anti- rabbit	rabbit IgG	HRP	goat	1 : 500000	Sigma-Aldrich Chemie GmbH, Steinheim, Germany
anti- mouse	mouse IgG Fc fragment	HRP	goat	1 : 10000	

Cy3: Indocarbocyanine
Cy2: Carbocyanine
Cy5: Indocarbocyanine
FITC: Fluorescein
HRP: Horseraddish-Peroxidase

2.47 Indirect immunofluorescence assay

The assay was performed with amoebal cultures containing chlamydial endosymbionts. Amoebae, devoid of endosymbionts, were used as negative controls.
Pre-immune sera, which were obtained prior to immunization of the respective animal, were tested to verify the specificity of the antibodies.

Solutions

1x PBS

10 mM Tris-HCl (pH 6.5)

0.05% Tween™ 20 in 1 x PBS

4% PFA

FA-block solution

Mowiol:

2.4 g Mowiol 4-88 were mixed with 6 g glycerine and 6 ml H_2O_{dd}. After adding 12 ml 0.2 M Tris-HCl (pH 8.5) the solution was stirred at 50-60°C until the Mowiol had dissolved completely. The solution was centrifuged at 7700x g for 15 min to remove air bubbles and the supernatant was collected and stored in aliquots at -20°C until further use.

Procedure

The following steps were performed at RT and all incubation steps were carried out on a shaking platform.
Already fixed cells were used for immunofluorescence analysis. Using methanol as a fixative, the cells could be directly incubated with 500 µl FA-block solution, whereas PFA fixed cells had to undergo a pre-treatment to permeabilice the cells.

1x PBS was removed and cells were incubated in 300 µl 0.05% Tween^{TM} 20 in 1x PBS for 25 min. After removing Tween from each well, 300 µl 10 mM Tris-HCl containing 5 µg/ml lysozyme were added and cells were incubated for 1 h. The permeabilized PFA fixed cells as well as the methanol fixed cells were covered with 500 µl FA-block solution in order to block unspecific binding sites. The blocking solution was initially replaced by the primary antibody (Table 22), appropriately diluted in FA-block solution, and incubated for 1 h to allow specific binding of the antibody. Cells were washed 3 times with 500 µl 1x PBS, followed by addition of the secondary antibody (Table 23), diluted in FA-block solution. After another hour of incubation in the dark, the secondary antibody was finally removed and the cells were again washed with 1x PBS as before. The cover slips were embedded in 1.5 µl Mowiol, placing the cover slips face-down on a glass slide, and stored in the dark at RT until further analysis by epifluorescence microscopy.

2.47.1 Immunofluorescence analysis of *E. coli* cells

Solutions

Methanol

4% PFA

FA-block solution

1x PBS

Citifluor

Procedure

Fixation of *E. coli* cells was carried out as described in 2.45 using a multiwell microscopic slide for fixation. 15 µl aliquots of *E. coli* cultures were pipetted onto one well, incubated for 20 min and finally fixed with the desired fixative.

The procedure for immunofluorescence was carried out as already depicted in 2.47, with the slight modification that incubation steps were not performed on a shaking platform but in a humid chamber. Furthermore, washing steps were reduced to one time washing with 1x PBS. Antibodies against the GST tag of overexpressed proteins and against general outer membrane structures of *P. amoebophila* are listed in Table 22.

Finally, slides were dried and stored in the dark until further analysis by epifluorescence microscopy. Slides were embedded in Citifluor and then stored at 4 °C.

2.48 Sodium dodecyl sulfate polyacrylamide gel electrophoresis (SDS – PAGE)

Solutions

- **Lower buffer**

Tris – HCl	90.8 g
10% (m/v) Sodium dodecyl Sulfate (SDS)	20 ml
H_2O_{dd}	ad 500 ml
pH 8.8	

- **Upper buffer**

Tris - HCl	30.3 g
10% SDS	20 ml
H_2O_{dd}	ad 500 ml
pH 6.8	

- **10 x SDS-PAGE running buffer**

Tris - HCl	30.2 g
Glycine	144 g
SDS	10 g
H_2O_{dd}	ad 1000 ml

- **4 x SDS - PAGE loading buffer**

Tris-HCl pH 6.8	2.42 g
SDS	8 g
Bromphenolblue	0.02 g
Glycerol	40 µl
Dithiothreitol (DTT)	6.2 g
H_2O_{dd}	ad 100 ml

Procedure

First, a 12.5% polyacrylamid gel was prepared according to the following standard protocol for 2 small gels:

Separating gel	
Lower buffer	2 ml
H_2O_{dd}	2.66 ml
Rotiphorese®NF-30%(w/v) Acrylamide/Bisacrylamide-solution	3.33 ml
10% (w/v) Ammoniumpersulfat (APS)	40 µl
N,N,N´,N´-tetramethylethane-1,2-diamine (TEMED)	8 µl
Stacking gel	
Upper buffer	0.63 ml
H_2O_{dd}	1.63 ml
Acrylamid/bisacrylamid solution	0.38 ml
10% APS	17.5 µl
TEMED	10 µl

For gel preparation four glass plates were set up in a BioRad Mini-PROTEAN casting stand. First, the separating gel was prepared. APS and TEMED were added at last to initiate polymerization. The solution was poured between two glass plates to about 3 cm below the rim and gels were overlayed with isopropanol to produce a smooth surface of the separating gel. After polymerization of the gel layer, the isopropanol was poured off and the stacking gel was prepared according to the standard reaction mixture. A layer of this solution was then applied on top of the separating gel and the combs were applied. Polymerized gels could either be wrapped in wet paper towels and saran wrap and stored at 4°C for a few days or used directly for SDS-PAGE.

For the separation of proteins, gels were inserted into a Mini-PROTEAN gel electrophoresis chamber filled with 1x SDS-PAGE running buffer. Pockets of the gel had to be rinsed shortly prior to application of the marker and the samples. Samples were heated to 95°C for 5 min before loading. Proteins were separated by applying a voltage of 60 – 110 V for 1.5 hours and the run was stopped when the marker front reached the bottom of the gel. The gel apparature was then dissembled and the stacking gel was removed from the separating gel.

2.48.1 Staining and destaining of SDS-PAGE gels using Coomassie brilliant blue staining solution

Solutions

- **Coomassie brilliant blue staining solution**

Methanol	500 ml
Acetic acid	100 ml
Coomassie Brilliant Blue G-250	2.76 g
H_2O_{dd}	ad 1000 ml

- **Destaining solution**

Acetic acid	50 ml
Ethanol	200 ml
H_2O_{dd}	ad 1000 ml

Procedure

After electrophoresis the separating gels were incubated in Coomassie brilliant blue staining solution for about 45 min on a rocking platform. Afterwards, the gels were transferred into destaining solution and destained on a rocking platform o/n. The gels were rinsed with H_2O_{dd} and digitalized by scanning.

2.48.2 Fixation, staining and destaining of SDS-PAGE gels using colloidal Coomassie staining solution

Solutions

- **Colloidal Coomassie solution**

$(NH_4)_2SO_4$	100 g
Orthophosphoric acid	20 g
Methanol	250 ml
Coomassie Brilliant Blue G-250	0.625 g
H_2O_{dd}	ad 1000 ml

- **Fixing solution**

Ethanol	800 ml
Acetic acid	200 ml
H_2O_{dd}	ad 2000 ml

Procedure

All following steps were carried out on a rocking platform.

The separating gels were first rinsed with H_2O_{dd} for 5 min, followed by incubation in fixing solution for about 20 min. Gels were rinsed 2 times for 10 min in H_2O_{dd} and stained with colloidal Coomassie o/n. Gels were destained by rinsing them 2 times for 30 min in H_2O_{dd} and finally scanned.

2.49 Western Blot analysis

Solutions

- **Transfer buffer**

Glycine	2.9 g
Tris-HCl	5.8 g
Methanol	200 ml
H_2O_{dd}	ad 1000 ml

- **10x TBS**

Tris-HCl	12.1 g
NaCl	43.8 g
H_2O_{dd}	ad 500 ml

pH 7.5; store at 4°C

- **1x TBS**

10 x TBS	100 ml
H_2O_{dd}	ad 1000 ml

- **TBS-T**

10x TBS	50 ml
Tween 20	0.5 ml
H_2O_{dd}	ad 500 ml

  store at 4°C

- **Developer and Fixer solution**

  SIGMA Kodak GBX Developer

  SIGMA Kodak GBX Fixer

  Developer and Fixer were diluted as recommended by the manufacturer

Procedure

Proteins were separated according to 2.48. Separating gels were equilibrated in transfer buffer for about 15 min. In the meantime a polyvinylidene fluoride (PVDF) membrane and 2 pieces of extra thick Whatman paper were cut to a size corresponding to the seperating gel. Since the PVDF membrane had to be activated, it was shaken in methanol for 5 min, followed by rinsing with H_2O_{dd} for 5 min. The membrane and the Whatman paper had to be equilibrated in transfer buffer for 5 min prior to building up the "blotting sandwich" (consisting of one piece of Whatman paper – membrane – gel – Whatman paper).
Transfer onto the membrane was performed by semi-dry blotting in a Trans-Blot® SD Semi-Dry Electrophoretic Transfer Cell, using settings as recommended by the manufacturer.

To prevent unspecific binding of antibodies, the membrane was incubated in 5% non-fat dry milk in 1x TBS on a rocking platform o/n. Blocking of the membrane was followed by incubation in 10 ml TBS-T containing the primary antibody (Table 22) for 1 hour. To remove excess primary antibody the membrane was washed 3 times in TBS-T for 15 min, followed by incubation in TBS-T with the corresponding HRP-labeled secondary antibody (Table 23) for 1 hour. After 3 additional washing steps for 10 min the membrane was treated with the Western Lightning Chemiluminesence Plus kit as recommended by the manufacturer. The membrane was exposed to a photographic film in the dark. The film was then developed with Developer Solution, fixed with Fixer Solution and washed in H_2O. Finally films were digitalized by scanning.

3 Results

3.1 Characterization of novel porins from P. amoebophila

3.1.1 Amplification of the genes encoding the putative porins pc0870, pc1077, pc1489 and pc1860, including changes in the leader sequence

After the design of specific primers (Table 13) for the genes of interest of *P. amoebophila*, a high-fidelity PCR was performed. Amplicons of the expected length were obtained for all genes, as listed in Table 20.

3.1.2 2-step cloning and clone screening

The four putative porins were cloned by following a 2-step cloning protocol (2.32). As a result, different constructs for overexpression experiments were obtained. Despite of low transformation efficiency, it was possible to verify at least two inserts with correct sequence and direction for each construct by several rounds of screening colonies from LB plates.

Figure 11 shows an example of pairwise alignment of the obtained sequence of pc1077 without leader sequence in comparison to the original sequence of pc1077 from the online environmental chlamydia genome database (http://mips.helmholtz-muenchen.de/genre/proj/uwe25/). All constructs used for further overexpression experiments showed at least 99.6 % amino acid sequence similarity.

```
                     10        20        30        40        50
Seq1              MRKILLTIMASLLSCSAAQAFWPEATDSSLEVGFGYRRDELKWKTRTGLD
                                        :::::::::::::::::::::::::::::
Seq2    FHTEFIKEEKLTMRGSHHHHHHGSACELGTFWPEATDSSLEVGFGYRRDELKWKTRTGLD
               50        60        70        80        90       100

               60        70        80        90       100       110
Seq1    SSDSGYSAASPFGAQSTLKWKNLNIWQIEARGEYVTCDNVYLRASGDYGWIVSGKNRDSD
        ::::::::::::::::::::::::::::::::::::::::::::::::::::::::::::::
Seq2    SSDSGYSAASPFGAQSTLKWKNLNIWQIEARGEYVTCDNVYLRASGDYGWIVSGKNRDSD
              110       120       130       140       150       160

              120       130       140       150       160       170
Seq1    YINAGEESQLEISRTHAKTRGHVYDVDVALGYQFKLCDDSFSVTPVVGYSWKGQHLKDRH
        ::::::::::::::::::::::::::::::::::::::::::::::::::::::::::::::
Seq2    YINAGEESQLEISRTHAKTRGHVYDVDVALGYQFKLCDDSFSVTPVVGYSWKGQHLKDRH
              170       180       190       200       210       220
```

```
               180       190       200       210       220       230
Seq1   LRFATSPIGESSSSSGLLRASSDYYDYSSSSSSSSSSNFHNRYNTRWNGPFVGVDFDYRI
       : ::::::::::::::::::::::::::::::::::::::::::::::::::::::::::
Seq2   LGFATSPIGESSSSSGLLRASSDYYDYSSSSSSSSSSNFHNRYNTRWNGPFVGVDFDYRI
               230       240       250       260       270       280

               240       250       260       270       280       290
Seq1   SCDLELFLDYEFHFAKYHAKADWKLRNDLPNGFHHRSKSSQGHVLDFGVKWDLDECWTLA
       ::::::::::::::::::::::::::::::::::::::::::::::::::::::::::::::
Seq2   SCDLELFLDYEFHFAKYHAKADWKLRNDLPNGFHHRSKSSQGHVLDFGVKWDLDECWTLA
               290       300       310       320       330       340

               300       310       320       330       340
Seq1   LKGGIQYFHARRGHDRSLVTKTEVGNVDTKCFVSIPLRDVKWCSGSVTFDVGMAF
       :::::::::::::::::::::::::::::::::::::::::::::::::::::::
Seq2   LKGGIQYFHARRGHDRSLVTKTEVGNVDTKCFVSIPLRDVKWCSGSVTFDVGMAFLQPSSTP
               350       360       370       380       390       400
```

Figure 11. **Output from PIR- protein pairwise alignment,** checking similarity of a sequence obtained after 2-step cloning of pc1077 to the original sequence of pc1077.
The Alignment shows 99.692% (= 1 mismatch, shown in red) identity (99.692% ungapped) in 325 aa overlap.

Seq1: pc1077, amino acid sequence obtained from the environmental chlamydia genome database
Seq2: obtained sequence for pc1077 without leader sequence in the vector pQE, translated into amino acids using the Expasy Proteomic Tools (http://www.expasy.ch/tools/dna.html)

M: Start-codon, HHHHHH: 6xHis-tag at N-terminus, derived from the vector, : start of sequence identity at amino acid 21, R-G: mismatch, STP Stop-codon
Abbreviations for amino acids are used according to the NC-IUB

3.1.3 Porin overexpression using different constructs in various *E. coli* strains

Vectors containing the correct porin sequence in-frame with the tag for purification were used for heterologous expression.

Different *E. coli* expression strains, temperatures, IPTG concentrations and media were used to create the optimal conditions for overexpression.

3.1.3.1 Overexpression in the vectors pet21b, pQE-30 and pet16b

The vector pet21b was first used for heterologous expression of the four porin candidates using different induction conditions, *E. coli* strains and media. Since this approach failed (Figure 12A), we used the vectors pQE-30 and pet16b for overexpression, again varying in the conditions for each approach (Table 24).

Table 24. Conditions used for overexpression of pc0870, pc1077, pc1489 and pc1860 in different expression vectors

Vector	Expression-culture media	IPTG concentration	Growing temperature of the expression culture	Harvest point	Pre-culture duration	*E. coli* strain
pet21b	LB	1 mM	37°C	6h	15 h o/n	BL21 (DE3)
	TB	0.5 mM	RT	4h	9 h o/n	C43
		0.1 mM				Rosetta (DE3)-pLysS
pQE-30	LB	1 mM	37°C	6 h	15 h o/n	M15
			37°C - RT*	3 h, 6 h		
			37°C - 20°C	3 h, 6 h		
pet16b	LB	1 mM	37°C - 37°C/20°C**	6 h	15 h o/n	BL21 (DE3)
		0.5 mM	37°C - 37°C/20°C	3h/6h**		
		0.2 mM	37°C - 37°C/20°C	3h/6h		

*37°C - RT: The *E. coli* culture was grown for 2 h at 37°C. Then expression was induced and the culture was grown at RT for 3 h or 6 h.
**37°C/20°C: After induction the expression culture was either grown at 37°C for 3 h or at 20°C for 6 h.

Although a lot of different constructs and conditions were tested, none of the four putative porins could be successfully overexpressed in these constructs. No difference between induced and non-induced cultures was detectable after IPTG induction and no band at the correct size (Table 20) could be obtained.

Some of the obtained negative results with the respective SDS-PAGE gels and Western blots are shown in Figure 12.

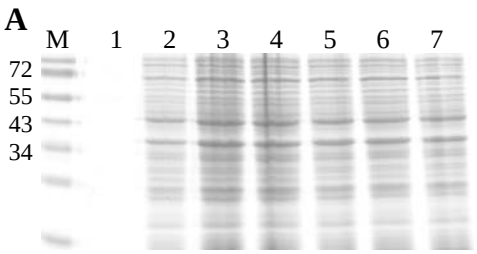

A. Porin overexpression of pc1489 in pet21b using *E. coli* Rosetta
M: prestained protein ladder (kDa), 1: empty, 2: *E. coli* protein lysate 4 h after induction of overexpression of pc1489 (pc1489 i.), 3: pc1489 i. for 6h, 4: *E. coli* protein lysate after 4 h of growing without induction of overexpression of pc1489 (pc1489 n.i.), 5: *E. coli* Rosetta without vector i. for 4h, 6: *E. coli* Rosetta without vector i. for 6h, 7: *E. coli* Rosetta without vector n.i.

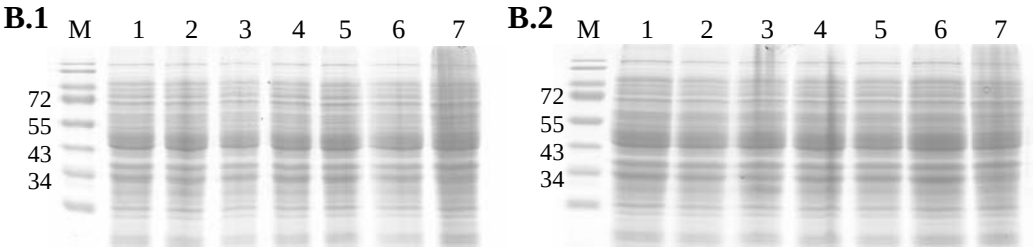

B. Porin overexpression of different constructs in pQE-30 using *E. coli* M15 comparing *E. coli* lysates 3h (B.1) and 6h (B.2) after induction
M: prestained protein ladder (kDa), 1: pc1860 i., 2: pc1860 n.i., 3: pc1077 i., 4: pc1077 n.i., 5: pc0870 i., 6: pc0870 n.i., 7: *E. coli* M15 without vector i.

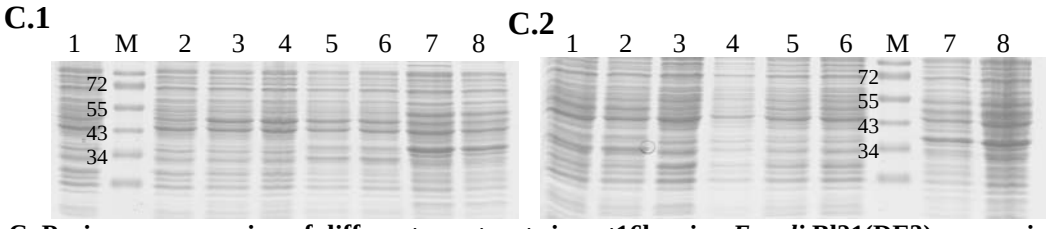

C. Porin overexpression of different constructs in pet16b using *E. coli* Bl21(DE3) comparing *E. coli* lysates 3h at 37°C (C.1) and 6h at 19°C (C.2) after induction
1: pc1077 i., M: prestained protein ladder (kDa), 2: pc1077 n.i., 3: pc1860 i., 4: pc1860 n.i., 5: pc0870 i., 6: pc0870 n.i., 7: *E. coli* BL21 (DE3) without vector i., 8: *E. coli* BL21 (DE3) without vector n.i.

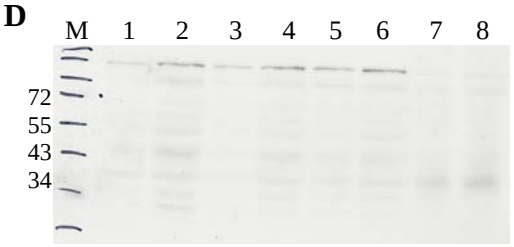

D. Verifying results of C.1 by Western blot analysis using anti-His antibodies. The film was exposed for 10 min. No bands of correct size were detected.
M: prestained protein ladder (kDa), 1: pc1077 i., 2: pc1077 n.i., 3: pc1860 i., 4: pc1860 n.i., 5: pc0870 i., 6: pc0870 n.i., 7: *E. coli* BL21 (DE3) without vector i., 8: *E. coli* BL21 (DE3) without vector n.i.

Figure 12. No detectable changes of expression levels after overexpression of the four putative porins in various *E. coli* strains (A, B, C, D).

3.1.3.2 Overexpression in the vector pgEX-4T-3 and effects of changes in the leader sequences of pc0870, pc1077 and pc1860

For further expression studies the vector pgEX was used, since this vector features a GST-tag with a molecular weight of 26 kDa suitable for masking toxic proteins in *E. coli*.
Gene expression form the vector pgEX-4T-3 results in a fusion of the GST-tag with the N-terminus of the porin. This fusion protein showed a higher molecular weight than the porin itself (Table 20).

Based on other studies (Findlay *et al.*, 2005), also changes in the leader sequence could have positive effects on the overexpression of porins. Special constructs were designed as described in 2.32 and used for additional expression experiments.
Heterologous expression was performed with constructs including or lacking a leader sequence and expression results were analyzed by SDS-PAGE and Western blot analysis.

Bands of the desired molecular weight could be observed on SDS-PAGE gels for pc0870 (Figure 13) and pc1077 (Figure 14) in both approaches and for pc1489 and pc1860 at least when using the vector pgEX (Figure 15 and Figure 16). For an additional identification of each porin fused to its tag, Western Blot analysis was performed detecting either the His-tag of the fusion-protein or the GST-tag with the help of HRP labeled antibodies. Since specific antibodies against pc1489 were available, they were also applied during Western blot analysis (Figure 15c).

Interestingly, results of Western blotting showed a possible processing of the porins, since additional bands at a molecular weight of ~26 kDa were detected, maybe displaying the cleavage of the leader sequence fused to the GST-tag at the N-terminus (Figure 13c and d, indicated by an arrow head).
Strong degradation effects were observed for pc1860 overexpressed in the vector pgEX (Figure 16c).

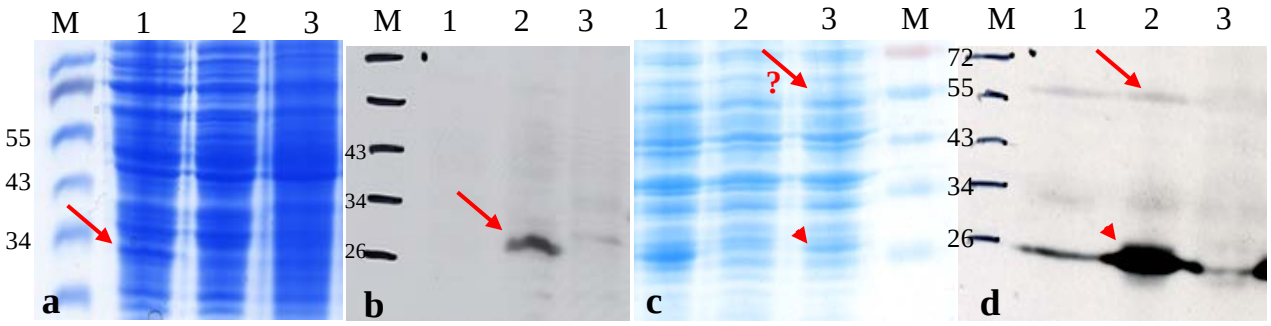

Figure 13. Overexpression of pc0870 checked by colloidal Coomassie staining and Western blot analysis

Bands of the correct and expected size are indicated by an arrow. Arrow heads indicate the possibly cut off leader sequence with the GST-tag.

a. Overexpression of pc0870 in pQE-30
M: prestained protein ladder (kDa), 1: *E. coli* protein lysate 4 h after induction of overexpression of pc0870 (pc0870 i)., 2: *E. coli* protein lysate after 4 h of growing without induction of overexpression of pc0870 (pc 0870 n.i.), 3: *E. coli* M15 without vector i.
b. Western blot analysis to verify overexpression of pc0870 in pQE-30 using anti-His antibodies. Film was exposed for 1 min.
M: prestained protein ladder (kDa), 1: pc0870 n.i., 2: pc0870 i., 3: *E. coli* M15 without vector i.
c. Overexpression of pc0870 in pgEX-4T-3
M: prestained protein ladder (kDa), 1: *E. coli* C43 without vector i., 2: pc0870 n.i., 3: pc0870 i
?: Coomassie staining did not show a clearly visible band of expected size, as indicated by the arrow.
d. Western blot analysis to verify overexpression of pc0870 in pgEX-4T-3 using anti-GST antibodies. Film was exposed for 10 min. Contrast was enhanced.
M: prestained protein ladder (kDa), 1: pc0870 n.i., 2: pc0870 i., 3: *E. coli* C43 without vector i.

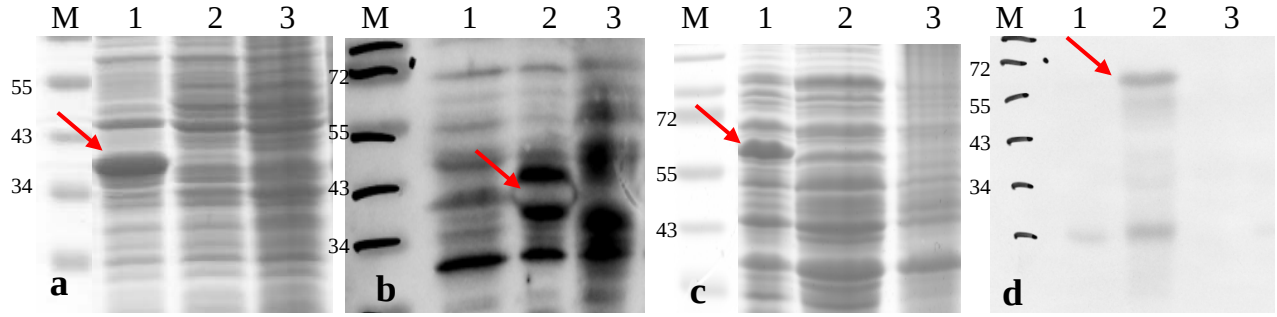

Figure 14. Overexpression of pc1077 checked by colloidal Coomassie staining and Western blot analysis

Bands of the correct and expected size are indicated by an arrow.

a. Overexpression of pc1077 in pQE-30
M: prestained protein ladder (kDa), 1: *E. coli* protein lysate 4 h after induction of overexpression of pc1077 (pc1077 i.), 2: *E. coli* protein lysate after 4 h of growing without induction of overexpression of pc1077 (pc1077 n.i.), 3: *E. coli* M15 without vector i.
b. Western blot analysis to verify overexpression of pc1077 in pQE-30 using anti-His antibodies. Film was exposed for 5 min.
M: prestained protein ladder (kDa), 1: pc1077 n.i., 2: pc1077 i., 3: *E. coli* M15 without vector i.
c. Overexpression of pc1077 in pgEX-4T-3
M: prestained protein ladder (kDa), 1: pc1077 i., 2: pc1077 n.i., 3: *E. coli* C43 without vector i.
d. Western blot analysis to verify overexpression of pc1077 in pgEX-4T-3 using anti-GST antibodies. The film was exposed for 2 sec.
M: prestained protein ladder (kDa), 1: pc1077 n.i., 2: pc1077 i., 3: *E. coli* C43 without vector i.

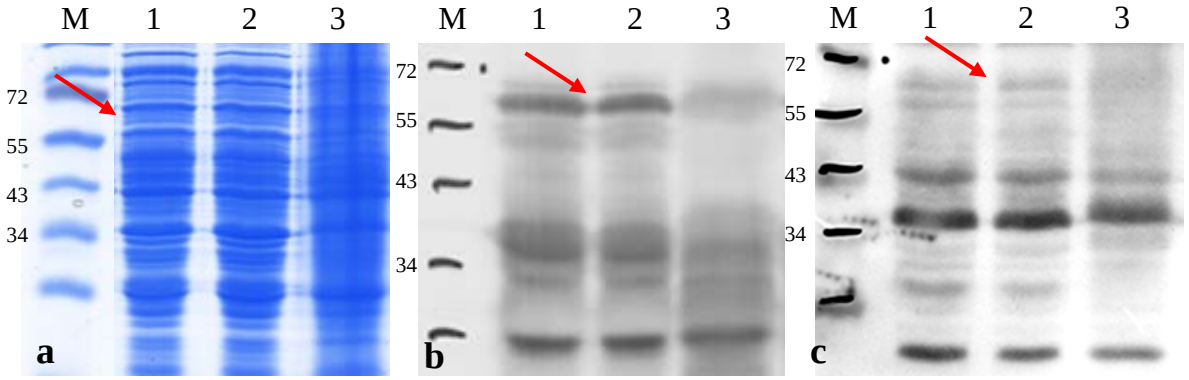

Figure 15. Overexpression of pc1489 checked by colloidal Coomassie staining and Western blot analysis

Bands of the correct and expected size are indicated by an arrow.

a. **Overexpression of pc1489 in pgEX-4T-3**

M: prestained protein ladder (kDa), 1: *E. coli* protein lysate 4 h after induction of overexpression of pc1489 (pc1489i.), 2: *E. coli* protein lysate after 4 h of growing without induction of overexpression of pc1489 (pc1489 n.i.), 3: *E. coli* C43 without vector i.

b.+c. Western blot analysis to verify overexpression of pc1489 in pgEX-4T-3 using anti-GST antibodies (b) and anti-pc1489-antibodies (c). The film was exposed for 1 min (b) and 5 min (c, contrast was enhanced).

M: prestained protein ladder (kDa), 1: pc1489 n.i., 2: pc1489 i., 3: *E. coli* C43 without vector i.

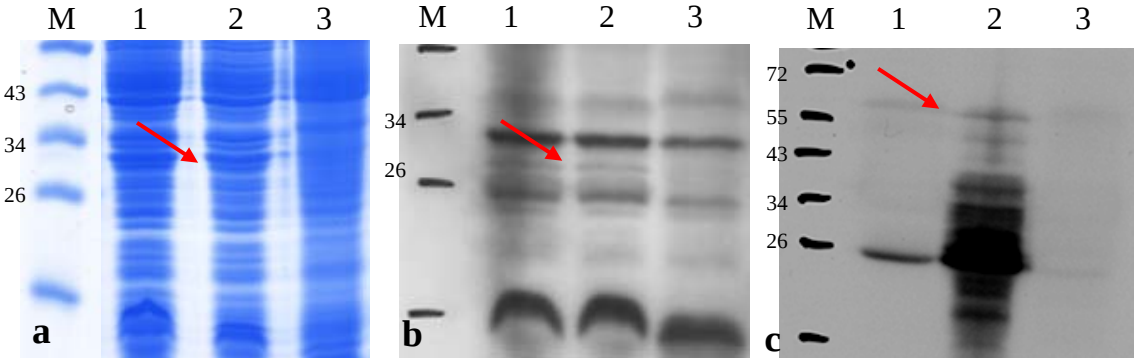

Figure 16. Overexpression of pc1860 checked by colloidal Coomassie staining and Western blot analysis

Bands of the correct and expected size are indicated by an arrow.

a. Overexpression of pc1860 in pQE-30

M: prestained protein ladder (kDa), 1: *E. coli* protein lysate 4 h after induction of overexpression of pc1860 (pc1860 i.), 2: *E. coli* protein lysate after 4 h of growing without induction of overexpression of pc1860 (pc1860 n.i.), 3: *E. coli* M15 without vector i.

b. Western blot analysis to verify overexpression of pc1860 in pQE-30 using anti-His antibodies. The film was exposed for 1 min.

M: prestained protein ladder (kDa), 1: pc1860 n.i., 2: pc1860 i., 3: *E. coli* M15 without vector i.

c. Western blot analysis to verify the overexpression of pc1860 in pgEX-4T-3 using anti-GST antibodies. The film was exposed for 10 sec. Contrast was enhanced.

M: prestained protein ladder (kDa), 1: pc1860 n.i., 2: pc1860 i., 3: *E. coli* M15 without vector i.

3.1.4 Hints for the formation of inclusion bodies and toxicity during porin overexpression in *E. coli*

If looking at the cell pellets after an overexpression of *E. coli* cells containing the expression construct or control cells without any vector, a remarkable difference could be observed. After harvesting, the transformed and consecutively induced cells resulted in smaller amounts of cells of white color, suggesting the formation of inclusion bodies. In contrast, cells without vector resulted in bigger brownish pellets.

During the process of 2-step cloning and subsequent overexpression of the porins pc1077 and pc0870, a reduced cell growth could be observed maybe due to the pore-forming characteristic of porins. Already after transformation of *E. coli* XL1blue with the overexpression constructs, some colonies did not grow well on the agar plates, probably displaying porin expression and incorporation into the outer membrane.

Badly grown colonies on a masterplate from screening for recombinant clones were compared with the respective screening results. Some clones regarded as positive in respect of containing pc1077 (Figure 17A, clones 1 and 11) or pc0870 (Figure 17A, clones 22 and 30) as insert, could be directly linked to bad growing on the masterplates as shown in Figure 17B (positive clones marked in red). However, some clones giving positive results for pc1077 in PCR (Figure 17A, clone 8) did not show bad growth on the masterplate (Figure 17B, clone 8). Since pgEX-specific primers were used for screening for recombinant clones, the true identity of the amplified fragment after PCR is not affirmed.

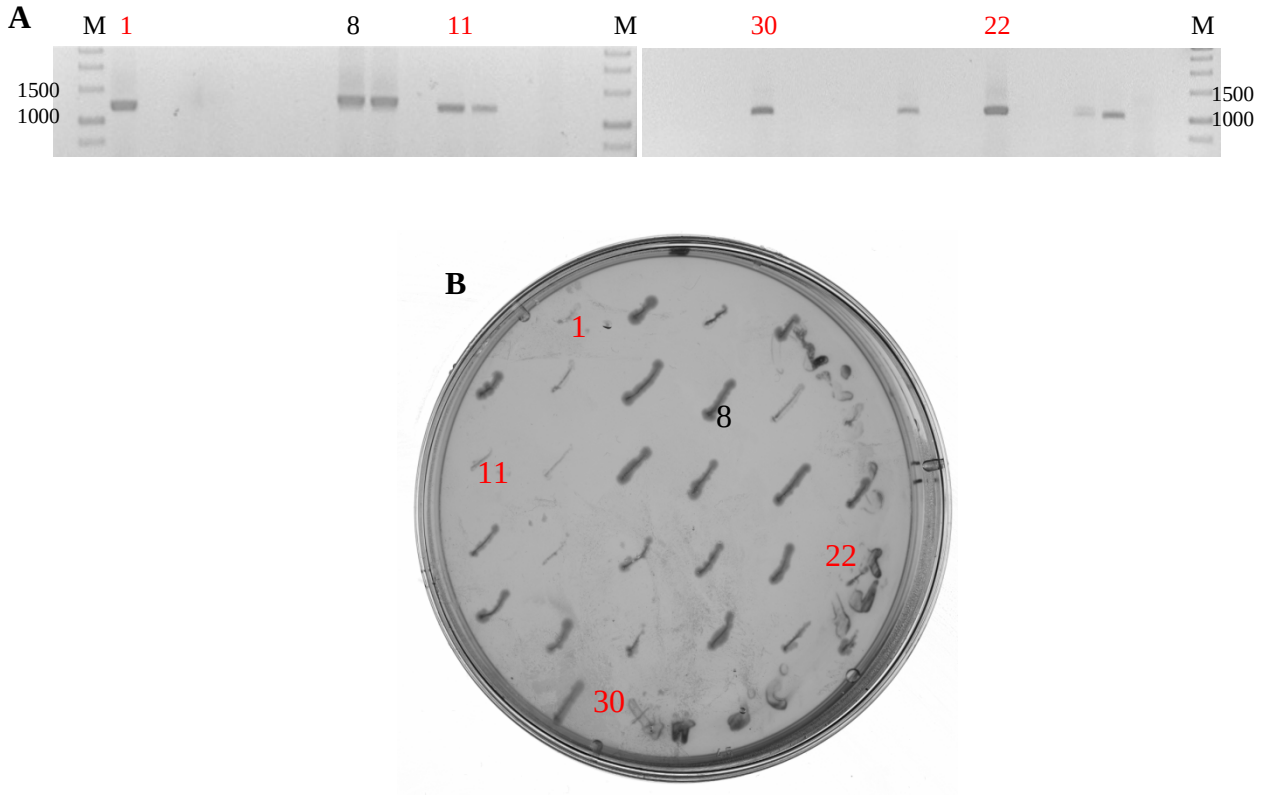

Figure 17. **Linking weak growth of transformed *E. coli* cells to the results of the screening for recombinant clones.**
A. Screening for recombinant clones of *E. coli* XL1blue containing pc1077 and pc0870 in the vector pgEX-4T-3. Clones 1 and 11 could be confirmed by sequencing to contain pc1077 as an insert. The clones 22 and 30 contain the correct sequence of pc0870as insert, according to sequencing results. M: DNA ladder 1kb
B. Masterplate from a screening for recombinant clones of pc1077 and pc0870.

3.1.5 Measurements of the optical density of *E. coli* C43 expression cultures

Taking a closer look at the cell growth during an overexpression, the optical density of induced and non-induced cells was measured at defined time-points to get some hints for pore-forming activity caused by porin expression. For this purpose, the construct pc1077 in the vector pgEX was used.

It could be shown in duplicates that the non-induced cells had grown to a much higher density than the induced cells four hours after induction (Figure 18A). Repetition of OD measurements starting directly after inoculation of the *E. coli* expression culture did not show drastic differences between the growths of induced and non-induced cells (Figure 18B).
Non-induced cells grew slightly better than the induced ones. However, results were not reproducible and effects of the inoculum size were considered.

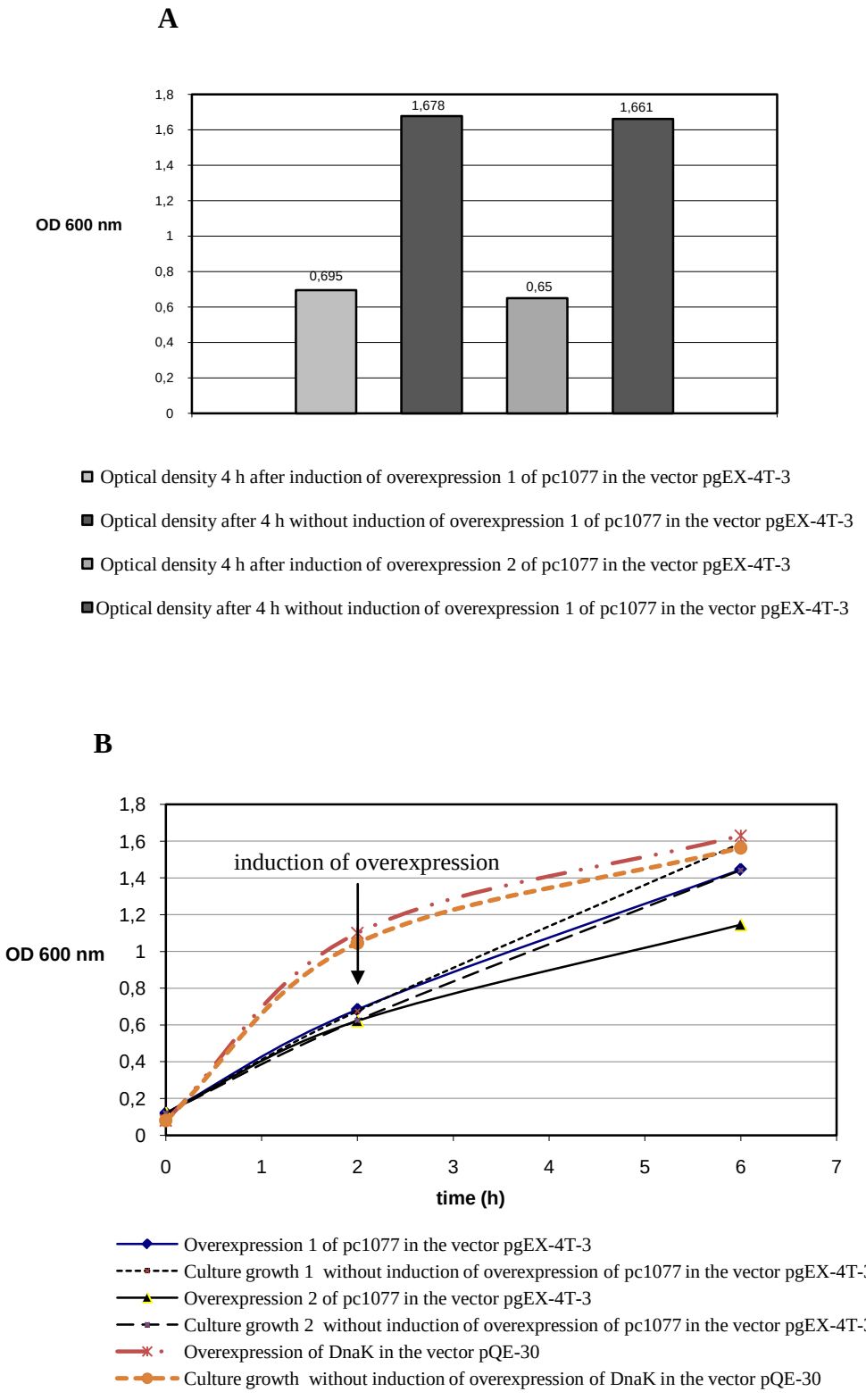

Figure 18. **OD measurments during porin overexpression**, concentrating on the construct pc1077 in the vector pgEX-4T-3 overexpressed in *E. coli* C43. Cultures overexpressing pc1077 showed a reduced cell density 4 h after induction of overexpression in comparison to a control culture, where overexpression was not induced (A). Differences in culture growth between induced and non-induced *E. coli* cultures were not always significant (B).

As a negative control the optical density of an *E. coli* culture expressing the cytoplasmic protein DnaK was tracked throughout the whole process (Figure 18B, red). No differences in the growing potential between induced and non-induced cultures were observed. Additionally, the inclusion membrane protein of *P. amoebophila* pc1111 in the vector pet16b (kindly provided by Eva Heinz) was overexpressed to get an idea of the growing behavior of an *E. coli* culture expressing non-toxic proteins. Again, no reduction in cell growth of the induced *E. coli* expression culture was observed (results not shown).

3.1.6 Indirect immunofluorescence experiments with *E. coli* cells after overexpression of pc1860 in the vector pgEX

In order to get more information about the localization of overexpressed porins in *E. coli*, immunofluorescence experiments with *E. coli* cells fixed after heterologous expression of pc1860 containing the leader sequence (2.47.1) were carried out.

Different antibodies were used for immunofluorescent staining of the cells, either targeting the GST-tag at the N-terminus of the porin or general outer membrane structures of *P. amoebophila*. Apparently, GST antibodies could bind in the induced *E. coli* C43 cells, whereas no cell staining got visible in the induced control cells without a vector if the same microscopic settings were used (Figure 19). However, despite of several tries, it was not possible to obtain reproducible results.

Looking at *E. coli* cells after induction in general, their morphology had changed evidently in comparison to non-induced cells. Due to the stress caused by protein overexpression the cells were elongated, whereas control cells without induction of overexpression showed coccoid morphology (results not shown).

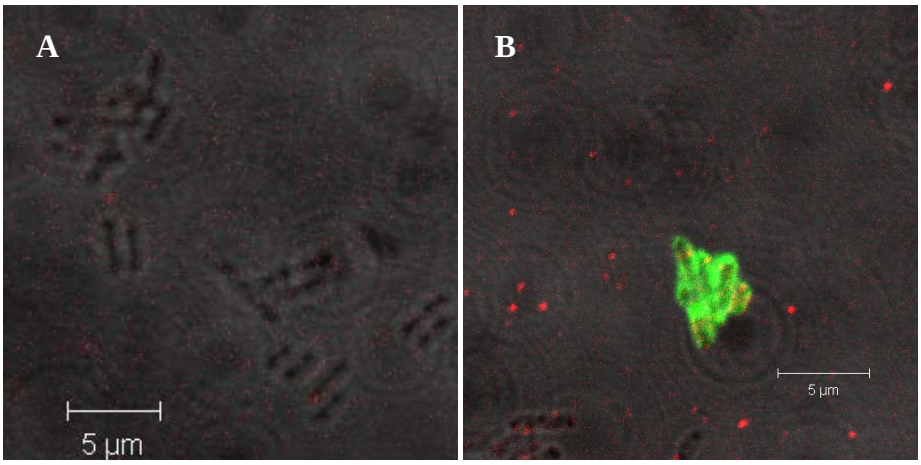

Figure 19. **Immunofluorescence analysis for the visualization of expressed pc1860.** The construct pc1860 in pgEX-4T-3 was overexpressed in *E. coli* C43 and detected by anti-GST-antibodies in green. Anti-Pam antibodies against general outer membrane components of *P. amoebophila* only show background signals (red). As a negative control empty *E. coli* C43 cells, equally induced, were investigated (A). Pictures were taken with exactly the same software and microscope settings.

3.1.7 Protein purification of pc1077 without leader sequence (noL1077)

The construct noL1077 could be successfully overexpressed (Figure 14). Thus, it was chosen for protein expression of pc1077 at large scale and consecutive purification via the His-tag.

As the harvested cells showed white color, indicating the possible formation of inclusion bodies, urea was used as a detergent during protein purification. Additionally, the whole approach was repeated using TB medium instead of LB medium and a growing temperature of 20°C after induction of overexpression. Interestingly, the pellet of an induced culture grown in TB showed hardly any differences in comparison to the non-induced cells after harvesting. The pellets had nearly the same appearance according to size and color, though the pellets of induced cells were a little bit brighter. Induced cells grown in LB resulted in small and white pellets, whereas the non-induced cells of the LB-approach looked similar to the pellets of TB-cultures. According to these findings, TB medium and a growing temperature of 20°C was chosen for an optimal yield during overexpression.

The collected fractions were analyzed by SDS-PAGE in order to detect the fraction containing the highest amount of purified protein (Figure 20). noL1077 was marginally eluted in the 60 mM to 100 mM imidazole fractions, while prominent bands for noL1077 were seen in the last 100 mM and first 300 mM imidazole fraction.

These eluates contained also some minimal amounts of other proteins (Figure 20, B3 and C1). In order to identify the purified protein as well as the additional bands, selected bands were analyzed by mass spectrometry.

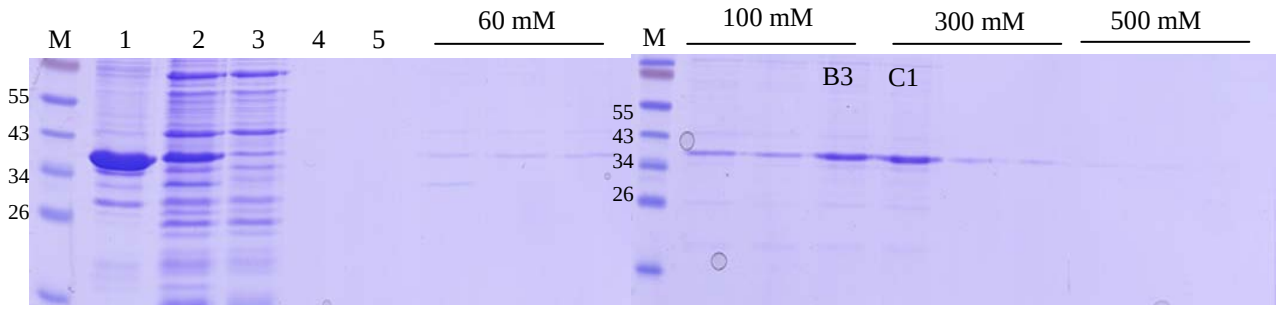

Figure 20. His-trap purification of noL1077 overexpressed in *E. coli* M15. Each imidazole concentration was applied three times, starting with 60 mM. The fractions B3 and C1 were containing the highest amount of purified protein.
M: prestained protein ladder, 1: pellet after sample preparation, 2: filtrate subjected to the column, 3: flow through during loading of the sample, 4: washing fraction, 5: flow through, collected while loading the first imidazole fraction
60-500 mM: used imidazole concentrations

3.1.8 Identification of protein bands by mass spectrometry

Proteins from fraction B3 and C1 were separated by SDS-PAGE. Three clearly visible protein bands (Figure 21) were chosen and subjected to analysis by nanoLC-MS/MS.

Interpretation of the output data of mass spectrometry showed that the dominant band 1 mostly contained the porin pc1077 as expected. All samples showed contamination with keratin, most likely introduced during sample preparation.

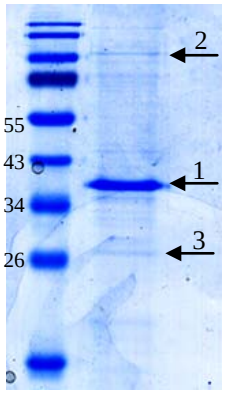

Figure 21. SDS-PAGE gel showing the purified pc1077 fractions B3 and C1. Arrows 1, 2 and 3 are pointing at the extracted bands

Band 2 and band 3 mainly showed hits for keratin, whereas results for band 3 reported an additional hit for pc1077. The appearance of the porin in this band of a lower molecular weight as expected (Table 20) could be due to degradation of the porin during the process of overexpression.

Additionally, all results were matched against an *E. coli* database to exclude the presence of *E. coli* porins in further functional analyses, but no significant hits were obtained.

Table 25. Hits for band 1, 2 and 3 for pc1077 based on the output data from mass spectrometry

	Band 1	Band 2	Band 3
Hit 1	Keratin, type II cytoskeletal 2 epidermal (Cytokeratin-2e)	PREDICTED: similar to Keratin, type I cytoskeletal 14 (Cytokeratin-14)	keratin 1 [Homo sapiens]
Hit 2	PREDICTED: similar to Keratin, type I cytoskeletal 14 (Cytokeratin-14)	keratin 1 [Homo sapiens]	epidermal cytokeratin 2 [Homo sapiens]
Hit 3	pc1077 Candidatus Protochlamydia amoebophila UWE25	epidermal cytokeratin 2 [Homo sapiens]	keratin 1 [Pan troglodytes]
Hit 4	PREDICTED: similar to keratin 1 isoform 7	type I keratin 16 [Homo sapiens]	PREDICTED: similar to Keratin, type I cytoskeletal 14 (Cytokeratin-14)
Detection of pc1077	Hit 3	no	Hit 14
Total number of hits	24	58	28

3.1.9 Immunofluorescence with *A. castellanii* Neff harboring *P. amoebophila* endosymbionts using anti-pc1077 antibodies

Antibodies against pc1077 were produced by Eurogentec (Seraing, Belgium) according to 2.42.

Applying pre-immune sera and subsequent bleeds in immunofluorescence (IF) experiments with uninfected *A. castellanii* Neff no signals could be detected, excluding the possible detection of amoeba proteins (results not shown).

Tests with the pre-immune sera were performed in the same dilutions as with the small, large and final bleeds. Unexpectedly, pre-immune sera of both rabbits showed signals if tested in IF experiments with E25-infected amoebae either due to unspecific binding of the antibodies or to a former chlamydial-infection of the rabbits. Results from Western Blot analysis (next chapter) promised insights into the unspecific binding capacities of the pre-immune sera.

The large bleed used in IF could not come up to expectations either, as testing the pre-immune serum in the same dilution as the antibody led to even stronger signals as obtained from the large bleed (Figure 22). No specific signals from the anti-pc1077 antibodies could be observed.

Also the overlay of signals from anti-pc1077 antibodies and the positive control against the cytoplasmic protein DnaK of *P. amoebophila* did not show overlapping signals (Figure 22B). This observation implied the detection of only unspecifically bound anti-pc1077 antibodies, since no halo-shaped signal from the outer membrane, surrounding the signals of anti-DnaK antibodies in the cytoplasm, was detectable.

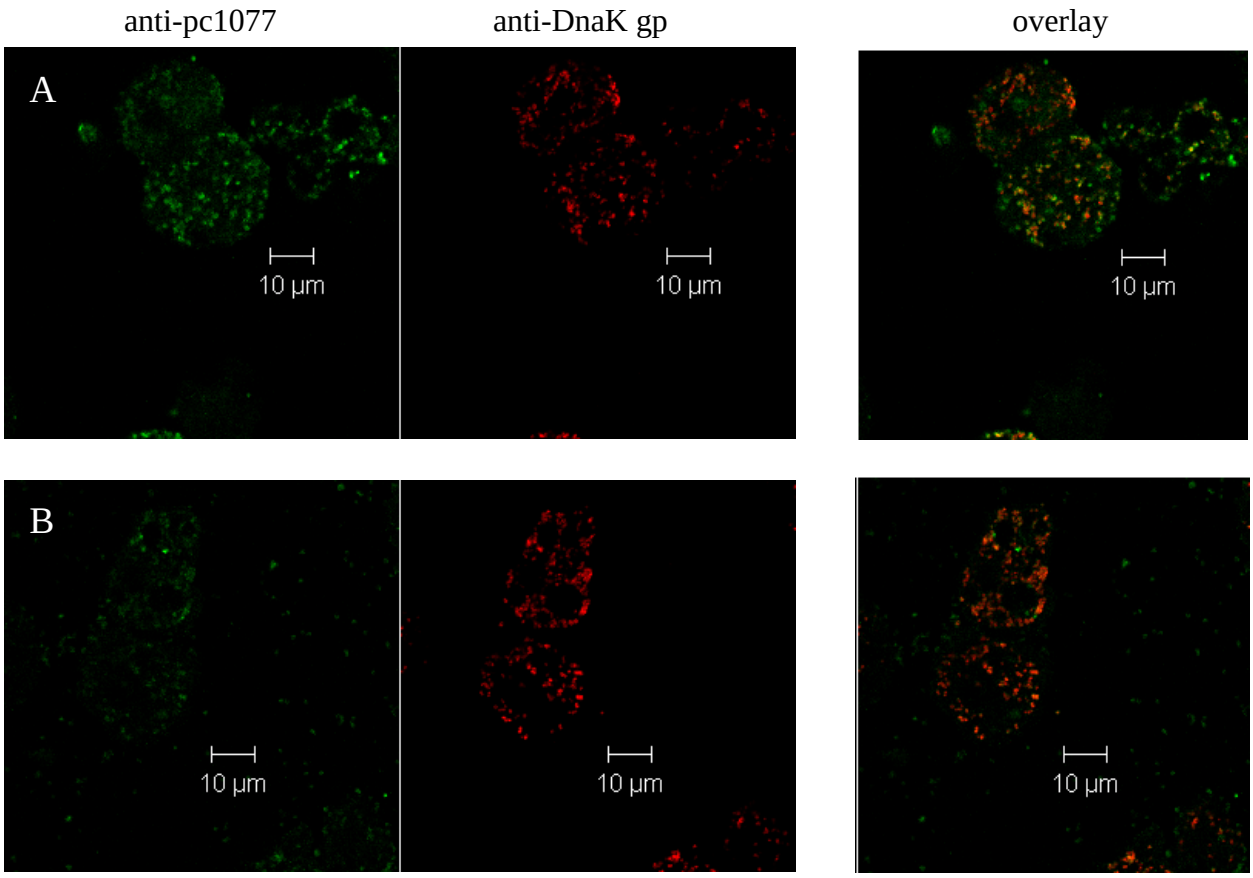

Figure 22. Specificity of the anti-pc1077 antibody was tested by immunofluorescence analysis.
B. The large bleed (green) was applied in a dilution of 1:100 and tested in E25-infected *A. castellanii* Neff. Antibodies against the cytoplasmic protein DnaK were used as a positive control, shown in red. No clearly overlapping signals could be observed.
A. In order to test the pre-immune serum for former chlamydial infections a dilution of 1:100 was applied in a parallel experiment, showing some strong unexpected signals (green).
Exactly the same microscopic settings were used for recording the pictures of A and B.

3.1.10 Western blot analysis with anti-pc1077 antibodies

For further investigation of the unexpected signals from the pre-immune sera in IF, Western blot analysis was performed with the large bleed as well as with the pre-immune serum of the rabbit.

Different dilutions of the large bleed and of the pre-immune serum were tested on the protein lysate after an overexpression of pc1077 in *E. coli* M15, resulting in a difference of the band pattern. Results for the pre-immune serum at low dilutions revealed a high unspecific background (results not shown). But Western blot using the large bleed at a dilution of 1:2000 demonstrated the specificity of the antibody by displaying an additional band at the expected size of about 37 kDa. The actual band of interest appeared as a strong white band in front of a high background, an indication for chosing a too low dilution of the respective antibody (Figure 23B, arrow). In comparison, the pre-immune serum applied in the same high dilution did not show any specific bands (Figure 23A).

For creating an even higher specificity of the anti-pc1077 antibody, suitable for its usage in IF experiments, an additional boost was considered.

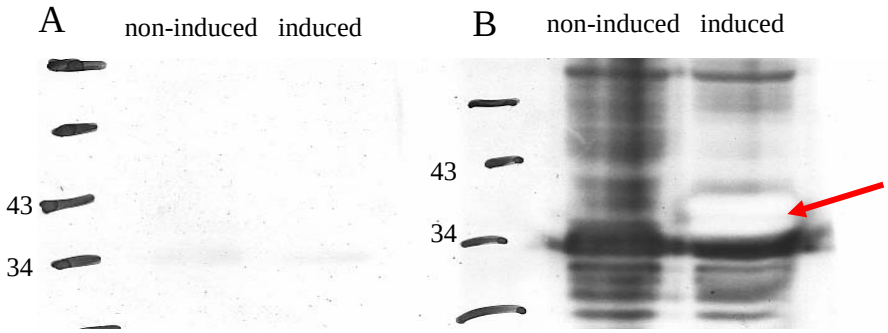

Figure 23. Western blot analysis to show specific binding of antibodies in the large bleed. Both the pre-immune serum (A) and the large bleed (B) were tested in a dilution of 1:2000 on a protein lysate after overexpression of pc1077 in *E. coli* M15. The secondary antibody was used 1:20000. The pre-immune serum just showed some weak unspecific bands at this high dilution, whereas the large bleed visualized a band of the expected size, indicated by an arrow. A higher dilution of the anti-pc1077 antibodies would reduce the high unspecific background.

3.1.11 Functional analysis of pc1077

In order to get an idea of the actual function of pc1077, lipid-bilayer measurements were performed to investigate the proposed pore-forming activity of this protein. The construct of pc1077 without leader sequence in the vector pQE-30 was overexpressed, purified and subjected to further analyses by lipid-bilayer measurements by Roland Benz.

A negative control of purified proteins of an overexpressed *E. coli* M15 culture containing only the empty pQE-30 vector was measured in parallel. Purification of this overexpression via a His-trap column resulted in hardly any detection of proteins by colloidal Coomassie staining, as expected.

Unfortunately, the measurements detected pores in the negative control due to the presence of the *E. coli* porin OmpF. Therefore, the measurements of the sample of purified pc1077 could not be considered as significant, since pore-forming activity could either be linked to a contamination with OmpF or as originally proposed linked to the porin of *P. amoebophila*. As a conclusion, no ascertained hint for the pore-forming activity of pc1077 was observed.

3.2 Transcription analysis

3.2.1 Defining the optimal settings for qPCR primers

Optimal conditions for the primer pairs q16S R+F and q1489 R+F (Table 16) were highly important, therefore different primer concentrations (15 pmol, 25pmol, 50 pmol and 75 pmol) were tested in each possible combination as well as various annealing temperatures. The optimal conditions for 16S R+F were set to a concentration of 25 pmol, whereas for 1489 R+F a concentration of 15 pmol was used. In both cases the annealing temperature was set to 60°C.

3.2.2 RNA isolation and control of RNA quality

Three independent biological replicates of RNA isolated at defined time points throughout an infectious cycle (0 h p.i., 24 h p.i., 48 h p.i. and 96h p.i.) were analyzed. RNA quality was tested in order to detect degradation effects resulting from the isolation procedure, but bands for 16S rRNA and 23S rRNA were obtained for all three replicates if loaded onto an agarose gel (Figure 24A).

The sample isolated 24h p.i. and the non-infected negative control, both descending from replicate 2, contained very low amounts of RNA, therefore no bands could be detected on the RNA gel (Figure 24A, replicate 2, lane 2 (24 h p.i.) and lane 5 (non-infected)).

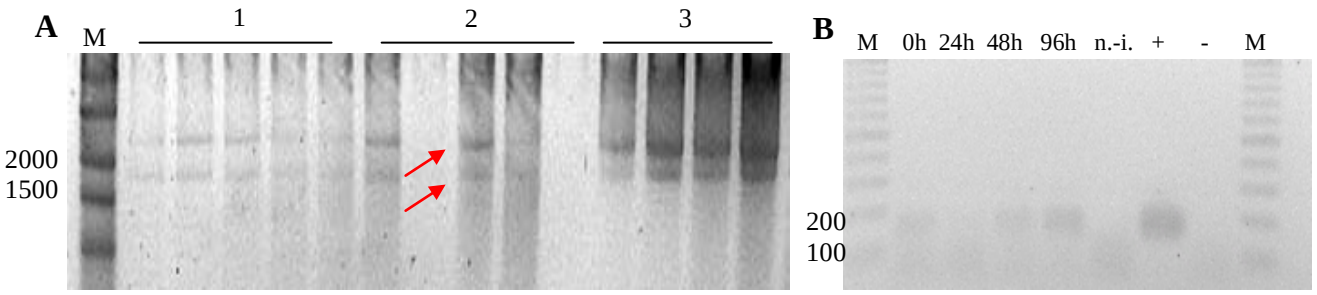

Figure 24. **Testing the quality of isolated RNA**
A. Bands for the 16S rRNA gene and the 23S rRNA gene could be detected on a 2% TAE-agarose gel as clearly defined bands, indicated by the arrows. 1, 2, 3 represent the 3 replicates, samples applied from 0 h to 96 h p.i. and non-infected sample (n.-i.). M: RNA ladder. Contrast was enhanced.
B. After the second DNase digestion co-extracted DNA of some samples was still amplified in PCR, visualized on a 2% TBE-agarose gel. DNA contaminations were detected using q1489 R+F. A positive (+) and a negative control (-) were included. M: 100 bp ladder

DNase digestion had to be performed three times in order to get rid of DNA, co-extracted during RNA isolation (Figure 24B). Finally, the primer pair q1489 R+F did not amplify the fragment of pc1489 in general PCR any more, approving the digestion of co-extracted DNA. The RNA sample which originated from the isolation 48 h p.i. still contained some DNA contamination after three times of DNase digestion. Hence, this sample was treated with and without reverse transcriptase in parallel during RT-PCR to get an idea of the effects of the remaining DNA in subsequent qPCR.

3.2.3 Optimization and quality control of the data output of qPCR using the iCycler software

First, the negative controls of the qPCR data had to be inspected to estimate reliability of the output data. Results from a qPCR run are shown in Figure 25. All three negative controls did not reach the treshhold for significant signals.

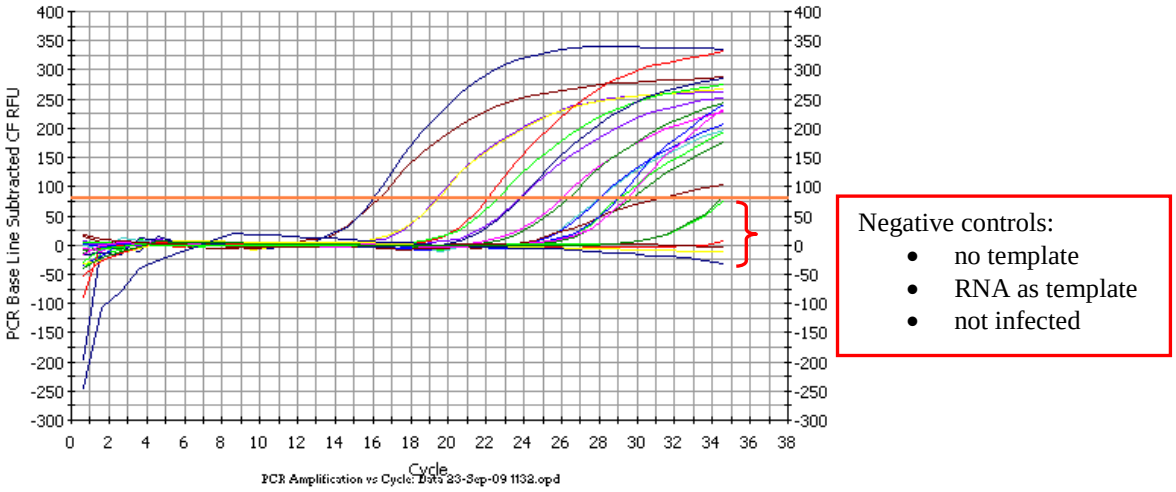

Figure 25. **Amplification graph for the fragment of pc1489 recorded during a qPCR run at cycle 2.** The orange line, representing the treshhold value, was not reached by the negative controls.
CF RFU: curve fit relative fluorescent units

The slope value of the standard curve of each qPCR run was inspected. If this value ranged from -3 to -3.6, the standard curve was used for further analysis (Figure 26, arrow). In all runs the slope value came up to this precondition by excluding standards which obviously deviated from the expected value.

Furthermore, PCR efficiency was expected to come up to 100% or even slightly more (Figure 26, arrow). Values much higher than 100% were due to the possible formation of primer dimers.

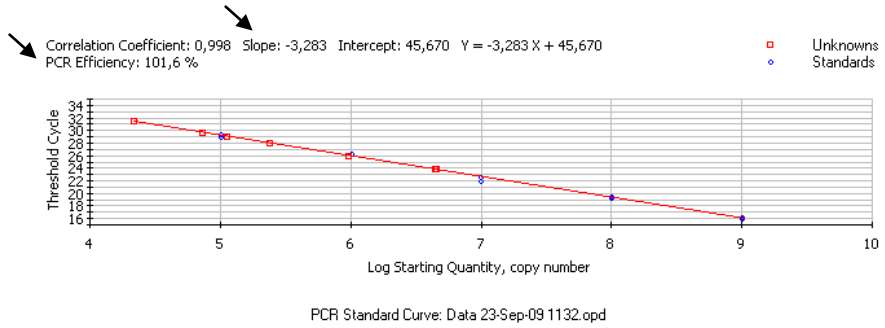

Figure 26. **Standard curve for the amplicons of pc1489** calculated with the help of the pc1489 standards (blue), unknowns were plotted in red, arrows were pointing out the important values. (Slope:-3.28, PCR efficiency: 101.6%, correlation coefficient: 0.998)

After each qPCR run, results were analyzed by agarose gel electrophoresis to check specific binding of the primer pairs (Figure 27). 16S R+F amplified a sequence of 88 bp, whereas the resulting amplicon using 1489 R+F consisted of 143 bp. As an additional proof of primer specificity, a melting curve was recorded at the end of each run, displaying the melting temperature (Tm) for each amplicon. Thus, if only one amplicon was produced during the run, as expected in the best case, just one Tm dominated throughout the melt curve data. Tm for the amplicon of pc1489 was set to 79°C (Figure 28, vertical orange line) and the amplicon of 16S separated at a Tm of 80°C. Melting curves of the negative control, containing no template, and the non-infected samples did not show a prominent Tm peak. The negative control –RT was characterized by a slightly shifted peak (Figure 28, red arrows), implying unspecific binding of the primer pairs with another amplification result.

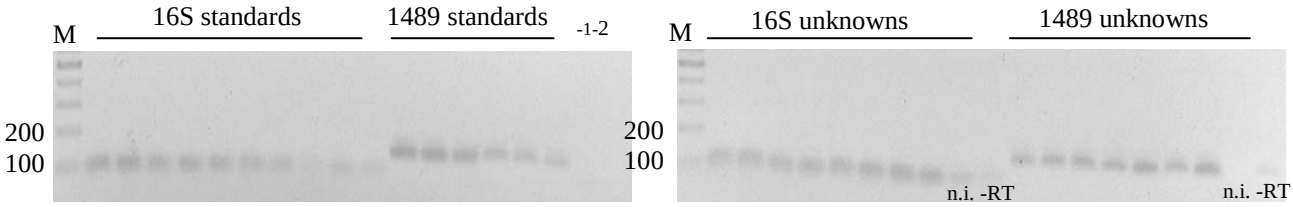

Figure 27. **2% agarose gel for showing the amplification results of a qPCR run**. 16S standards were applied in duplicates from 10^9 to 10^5, 1489 standards were applied once with exception of 10^9. NTCs were represented by -1 for 16S and -2 for 1489. Unknowns were applied in duplicates starting with 0h, except the following: non-infected (n.i.) and without reverse transcription (–RT) samples of 16S and 1489 and 96h p.i of pc1489 were only applied once.
M: 100 bp ladder

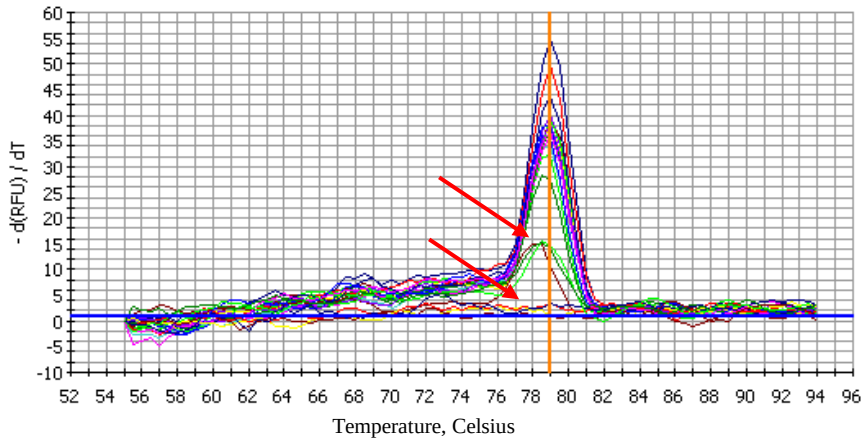

Figure 28. **Melting curve for the pc1489 amplicons after a qPCR run.** For each reaction one specific melting temperature was figured out. Production of always the same amplicon should end up in only one common Tm. Red arrows are indicating different Tms for the negative controls.
-d(RFU)/dT: change of fluoresecent units with time

3.2.4 Summary of all qPCR runs

qPCR was performed in duplicates with three biological replicates, finally producing data from 6 different runs:

- Run 1 and Run 2: RNA kindly provided by Albert, but data from Run 1 were not included in further analyses, as standard curve data were not reliable
- Run 3 and Run 4: RNA isolated from infectious cycle 1
- Run 5 and Run 6: RNA isolated from infectious cycle 2

An overview of all runs, except Run 1, is shown in Figure 29. No outstanding differences could be observed between the single runs, displaying about 10000 times less transcripts of pc1489 than transcripts of the 16S rRNA at 0 h p.i..

The mean values for each time point were calculated for further investigation and the lowest value at 24 h p.i. was used as starting-point for subsequent calculations.

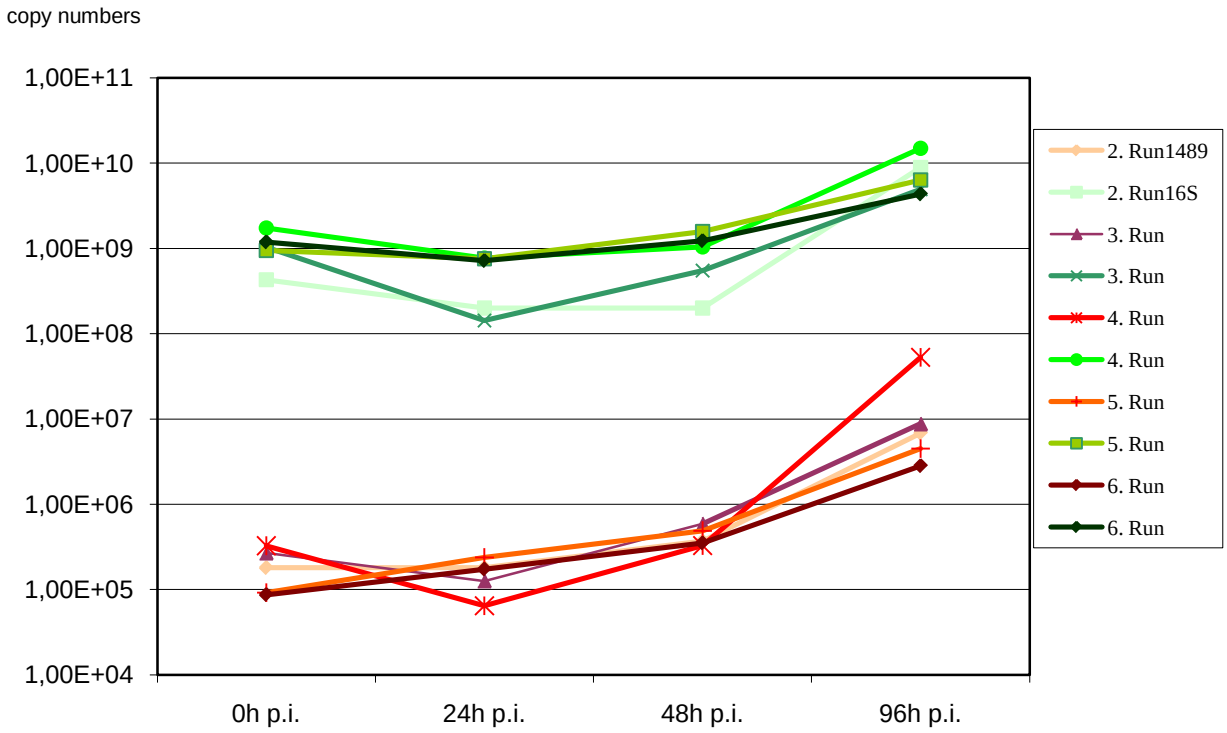

Figure 29. **Results of 5 qPCR runs**. Red colored lines are displaying values for pc1489, lines in green are representing values for the 16S rrNA. Templates were diluted 1:10. The first run was excluded from analyses.

Changes in the transcription level got visible by comparing the copy numbers of pc1489 and the 16S rRNA at different time points. The increase of both was set in relation to the respective lowest value at 24 h p.i..

The copy numbers of the 16S rRNA showed an increase of more than 10 times from 24 h p.i. to 96 h p.i., reflecting the expected growth of the bacterial community. The increase of copy numbers of pc1489 from 24 h p.i. to 96 h p.i. was more evident, since a 100 fold rise was observed (Figure 30A).

The copy numbers of pc1489 were normalized to those of the 16S rRNA in order to produce representative values displaying the actual changes of transcription throughout an infectious cycle not due to expected bacterial replication. Normalized copy numbers of pc1489 demonstrated a 10 fold increase from 24 h p.i. to 96 h p.i. (Figure 30B).

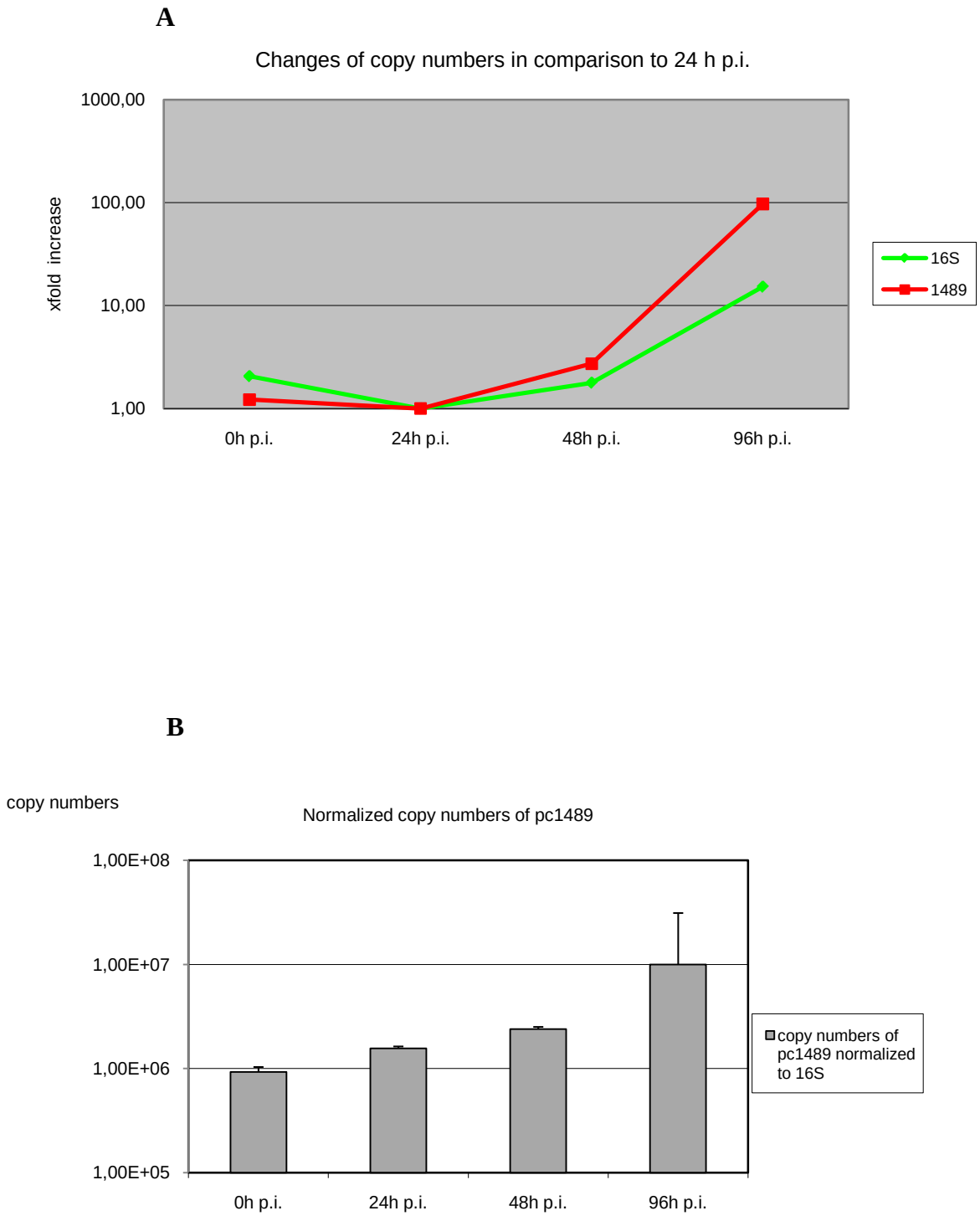

Figure 30. **Different transcription levels of the 16S rRNA and pc1489 during an infectious cycle (**displaying the mean values).
A. Increase of both copy numbers of the 16S rRNA and copy numbers of pc1489 in relation to the lowest copy number at 24 h p.i.
B. Copy numbers of pc1489 normalized with the help of the corresponding values for the 16S rRNA.

3.3 Generation of polyclonal antibodies against cytoplasmic proteins

3.3.1 Amplification of pc1499 (DnaK) and pc0595 (EF-TU), 2-step cloning and clone screening

Specific primers (Table 14) for pc1499 and pc0595 of *P. amoebophila* UWE25 were designed and amplificates from a high-fidelity PCR showed the expected length of 1965 bp for pc1499 and 1185 bp for pc0595.

Cloning was performed following a 2-step cloning protocol. It required several rounds of screening to finally detect amplicons with the correct and expected sequence length. For each construct two clones with correct inserts were verified by pQE/pgEX screening and sequencing.

Sequencing of the clones of DnaK was linked to some problems due to the length of its sequence. Despite of forward and reverse sequencing, it was not possible to obtain the whole length sequence of 1965 bp. Hence, pc1499 clones were only identified by their start- and end-sequences, thereby showing up to 100% similarity to the original sequence part.

3.3.2 Overexpression of DnaK in the vector pQE-30 and EF-TU in the vector pgEX-4T-3

After heterologous expression in an adequate *E. coli* strain, the expression level was inspected by colloidal Coomassie staining and Western blot analysis. Based on the amount of overexpressed protein the constructs pc1499 (DnaK) in the vector pQE-30 and pc0595 (EF-TU) in the vector pgEX-4T-3 were used for further investigations.

Bands of the expected molecular weight of 71 kDa could be observed for DnaK (Figure 31, arrows). According to colloidal Coomassie staining, the overexpression of DnaK resulted in a very strong signal. This high amount of detectable DnaK led to high background signals in Western blot analysis with anti-His antibodies (Figure 31B). The signals from DnaK visually intensified the additional bands, resulting from other proteins containing histidines.

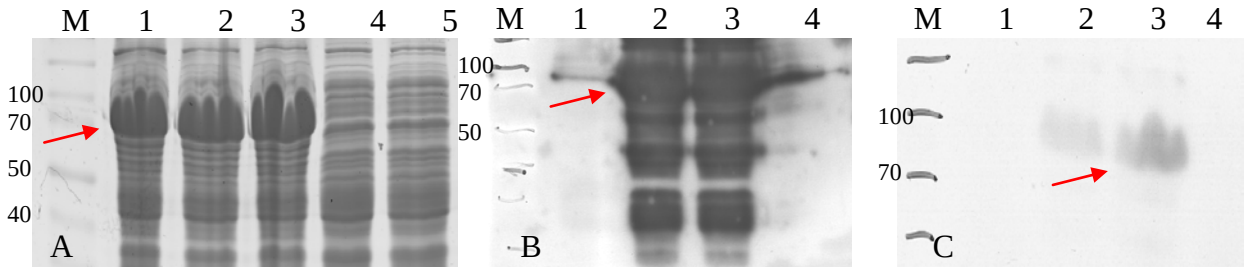

Figure 31. Overexpression of pc1499 (DnaK) in pQE-30 using *E. coli* M15 and different IPTG concentrations for induction. Results shown with colloidal Coomassie stainig (A) and Western blot using anti-His antibodies (B) and anti-DnaJ antibodies (C). Films were exposed for 30 sec.
A. M: multicolor protein ladder (kDa), 1: *E. coli* protein lysate 4 h after induction of overexpression of pc1499 (pc1499 i.) with 1mM IPTG, 2: pc1499 i., 0.5 mM IPTG, 3: pc1499 i., 0.1 mM IPTG, 4: *E. coli* protein lysate after 4 h of growing without induction of overexpression of pc1499 (pc1499 n.i.), 5: *E. coli* M15 without vector i., 1mM IPTG
B.+C. M: multicolor protein ladder (kDa), 1: *E. coli* M15 without vector i., 1mM IPTG, 2: pc1499 i., 0.5 mM IPTG, 3: pc1499 i., 1 mM IPTG, 4: pc1499 n.i.

The expected molecular weight of EF-TU was calculated by adding 26 kDa for the GST-tag to the original weight of 43 kDa, resulting in a weight of 69 kDa. This GST-fusion protein was detected as an additional band at ~70 kDa after induction of overexpression of EF-TU (Figure 32, arrows).

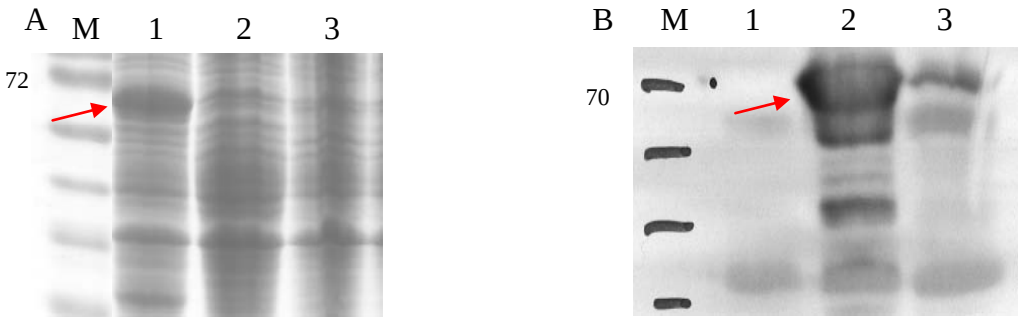

Figure 32. Overexpression of pc0595 (EF-TU) in pgEX-4T-3 using *E. coli* BL21 (DE3) shown by colloidal Coomassie staining (a) and Western blot analysis (b) usind anti GST-antibodies (1:5000). The film was exposed for 20 sec.
A. M: prestained protein ladder (improved), 1: *E. coli* protein lysate 4 h after induction of overexpression of pc0595 (pc0595 i.), 2: *E. coli* protein lysate after 4 h of growing without induction of overexpression of pc0595 (pc0595 n.i.), 3: *E. coli* BL21 (DE3) without vector i.
B. M prestained protein ladder, 1: *E. coli* BL21 (DE3) without vector i., 2: pc0595 i., 3: pc0595 n.i.

3.3.3 Purification of pc1499 (DnaK)

DnaK in the vector pQE-30 was chosen for further protein expression at large scale followed by purification via the His-tag using an imidazole gradient (60 mM – 100 mM- 300 mM- 500 mM). SDS-PAGE analyses showed elution of the protein at nearly all imidazole concentrations and many additional protein bands. Thus, additional imidazole steps (30 mM, 40 mM, 50 mM, 55 mM, 70 mM, 80 mM) were included in order to improve the purity of the overexpressed protein. After this optimization process, fractions were collected again and analyzed with SDS-PAGE (Figure 33) in order to detect the fraction containing the highest amount of purified protein.

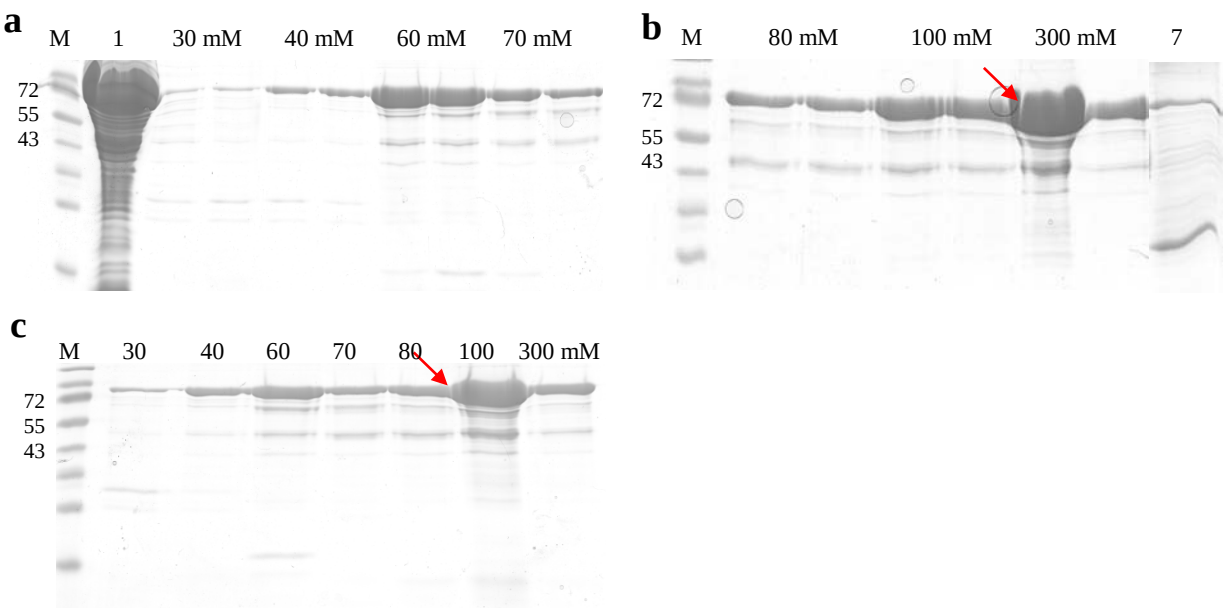

Figure 33. Protein fractions after purification of DnaK using a His-trap column to identify the fraction containing the highest and purest amount of desired protein. Results are visualized by colloidal Coomassie staining of SDS-PAGE gels. a and b show the first and second eluat-fractions, in c the third fraction of each imidazole step was applied.
a. M: prestained protein ladder (kDa), 1: filtrate after sample preparation, 30-70 mM: applied imidazole concentrations
b. M: prestained protein ladder (kDa), 7: pellet after sample preparation, 80-300 mM: applied imidazole concentrations
c. M: prestained protein ladder (kDa), 30-300 mM: applied imidazole concentrations

DnaK was still - but most of the time marginally - eluted in all imidazole fractions. The most prominent band for DnaK was seen in the first 300 mM imidazole fraction (Figure 33b, arrow). Also the last 100 mM fraction yielded a notable amount of protein.

3.3.4 Identification of protein bands by mass spectrometry

The selected eluates from purification of DnaK still contained some minimal amounts of other proteins (Figure 33b+c), which could disrupt antibody generation. Therefore, two of these additional bands as well as the dominant band were extracted and subjected to nanoLC-MS/MS in order to ensure purity of purified DnaK for the following antibody generation. Additionally, bands obtained after overexpression of the protein EF-TU were analyzed.

Mass spectrometry approved high purity of DnaK. The dominant band featuring the expected weight of 71 kDa as well as the other bands, considered as possible contaminations, could be identified as DnaK (Table 26). Moreover, a contamination with keratin was detected in all samples most probably arising from the process of sample preparation.

Also EF-TU was identified by mass spectrometry, since the analyzed band contained a hit for pc0595 (EF-TU) beside some additional hits for keratin.

Table 26. Hits for bands 1, 2 and 3 for DnaK and the band for EF-TU based on the output data of mass spectrometry

	Band 1 DnaK	Band 2 DnaK	Band 3 DnaK	EF-TU
Hit 1	pc1499 Candidatus Protochlamydia amoebophila UWE25	pc1499 Candidatus Protochlamydia amoebophila UWE25	pc1499 Candidatus Protochlamydia amoebophila UWE25	pc0595 Candidatus Protochlamydia amoebophila UWE25
Hit 2	keratin 1 [Homo sapiens]	keratin 1 [Homo sapiens]	Keratin, type II cytoskeletal 2 epidermal (Cytokeratin-2e)	ECOLI 60 kDa chaperonin (Protein Cpn60)
Hit 3	Keratin, type II cytoskeletal 2 epidermal (Cytokeratin-2e)	PREDICTED: similar to Keratin, type I cytoskeletal 14 (Cytokeratin-14)	keratin 1 [Homo sapiens]	HUMAN Keratin, type II cytoskeletal 1 (Cytokeratin 1)
Hit 4	PREDICTED: similar to Keratin, type I cytoskeletal 14 (Cytokeratin-14)	PREDICTED: similar to keratin 2a [Macaca mulatta]	PREDICTED: similar to Keratin, type I cytoskeletal 14 (Cytokeratin-14)	EFTU_ECOLI Elongation factor Tu
Total number of hits	13	35	20	19

3.3.5 Immunofluorescence experiments and Western blot analysis showing the specificity of anti-DnaK antibodies

Antibodies against DnaK were raised in both guinea pig and chicken by Eurogentec (Seraing, Belgium) and localization of DnaK was studied by immunofluorescence analysis using *A. castellanii* Neff harboring *P. amoebophila* endosymbionts. Pre-immune sera from the respective animal were used as negative control.

3.3.5.1 Immunofluorescence analysis with antibodies against DnaK obtained by the immunization of two guinea pigs (anti-DnaK gp)

Initial tests with the pre-immune serum in IF showed no signals when using an appropriate dilution of 1:1000 after inactivation (data not shown).

To visualize the localization of DnaK in *P. amoebophila* anti-DnaK antibodies were used simultaneously with anti-Pam antibodies, targeting the immunodominant components of the outer membrane of *P. amoebophila*, and anti-pc1489 antibodies, targeting the porin pc1489 in the outer membrane of *P. amoebophila* (kindly provided by Karin Aistleitner).
The first bleed already showed knob-shaped signals located in the cytoplasm of *P. amoebophila*, suggesting detection of DnaK. In support of this, the overlay of signals showed that the red signal for DnaK was surrounded by signals for the outer membrane originating from anti-Pam (blue) as well as from anti-pc1489 (green) antibodies (Figure 34B).

In parallel, the first bleed was used in amoeba cells without endosymbionts (Figure 34A). Antibodies from one guinea pig showed signals, suggesting unspecific binding to the mitochondria of amoebae. While testing the second and the final bleed from this guinea pig under the same conditions, the detection of mitochondria was reduced (results not shown).

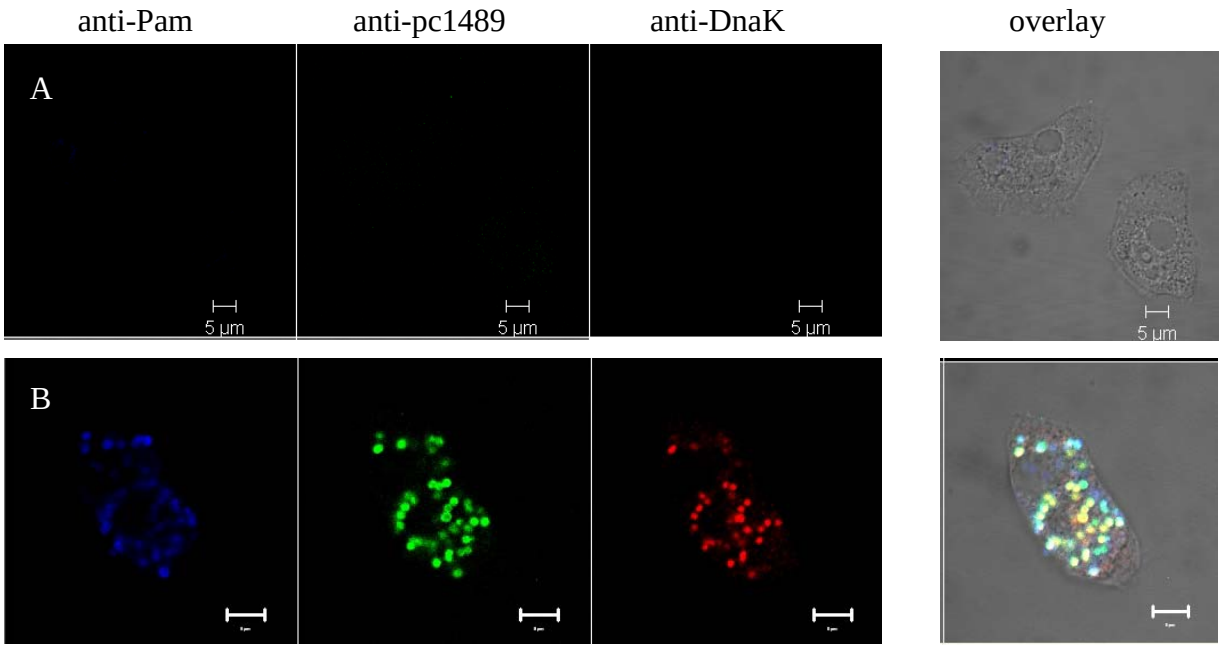

Figure 34. Immunofluorescence analysis using anti-DnaK gp antibodies. No signals were observed in uninfected amoebal cells (A) whereas *P. amoebophila*-infected amoebal cells showed signals detecting the endosymbionts (B). The overlay of signals visualizes localization of the signals for DnaK (red) in the cytoplasm of *P. amoebophila*, surrounded by signals for the outer membrane (blue, green). The four pictures of both A and B represent identical microscopic fields. Pictures of A and B were taken with the same microscope settings. Bars 5µm.

Additional assays were performed using the second and the final bleed, including PFA fixed cells as well as methanol fixed cells. No differences in the location of signals could be observed. The expected intracellular localization was clearly visualized (Figure 35) and this newly generated antibody can be used as an intracellular standard in future immunofluorescence experiments.

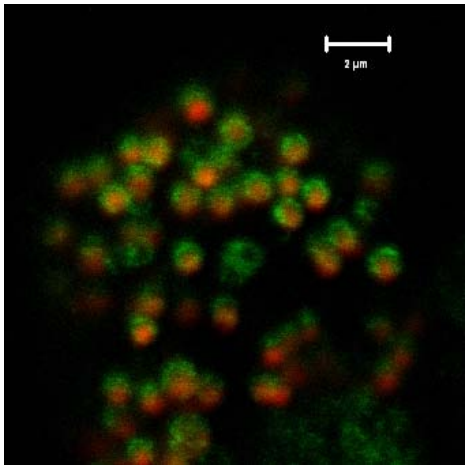

Figure 35. Showing the intracellular localization of anti-DnaK antibodies by immunofluorescence analysis. Antibodies used for visualizing the outer membrane (anti-Pam) are shown in green whereas anti-DnaK appears in red. Bar 2 µm.

3.3.5.2 Cross-reactivity of anti-DnaK antibodies in other chlamydia-like bacteria

The anti-DnaK antibody was considered to be used as a standard antibody in immunofluorescence experiments. Thus, some additional experiments were performed to detect *Waddlia chondrophila* by these newly generated antibodies in IF.
Signals indicating a *Waddlia chondrophila* infection of amoebae could be observed as shown in Figure 36 (pictures taken by Karin Aistleitner), offering a new method for detecting these chlamydia-like bacteria besides of DAPI staining and fluorescent-in-situ-hybridization.

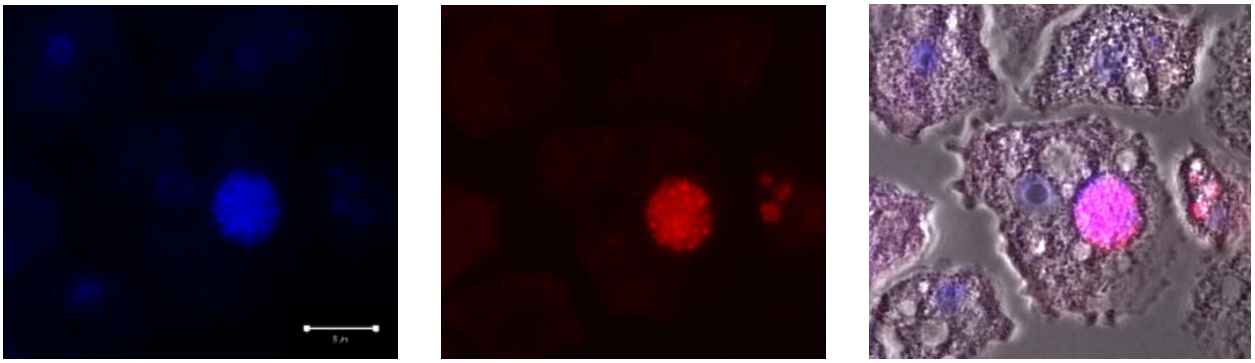

Figure 36. Detection of a homologue of DnaK by anti-DnaK antibody in *Waddlia chondrophila*. Bacteria are blue due to DAPI staining. The antibody against DnaK shows red signals. Bar 5 µm.

3.3.5.3 Western blot analysis with anti-DnaK gp antibody

Specificity of anti-DnaK gp was tested by Western blot analysis. For this purpose, either *E. coli* M15 cells, harvested after an overexpression of DnaK, or amoebae harboring *P. amoebophila* were applied. Specific detection of DnaK could be shown in both approaches, since distinct bands at a molecular weight of 71 kDa were present (Figure 37). The overexpression of DnaK has always yielded high amounts of protein, explaining the strong signal (Figure 37, lane 2) resulting from this approach.

Moreover, no unspecific binding to amoeba proteins was detectable in Western blot (Figure 37B).

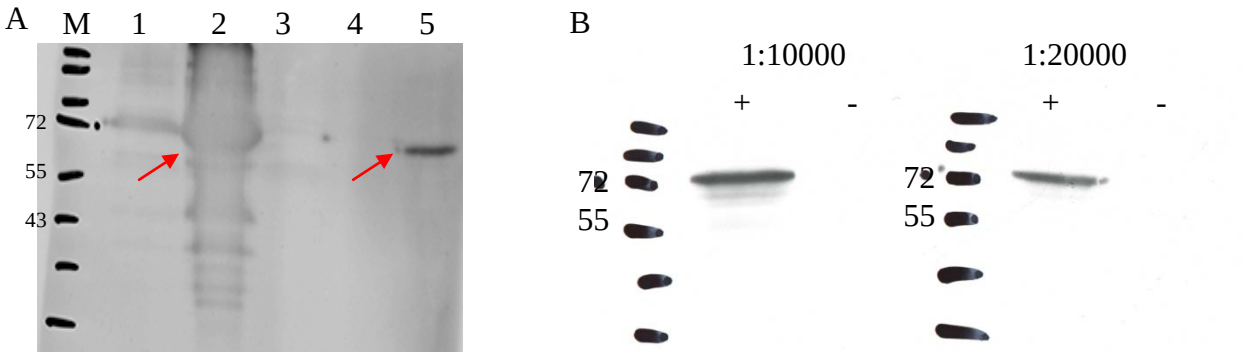

Figure 37. Western blot analysis to show specificity of anti-DnaK gp.
A. Antibodies were tested at a dilution of 1:2000 to detect a specific signal after overexpression or DnaK in amoebae infected with *P. amoebophila*. Film was exposed for 10 sec.
M: prestained protein ladder (kDa), 1: *E. coli* protein lysate after 4 h of growing without induction of overexpression of DnaK (DnaK n.i.), 2: *E. coli* protein lysate 4 h after induction of overexpression of DnaK (DnaK i.), 3: *E. coli* M15 without vector i., 4: uninfected *A. castellanii* Neff, 5: E25-infected *A. castellanii* Neff

B. Anti-DnaK gp was tested in various dilutions to demonstrate detection of *P. amoebophila*-infected amoebae by Western blot.
+: *P. amoebophila*-infected *A. castellanii* Neff, -: uninfected *A. castellanii* Neff
1:10000, 1:20000: applied dilutions of the anti-DnaK antibody

3.3.5.4 Immunofluorescence analysis with antibodies against DnaK obtained by the immunization of one chicken (anti-DnaK chick)

After purification of the specific antibodies out of egg-yolks, they were applied in immunofluorescence analysis for visualization of DnaK in *P. amoebophila*.
IF with the purified pre-immune yolks, diluted 1:100 after inactivation of antibodies, showed no signals in *A. castellanii* Neff harboring *P. amoebophilus* endosymbionts (data not shown).

The concentration of antibodies was really low in all three egg-yolk collections, thus dilutions up to 1:1 were used for indirect immunofluorescence to observe signals. The pre-immune yolk always had to be tested in parallel in the same dilution, leading to detection of unspecifically bound antibodies at this low dilution. Consequentially, the anti-DnaK chick antibody was regarded as too weak for usage in IF experiments and an additional antigen boost was ordered after the end of the immunization program in order to stimulate a stronger immune response.

Repeating the assay with this additional egg-yolk collection in a 1:100 dilution after antibody inactivation, signals could be observed resembling those for anti-DnaK gp antibodies (Figure 38B).

The specific antibody was used simultaneously with anti-Pam antibodies for the detection of outer membrane structures of *P. amoebophila*. Again, knob-shaped signals for DnaK (shown in red) were observed and in an overlay of signals the intracellular localization of DnaK could be clearly visualized (Figure 38B, overlay). Already inactivated antibodies could be applied in a dilution of up to 1:1000. No signals were detected when applying the same antibody on non-infected amoeba cells (Figure 38A) as a negative control, resembling the results of the pre-immune yolk tested in a dilution of 1:1000 in *P. amoebophila*-infected amoebae (data not shown).

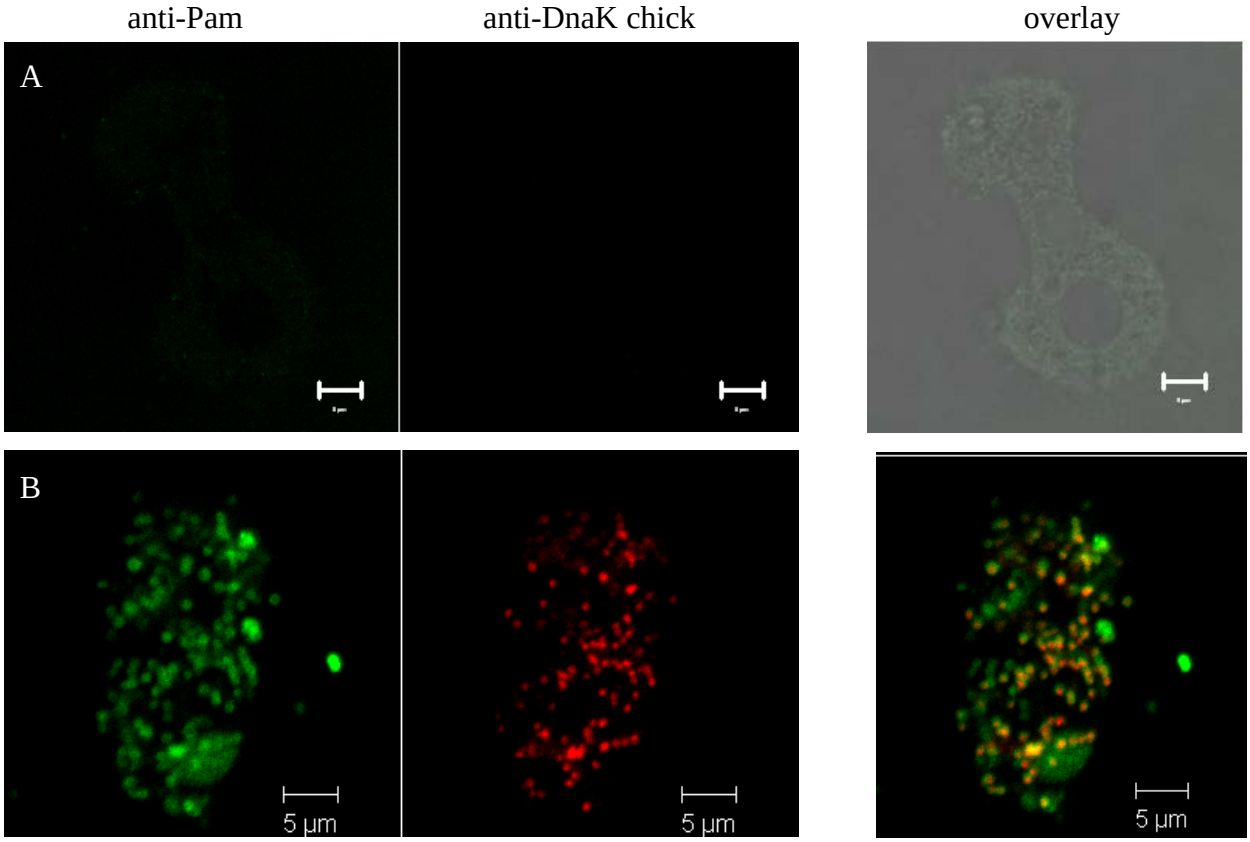

Figure 38. **Localization of DnaK visualized by immunofluorescence analysis.** Knob-shaped signales of DnaK can be seen in red surrounded by the green signals of anti-Pam (B).
No signals were observed in empty Neff if using anti-DnaK chick in the same dilution of 1:1000 (A). Bars 5 µm.

3.3.5.5 Western blot analysis with anti-DnaK chick antibody

Western blot using anti-DnaK chick was performed in the same way as done before with anti-DnaK gp. The tested ratio of inactivated antibody was 1:500, applying the pre-immune yolk in the same dilution in a parallel experiment.

Results resembled those of anti-DnaK gp shown in Figure 37A. A strong signal emerging from the overexpression of DnaK in *E. coli* was observed. As expected, the pre-immune serum showed no specific signals at all (results not shown).

4 Discussion

4.1 Towards the characterization of novel porins from P. amoebophila

The major aim of this study was to illuminate the nature and function of the four members of a recently discovered putative porin family. Heterologous expression followed by antibody production and lipid-bilayer measurements were performed to investigate the localization and function of the porin candidates.

Our knowledge about the outer membrane of environmental chlamydiae is still limited. No homologue of the major outer membrane protein (MOMP), the most dominant component of the outer membrane in the *Chlamydiaceae*, could be identified (Caldwell *et al.*, 1981), thus great differences in comparison to the clinical chlamydiae are assumed.

Recent studies provided first insights into the outer membrane composition of this novel chlamydial lineage by combining 1D and 2D gel electrophoresis with mass spectrometry (Heinz, 2008). Heinz *et al.* suggested a novel porin family that could be responsible for the functional substitution of MOMP (Heinz, 2008).
In silico analysis predicted a beta-barrel structure for two of these putative porins, namely pc1489 and pc1077, a characteristic feature of porins in general (Nikaido, 2003). The high abundance of pc1489 and pc1077 in outer membrane fractions additionally contributes to speculations about the importance of these potential porins (Heinz, 2008). As a result, the localization of pc1489 to the outer membrane and its function as a porin have already been shown in a previous study (Aistleitner, 2009).

4.1.1 Overexpression of outer membrane proteins – problems and solutions

Gene sequences are characterized by unique and subtle structural features, which may complicate gene expression as well as translational efficiency of mRNA, individual protein folding and degradation effects. Being aware of this, only some empirical “rules” but no standard procedure for protein overexpression exist (Makrides, 1996). Even though standing out due to extensive knowledge on its genetics and molecular biology, *E. coli* must not be seen as the answer for an efficient overexpression for every gene.

Even 30% of proteins from *E. coli* itself cannot be successfully overexpressed in the *E. coli* expression system (Vincentelli *et al.*, 2003).

4.1.1.1 Effects of different E. coli *strains for the overexpression of the four porin candidates*

Studies have shown that especially overexpression of outer membrane proteins is problematic, often achieving no efficient overexpression, since toxicity to the host is a common phenomenon observed during heterologous expression (Wagner *et al.*, 2006). In the present study various *E. coli* strains were tested in combination with different expression vectors for heterologous expression of the four putative porins, expecting improvement of the expression levels.

This work included experiments using the *E. coli* strain C43, a member of the so-called "Walker strains" derived from *E. coli* BL21 (DE3) (Miroux and Walker, 1996). Various studies could show that the use of *E. coli* C43 as an expression host correlates with successful overexpression of membrane components (Miroux and Walker, 1996; Rogl *et al.*, 1998; Korepanova *et al.*, 2001).

In most *E. coli* strains used for heterologous expression of proteins transcription is conducted at a very high speed, leading to high amounts of protein, which cannot be processed that quickly. Therefore, the process of insertion into the outer membrane is inhibited (Iost *et al.*, 1992). The Walker strains feature mutations in the lacUV5 promoter region, which exclusively controls the T7 RNA polymerase that is used to drive recombinant protein production in *E. coli* (Miroux and Walker, 1996). As the high transcription level can be reduced by these mutations, the Walker strain C43 was used for overexpression of the four putative porins. A low transcriptional rate would contribute to correct folding and processing of these outer membrane components without aggregation and further formation of inclusion bodies.

However, the use of *E. coli* C43 did not lead to a successful overexpression of the constructs based on the vectors pet21b and pet16b.

4.1.1.2 Effects of different vectors and tags for purification of overexpressed porin candidates

Different constructs were designed for an optimized heterologous expression of the four putative porins in *E. coli*.

Porins feature a leader sequence at the N-terminus, necessary for directing the nascent polypeptide to the outer membrane, where this "leader" gets finally cleaved (Mizuno *et al.*, 1983). Therefore, we focused on the vector pet 21b, featuring a 6x His at the C-terminus, which would not be affected by the cleavage of the N-terminal leader sequence of porins. This vector was successfully applied during overexpression of outer membrane proteins of *E. coli* (Shin *et al.*, 2005) and *Rickettsia japonica* (Uchiyama *et al.*, 2006), but no detectable overexpression of the porin candidates was achieved in the present study.
In addition, the vector pet16b was used, which has been successfully applied for the overexpression of inclusion membrane proteins of *P.amoebophila* (Heinz, 2004) and membrane proteins from *Mycobacterium tuberculosis* (Korepanova *et al.*, 2005). Also this attempt of heterologous expression of the porins failed during our work.

The vector pQE-30, based on the T5 promoter transcription–translation system (Bujard *et al.*, 1987), was further chosen for overexpression. Efficient repression of the powerful T5 promoter is ensured by the presence of high levels of the *lac* repressor protein. Therefore, an *E. coli* strain featuring the plasmid pREP4 is required for overexpression, since this plasmid constitutively expresses the *lac* repressor (Farabaugh *et al.*, 1978). As a result, our constructs based on the vector pQE-30 could not be overexpressed in *E. coli* C43 due to the requirement of the *E. coli* M15 host strain (Quiagen, The QIAexpressionist). Using this strain and the vector pQE-30 did not lead to a successful overexpression of native-leadered porin candidates, either.

There is an ongoing discussion in the literature about the effects of different fusion tags, since in general they are thought to have little influence on protein structure (Scholtz, 1995). However, it has been demonstrated that terminal extensions may change protein stability and folding properties (Korepanova *et al.*, 2001). A study by Alam *et al.* showed that some proteins are completely insoluble with an N-terminal histidine tag, whereas a C-terminal tag contributes to solubility in a favourable way (Alam *et al.*, 2002).

To date, polyhistidine tags (His-tags) are considered to be most effective for the expression of soluble proteins (Edwards *et al.*, 2000). Considering this and standing out due to it easy handling, this work focused on using the His-tag (Porath, 1992) as well as the GST-tag, encoding the glutathione-S-transferase (Smith and Johnson, 1988). The latter tag is characterized by the GST molecule featuring a molecular weight of 26 kDa, providing a possibility for masking a toxic protein (Terpe, 2003).

We used the vector pgEX-4T-3, which leads to an N-terminal fusion of the expressed protein with GST. The putative porins are considered to be problematic during overexpression due to their lethal effects, hence, the GST-tag may hide the original function from the *E. coli* host to finally get expressed and even processed without being recognized as harmful for the host cell. In addition, all pgEX vectors are engineered with an internal *lac*Iq gene which contributes to repression of the *tac* promoter, thus maintaining tight control over expression of the insert (GST Gene Fusion System, Amersham Biosciences).

Constructs based on the vector pgEX-4T-3 were overexpressed in *E. coli* C43 for low expression rates as well as in *E. coli* BL21(DE3), both strains deficient in known cytoplasmic protease gene products, as OmpT, DegP or HtpR. This special feature may assist in the expression of fusion proteins by minimizing the effects of proteolytic degradation by the host (Grodberg and Dunn, 1988; Strauch and Beckwith, 1988; Sugimura and Higashi, 1988).

Interestingly, the vector pgEX-4T-3 turned out to feature optimal conditions for heterologous expression of each of the four porins. We assumed that Western blot analysis showed processing of the proteins, since an additional band at about the expected molecular weight of the GST-tag (26 kDa), which was originally fused to the N-terminus of the leader sequence, got visible after overexpression. However, GST-fusion proteins are supposed to be quite unstable and spontaneous cleavage events of the GST-tag appear frequently (GST Gene Fusion System, Amersham Biosciences). Therefore, detection of a separated GST-tag by Western blot analysis does not directly imply correct processing and cleavage of the leader sequence.

4.1.1.3 Effects of changes in the leader sequence and the formation of inclusion bodies

Frequently, overexpression of membrane proteins can be achieved, though only in connection with the formation of inclusion bodies and no successful way of refolding into functional proteins (Drew *et al.*, 2003). Studies dealing with MOMP of clinical chlamydiae demonstrated the effects of changes in the leader sequence by comparing the expression levels of various constructs (Findlay *et al.*, 2005). Findlay *et al.* could show that overexpression of leaderless MOMP is connected to protein misfolding and aggregation, contributing to the formation of inclusion bodies and requiring refolding of the protein. Heterologous expression of MOMP was improved by using either the native leader or the *E. coli* OmpT leader under slow induction conditions (Findlay *et al.*, 2005).

These studies have clearly demonstrated that successful expression and processing apparently depend on the precise leader sequence (Findlay *et al.*, 2005). Based on these findings, our additional approach for porin overexpression contained a total cut-off of the signal sequence as well as its substitution with the *E. coli* leader sequence of the *ompT* gene (Baneyx, 1999). Using an *E. coli* leader sequence is supposed to affect correct processing in a favorable way (Baneyx, 1999). Correct incorporation into the outer membrane of *E. coli* would further offer the opportunity for functional analysis *in vivo*, testing transportation behavior in respect of nutrients or antibiotics, further illuminating the nature of the putative porins. Unfortunately, heterologous expression of pc1860, after substitution of its native leader sequence with the *E. coli* OmpT leader sequence, did not lead to detectable amounts of overexpressed protein.

During this work we had to cope with inclusion bodies, especially when using leaderless porins for overexpression experiments, being consistent with the findings for leaderless MOMP (Findlay *et al.*, 2005) and other leaderless outer membrane proteins (Bannwarth and Schulz, 2003). Inclusion bodies were visible as white colonies and pellets during and after overexpression experiments, implying problems for the *E. coli* host while dealing with this foreign protein.

Using the online tool “Recombinant protein solubility prediction” (www.biotech.ou.edu) we inspected the probability of inclusion body formation after overexpression of the porins. This method is based on six parameters only derived from the protein´s amino acid composition (Wilkinson and Harrison, 1991).

We compared the values for the four porin candidates with the cytoplasmic protein DnaK in Table 27, showing that the formation of inclusion bodies during overexpression of the porins was highly likely.

Table 27. Probability of the formation of inclusion bodies after overexpression of the porins using the online tool "Recombinant protein solubility prediction" (www.biotech.ou.edu)

Protein	Solubility prediction	Hints for inclusion bodies after overexpression
pc0870	85 % insoluble	yes
pc1077	80 % insoluble	yes
pc1489	79 % insoluble	yes
pc1860	88 % insoluble	yes
DnaK	58 % soluble	no

The aggregation of toxic proteins in inclusion bodies is an advantage if high amounts of pure protein are needed, as it contributes to suppression of the lethal effect on the host cells (Makrides, 1996). Since antibody production requires proteins of high purity and high concentration, the present study used the overexpression approach of the porin pc1077 without leader sequence for the generation of antibodies despite of the formation of inclusion bodies.

Inside inclusion bodies the overexpressed proteins are typically found in an insoluble and biologically inactive form. To address the problem of correct refolding chromatography or refolding in solution are proposed (Swietnicki, 2006). In addition, Singh *et al.* could show that mild solubilization contributes to high recovery of the bioactive native confirmation of proteins (Singh and Panda, 2005).

4.1.2 Hints for toxicity

The toxic effect of porins is derived from pore-forming activities by building holes in the outer membrane of *E. coli* cells with lethal effects (Koehler *et al.*, 1992; Findlay *et al.*, 2005). As different studies have already shown, the maintenance of a stable clone for MOMP turned out to be problematic (Pickett *et al.*, 1988; Koehler *et al.*, 1992) and this was also true in the present study during overexpression of the porins from *P. amoebophila*.

Studies by Koehler *et al.* visualized the lethal effects of MOMP for a foreign host by comparing induced and non-induced cells. Colony-forming-units were plotted over time, resulting in a dramatic drop already 10 min after induction, which was not as obvious in the actual cell culture (Koehler *et al.*, 1992). Notable hints for toxicity could hardly be observed in our studies of the four putative porins, since OD measurements at 600 nm revealed only slight differences between induced and non-induced *E. coli* cultures. In fact, differences in the cell density could only be observed for the induced culture expressing the porin pc1077 in the vector pgEX, therefore giving considerable evidence for pore-forming activity and resulting in reduced growing potential of the *E. coli* expression culture. Thus, it can be assumed that pc1077 features functional characteristics of a porin, but OD measurements did not show the final proof.

As a negative control, OD measurements during an overexpression of the cytoplasmic protein DnaK and the inclusion membrane protein pc1111 (kindly provided by Eva Heinz) were performed. The growth potential of *E. coli* cultures expressing the constructs for these two proteins did not show changes in comparison to *E. coli* cells without induction of overexpression, demonstrating that proteins of *P. amoebophila* are not *per se* toxic for *E. coli*. But effects of the tag or even the vector itself could contribute to wrong interpretations of the optical density of induced *E. coli* expression cultures. In fact, previous studies demonstrated that plasmids and associated tags even without any insert can have lethal effects on *E. coli* host cells (Miroux and Walker, 1996; Dumon-Seignovert *et al.*, 2004; Wagner *et al.*, 2007).
Thus, it remains questionable to directly link reduced growing potential to lethal effects due to pore-forming activities of the porins.

An observation after transformation of the respective *E. coli* cells with the construct for overexpression hints at toxic effects of the porin candidates pc1077 and pc0870, though. Reduced growing potential on agar plates could be directly linked to positive screening results, since badly grown clones were shown to carry a plasmid with the desired porin as insert.
This observation gives an additional proof of correct processing, incorporation into the outer membrane and negative or even lethal effects for *E. coli* host cells.

4.1.3 Disulfide bridges of the putative porins in a reducing environment

According to sequence analyses, the four putative porins of *P. amoebophila* contain a high number of cysteines, an unexpected feature of porins in general (Nikaido, 2003). Challenges of expressing disulfide-rich proteins arise from the reducing conditions of the cytoplasm of *E. coli* cells (Stewart *et al.*, 1998). As disulfide formation requires cysteine oxidation, this process naturally takes place within the periplasmic space in *E. coli*.

Heterologous expression of the porins in an *E. coli* host cell takes place in the cytoplasm of the cell, thereby exposing the newly processed protein to a more reducing potential (Baneyx and Mujacic, 2004). Little is known about the involvement of intramolecular disulfide bonds for correct structural folding of cysteine-rich proteins. Hence, an overexpression of these putative porins in a reducing environment would probably result in formation of aggregates and inclusion bodies.

Considering these general findings, an explanation for the failure of different overexpression constructs of the putative porins during this work can be hypothesized. In many approaches no changes in the expression level could be detected possibly due to unfolding or aggregation of proteins. Therefore, an unexpected running behaviour on SDS-PAGE gels seems possible.

4.1.4 Localization of pc1860 in the outer membrane of *E. coli* host cells

After heterologous expression of MOMP in *E. coli*, immunofluorescence experiments with anti-MOMP antibodies clearly visualized the localization either in the outer membrane of the *E. coli* host cells or in inclusion bodies if a construct without leader sequence was overexpressed (Findlay *et al.*, 2005).

We wanted to demonstrate incorporation of the porin pc1860 into the outer membrane, after correct processing and folding, by immunofluorescence analysis with *E. coli* cultures after an overxpression of native-leadered pc1860 in the vector pgEX. By comparing induced *E. c*oli C43 cells without a vector and an induced expression culture of the same strain, indications for incorporation into the outer membrane got visible.

Signals of the anti-GST antibody appeared in the induced expression culture, but not in the control cells, suggesting an expression of pc1860 as a fusion protein with GST. Detection of the N-terminal GST-tag in the outer membrane would reflect problems during processing (Mizuno *et al.*, 1983). Cutting off the leader sequence, fused to GST, seemed to be disturbed leading to incorporation of the whole length protein into the outer membrane. Arguing against a proper incorporation, it could be hypothesized that the porin was just expressed as a fusion protein with GST, without processing and translocation to the correct place.

Another theory suggests that the signal peptide, linked to the GST-tag, was cut off and the mature porin was exposed to the surface. Hence, staining with anti-GST antibodies would detect the signal peptides tagged with GST and not the actual porin of interest.

4.1.5 Localization of the porin candidate pc1077

Pc1077 and pc1489 are considered to be responsible for the substitution of MOMP of the *Chlamydiaceae* (Heinz, 2008), hence their localization in the outer membrane of *P. amoebophila* should get clearly visible by staining with specific antibodies. Previous studies using anti-pc1489 antibodies showed a halo-shaped signal, consisting of single signals from incorporated pc1489 in the outer membrane (Aistleitner, 2009). Moreover, pc1489 was successfully visualized as a component of the outer membrane by transmission electron microscopy (pictures taken by Jacqueline Montanaro).

As pc1077 and pc1489 could be equally detected in outer membrane fractions (Heinz, 2008), maybe due to their high occurrence, we suggested that pc1077 and pc1489 are functionally interacting or even linked to each other. Antibodies against pc1077 could be used for further analysis of interactions between pc1489 and pc1077, either during immunofluorescence experiments or for Western blot analysis, maybe contributing to our understanding of the unexpected running behavior of pc1489 on SDS-PAGE gels, since this phenomenon was observed in Western blots by Karin Aistleitner.

4.1.5.1 Unexpected signals from the pre-immune serum in immunofluorescence analysis

Unexpected signals were observed when using the pre-immune serum on *P. amoebophila*-infected amoebae. Since chlamydiae are ubiquitous (revisited by Horn, 2008), a former chlamydial infection of the rabbits is a possible explanation. In this case, chlamydia-specific antibodies would have already been present before the actually planned immunization.

Notably, Western blot analysis confirmed that the large bleed contained pc1077-specific antibodies, visualized by an additional band at the expected molecular weight beside the unspecific background in *E. coli*. Evidence for specificity of the anti-pc1077 antibody is given, though a successful usage in IF was not realized.

Recent studies on outer membrane fractions of *P. amoebophila* proved the fact of specific binding capacities of anti-pc1077 antibodies in comparison to the pre-immune serum. Detection of pc1077 (39 kDa) was clearly demonstrated in Western blot experiments beside the detection of bands of lower molecular weight than expected, when using anti-pc1077 antibodies (analysis done by Karin Aistleitner). These findings are in accordance with results of mass spectrometry performed with COMC, where pc1077 was also detected in bands of lower molecular weight than 39 kDa (Heinz, 2008). To date, further processing of pc1077 or degradation effects represent unknown issues and remain to be analyzed.

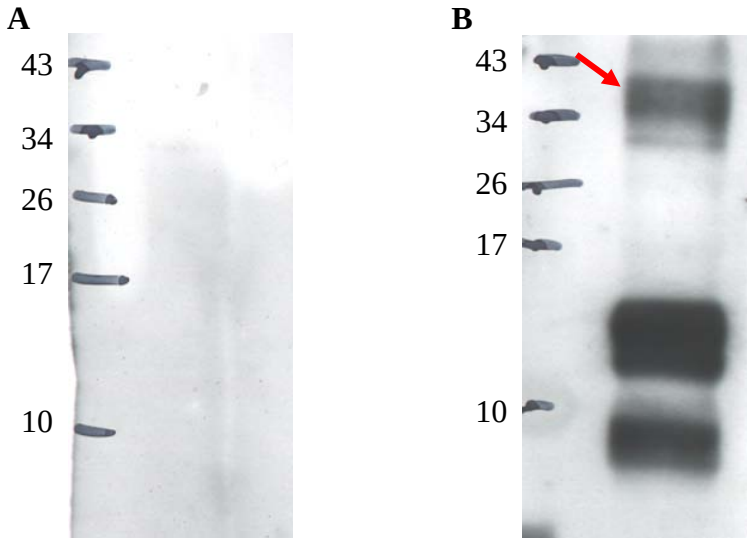

Figure 39. Detection of pc1077 in the outer membrane fraction of *P. amoebophila* by anti-pc1077 antibodies (B, red arrow). In comparison, the pre-immune serum did not show any signals at all (A). Additional bands of lower molecular weight than expected were visualized by anti-pc1077 maybe due to degradation and further processing of the porin pc1077. Antibodies were applied 1:500.

4.1.5.2 Immunogenic potential of pc1077

In contrast to naturally folded pc 1489 (Aistleitner, 2009), pc1077 without leader sequence cannot be considered as a highly immunogenic antigen, since the reaction of the immune system and the production of specific antibodies seems to be repressed. Even with the large bleed, no strong and specific signals for the outer membrane could be observed by IF.

The weak specificity of anti-pc1077 antibodies in immunofluorescence experiments potentially reflects problems during the process of purification. The involvement of co-purified *E. coli* proteins has to be considered (Graslund *et al.*, 2008), therefore triggering the antibodies against additional proteins of *E. coli* origin and leading into weak affinity to the original target pc1077.

Low immunogenic reactions may correlate with the use of urea as a strong denaturing agent during protein purification (Brandts and Hunt, 1967). The application of urea got essential, since insoluble pc1077 aggregated in inclusion bodies during the process of overexpression, but maybe affected the potential of pc1077 as an antigen in a negative way. Defolding and denaturing of proteins are considered to have non-predictable consequences during immunogenic reactions of the host´s immune system. The major antigenic determinant could be lost after denaturation in 8M urea (Ishizaka *et al.*, 1975), contributing to reduced specificity of the antibody if encountering the mature and correctly folded protein *in vivo* or fixed.

In an additional approach, purification without urea was performed. Although the amount of soluble protein was considerably low, one of the purified fractions appeared suitable for further analysis by showing an adequate amount of pc1077 and a high grade of purity. To date, the effects of using pc1077 in its natural folding for the production of specific antibodies were not known.

4.1.6 Functional analysis of pc1077

In general, lipid bilayer measurements provide the opportunity for an accurate determination of existing pore-forming proteins in a sample (Benz *et al.*, 1988; Findlay *et al.*, 2005). As the function of pc1489 as a porin was confirmed already with the help of this method (Aistleitner, 2009), it was also applied to elucidate the functional nature of pc1077 in more detail. A functional similarity could be reasoned (Heinz, 2008).

The amino acid sequence similarity within the four members of the putative porin family of *P. amoebophila* was determined as 22-28% (Heinz, 2008), but a functional prediction based on similarities only is not possible. However, in the COMC of *C. trachomatis* a protein with about 20% sequence identity to MOMP could be identified. This protein known as PorB was shown to have an even more specific porin function compared to MOMP (Kubo and Stephens, 2000). In contrast, the three dominant porins of *E. coli*, OmpC, OmpF and PhoE, share about 60 % sequence homology and just vary slightly in ion-selectivity and pore size (Mizuno *et al.*, 1983).

Also MOMPs of *C. psittaci* and *C. trachomatis* differ significantly in ion selectivity, suggesting that selectivity for cations or anions results from the variable domains exposed to the surface (Hughes *et al.*, 2001). Referring to these findings, the putative porins of *P. amoebophila* could show functional differences, including different expression patterns during an infectious cycle or variations in the ion-selectivity.

During lipid bilayer measurements, the sample which is supposed to contain a porin is added to artificial lipid bilayers followed by a stepwise increase in conductance. Each step indicates incorporation of one pore into the membrane (Benz *et al.*, 1988). Unfortunately, lipid-bilayer measurements could not give the expected proof of the function of pc1077 as a porin, since we had to encounter some unexpected problems with the negative control. This negative control was created under exactly the same conditions as the actual sample after overexpression of pc1077. However, a contamination with the *E. coli* porin OmpF (Mizuno *et al.*, 1983) was detectable in the negative control, making the data obtained by these lipid-bilayer measurements insignificant. Even though pores were detected in the sample, it remains questionable whether they actually originated from a contamination with *E. coli* porins or from the analyzed putative porin pc1077.

This work did not concentrate on correct refolding of pc1077, thus its purification out of inclusion bodies may also have negative effects on functional analysis of pc1077 by lipid-bilayer measurements.

4.1.6.1 Avoiding contaminations with the E. coli *porin OmpF*

The co-purification of OmpF with a His-trap column cannot be explained easily (Graslund *et al.*, 2008). Interestingly, only one histidine resides in the amino acid sequence of OmpF, making the co-purification of this *E. coli* porin even more inexplicable (Klebba *et al.*, 1990).

One single porin represents the detection limit of lipid-bilayer measurements, hence the use of other purification methods could ensure samples of high purity without *E. coli* contaminations. Separation of pc1077 from OmpF seems to be possible due to differently predicted isoelectric points (Tudor and Karp, 1994; environmental chlamydia genome database). Also anti-OmpF antibodies could be used to detect contaminations in future approaches (Fourel *et al.*, 1992).

Repetition of lipid-bilayer measurements is planned, analyzing purified pc1077 which was not exposed to the strong denaturing agent urea and did not undergo the process of precipitation after purification in order to maintain the natural secondary structure of pc1077. Additionally, unspecific binding of proteins with no His-tag, like *E. coli* porins, to a His-trap column may be reduced due to the natural folding of proteins, which have not been denatured by urea.

The aggregation and binding of unspecific proteins to the matrix can be assumed if no His-tagged proteins are bound to the column (Waugh, 2005). But even in the presence of His-tagged pc1077, showing high affinity to the binding matrix, a co-purification cannot be excluded, since again *E. coli* proteins could stick unspecifically to the column followed by co-elution at a distinct imidazole concentration. Also the impact of urea has to be considered, as discussed above.

Knock-out strains offer the perfect possibility to exclude a possible contamination with *E. coli* porins (Bannwarth and Schulz, 2003). As an example, *E. coli* BL21*(DE3)omp8* is a porin-deficient strain that lacks the outer membrane proteins OmpF, OmpC, OmpA, and LamB (Prilipov *et al.*, 1998). Hence, successful overexpression of pc1077 in this strain seems to be possible followed by purification, where the co-purification of other *E. coli* porins can be reduced. Though the expression construct of pc1077 without leader sequence is based on the vector pQE-30, which requires the *E. coli* M15 strain, characterized by containing the plasmid pREP4, as host. The *lac* repressor encoded on this plasmid ensures a tightly regulated expression and the optimal conditions for the process of overexpression (The QIAexpressionist, Quiagen).
Nevertheless, pQE-30 has been successfully tested in other *E. coli* expression strains during our work, leading to detectable levels of heterologously expressed porins.

As a conclusion, these different methods provide the opportunity to finally create samples applicable for lipid-bilayer measurements.

4.2 Transcription analysis of pc1489 during an infectious cycle

Recent studies demonstrated that the porin pc1489, one member of the novel putative porin family of *P. amoebophila*, is present throughout the whole developmental cycle by using specific antibodies (Aistleitner, 2009). Hence, the presence of this protein in EBs as well as in RBs was proven, comparable to results of studies with MOMP of clinical chlamydiae (Hatch *et al.*, 1986). However, increased signal intensity at later time points could not be clearly explained. Incorporation of newly synthesized pc1489 into the outer membrane or structural changes of pc1489, which led to better binding of anti-pc1489 antibodies to its target protein, could be responsible for this increase in signal intensity at later time points of the developmental cycle (Aistleitner, 2009).

We studied the expression pattern of pc1489 during a developmental cycle, based on studies with clinical chlamydiae (Belland *et al.*, 2004; Maurer *et al.*, 2007). Accordingly, we chose distinct time points for the transcription analysis of pc1489 until 96 h post infection (h p.i.). This last time point represents the end of one complete developmental cycle of *P. amoebophila* and is characterized by the release of infectious EBs (König, 2008).

4.2.1 Gene expression profiles - early vs. late genes

Studies of pathogenic chlamydiae identified subsets of genes belonging to different clusters, according to their transcriptional pattern throughout an infectious cycle (Belland *et al.*, 2003; Gomes *et al.*, 2005; Maurer *et al.*, 2007)). Different gene categories, like the “early” and the “late” gene-clusters, were proposed. Additionally to the third “mid” genes, Mäurer *et* al proposed a fourth cluster class, the so called “tardy” genes (Maurer *et al.*, 2007).

A previous study concentrated on the expression pattern of the heat shock protein GroEL of *P. amoebaphila*, identifying GroEL as a member of the immediate-early genes (Haider, 2004). According to the findings of Belland *et al*., this heat shock protein is involved in processes occurring quite early during an infection. Haider *et al.* observed an increase of transcription at 24 h p.i. (Haider, 2004), whereas GroEL of *C. trachomatis* showed changes in the expression levels already within 6 h p.i. (Belland *et al.*, 2003; Gomes *et al.*, 2005).

We focused on the expression profile of the porin pc1489 of *P. ameobophila*. Previous studies with *C. trachomatis* and *C. pneumoniae* could show that especially genes encoding structural components for outer membrane stability are associated with the late gene cluster, like the cysteine-rich proteins OmcA and OmcB (Belland *et al.*, 2003; Gomes *et al.*, 2005; Maurer *et al.*, 2007). Moreover, it was shown that expression of *ompA* encoding MOMP of *C. trachomatis* was upregulated later in the development in comparison to the heat shock protein GroEL (Gomes *et al.*, 2005). Hence, we aimed to identify the cysteine-rich porin pc1489 as a possible member of the "late" gene-cluster expecting a similar expression pattern as outer membrane components of clinical chlamydiae.

Transcription analysis showed a 10-fold increase of normalized pc1489 RNA at the latest time point 96 h p.i., being in accordance with characterization as a late gene. However, it does not demonstrate the drastic differences like the expression profile of *ompA* in *C. trachomatis*, where a 17-fold increase between 6 and 24 h p.i. was observed (Gomes *et al.*, 2005). In *C. trachomatis*, the time point 24 h p.i. is associated with the beginning of late stages of the developmental cycle. At this growth phase a lot of membrane components for newly formed organisms are needed (Hatch *et al.*, 1986).

4.2.2 pc1489 carry-over mRNA

Interestingly, the copy numbers of pc1489 seem to be notably high throughout the whole developmental cycle. This observation suggests that high rates of carry-over mRNA from RBs to EBs correlate with the high importance of pc1489 in the outer membrane. This would be in accordance with findings of MOMP, as Gomes *et al.* detected a constantly higher level of *ompA* mRNA in comparison to groEL mRNA throughout the development, including a high level of carry-over mRNA at 2 h p.i. (Gomes *et al.*, 2005).

The decrease of transcripts 24 h p.i. is not reflecting a transcriptional decrease but since not all EBs are able to infect a host cell at 0 h p.i., the excess EBs and their mRNA were removed after this initial infection, leading to a decrease in detectable mRNA 24 h p.i.. Carry-over mRNA does not always appear to be translationally active immediately, since studies of clinical chlamydiae could show that *omcA* mRNA is not directly linked to *omcA* synthesis early in infection (Hatch *et al.*, 1986; Douglas and Hatch, 2000).

Findings of qPCR of the present study primarily reflect that the expression profile of pc1489 resembles those of other outer membrane proteins of the *Chlamydiaceae* (Belland *et al.*, 2003; Maurer *et al.*, 2007). An up-regulation during late stages of the developmental cycle identified pc1489 as a member of the "late" gene-cluster and clearly visualizes the importance of pc1489 in processes of re-differentiation from RBs to infectious EBs. High amounts of carry-over mRNA further suggest a high importance of pc1489 as an outer membrane component in general.

4.3 Conclusion

4.3.1 Characterization of novel porins from *P. amoebophila*

Outer membrane proteins of *P. amoebophila* are considered to be key players in the initial steps of host cell invasion. In this work, preliminary insights into the nature of the four members of a recently discovered putative porin family were obtained. Although porin function and localization were not clearly identified, constitutive experiments promise to show significant results. Successful overexpression of each of the four putative porins represents the optimal basis for future studies focusing on the nature, structure or function of outer membrane proteins.

Moreover, the developmental expression of pc1489, one member of the putative porin family, was analyzed. An increased transcription of pc1489 towards the end of the cycle identified this porin as a "late" gene with an important role throughout the whole cycle. High amounts of transcripts were detectable in both EBs and RBs validating the results of previous immunofluorescence experiments (Aistleitner, 2009).

4.3.2 Generation of an internal standard for immunofluorescence experiments

The heat-shock protein DnaK was chosen for the generation of a new standard antibody characterized by intracellular localization. These intracellular signals for DnaK help to show permeability of cells if other antibodies were applied simultaneously.

Since DnaK is a highly conserved protein throughout different organisms, antibodies against DnaK of *P. amoebophila* also detect homologues of this protein in *Waddlia chondrophila* and *Simkania negevensis* (analyses done by Karin Aistleitner and Barbara Sixt).

As a conclusion, anti-DnaK antibodies were created and the usage as a new standard antibody in immunofluorescence experiments was successfully tested.

5 Summaries

5.1 Abstract

The phylum *Chlamydiae* comprises important pathogens for humans and animals. They all share an obligate intracellular lifestyle and a characteristic biphasic developmental cycle. Attachment and entering a host cell represent crucial steps, and outer membrane proteins are considered to be key players during these first steps of infection.

This work focused on the characterization of four putative porins from *P. amoebophila* - pc0870, pc1077, pc1489 and pc1860 - which are proposed for being responsible for the substitution of the major outer membrane protein (MOMP) of the *Chlamydiaceae*. Using *E. coli* for heterologous expression of these four porin candidates, various expression vectors were tested in different *E. coli* strains under optimized conditions. Finally, all members of the putative porin family were successfully overexpressed, as shown by SDS-PAGE and Western blot analysis, and used for further analysis.

During heterologous expression we tried to detect toxic effects of the putative porins if processed correctly and incorporated into the outer membrane of *E. coli*. Thereby formed channels are supposed to have lethal effects on the foreign host. However, measurements of the optical density did not contribute to a functional characterization of the putative porins. Also lipid-bilayer measurements, suitable for an accurate determination of existing pore-forming proteins, did not validate the function of the putative porins because of contaminations with the *E. coli* porin OmpF in the negative control. Moreover, antibodies against one of the putative porins, namely pc1077, were generated to visualize localization of the proposed porin in the outer membrane of *P. amoebophila* by immunofluorescence analysis.

Additionally, qPCR promised new insights into the transcriptional profil of the porin pc1489. Based on findings of outer membrane proteins of clinical chlamydiae, pc1489 is regarded as a member of the late gene cluster, being important during late stages of the developmental cycle. This supports the theory of pc1489 as a key player during the process of re-differentiation from RBs to EBs, where outer membrane stability is of particular importance.

A third project focused on the generation of a standard antibody for immunofluorescence analyses. If antibodies targeting outer membrane components of *P. amoebophila* are applied, a standard antibody against an intracellular protein has to be used simultaneously in order to demonstrate permeability of the cells. For this purpose, the cytoplasmic protein DnaK was successfully overexpressed in *E. coli*, followed by generation of specific antibodies. The specificity of these anti-DnaK antibodies was successfully tested in immunofluorescence experiments by showing intracellular localization and was also proven by Western blot analysis. In addition, cross-reactivity of this new standard antibody was tested, since DnaK is a highly conserved protein throughout different organisms. As a result, antibodies against DnaK of *P. amoebophila* also detect homologues of this protein in *Waddlia chondrophila* and *Simkania negevensis.*

This work is regarded as a basis for follow-up studies of the structure and function of outer membrane components from *P. amoebophila* and their involvement during initial stages of host-cell invasion.

5.2 Zusammenfassung

Das Phylum *Chlamydiae* beinhaltet einige wichtige bakterielle Krankheitserreger, die sowohl für den Menschen als auch für die Tierwelt eine potentielle Gefahr darstellen. Alle Chlamydien zeichnen sich durch eine obligat intrazelluläre Lebensweise aus, die mit einem charakteristischen Lebenszyklus in Verbindung gebracht werden kann. Eine kritische Phase stellt dabei das Eintreten des Bakteriums in die eukaryotische Wirtszelle dar, bei der Außenmembranproteinen eine wichtige Rolle spielen.

Im Zuge dieser Diplomarbeit wurde an der Charakterisierung einer kürzlich entdeckten Porin-Familie aus *P. amoebophila* gearbeitet, deren Mitglieder - pc0870, pc1077, pc1489 und pc1860 - möglicherweise die Funktion des „major outer membrane protein“ (MOMP) der klinischen Chlamydien ersetzen könnten. *E. coli* wurde als geeignetes Modelsystem herangezogen, um die vier potentiellen Porine unter optimalen Bedingungen heterolog zu exprimieren. Dafür wurden verschiedene Expressionsvektoren in unterschiedlichen *E. coli* Stämmen eingesetzt. Als Ergebnis konnte schlussendlich die Überexpression von allen vier Porin-Kandidaten mittels SDS-PAGE und Western Blot Analyse detektiert und für weiterführende Experimente verwendet werden.

Mit Hilfe heterologer Expression sollten mögliche toxische Auswirkungen der potentiellen Porine auf die *E. coli* Wirtszelle nachvollzogen werden. Mittels Messungen der optischen Dichte konnte jedoch nicht eindeutig gezeigt werden, dass die Porine Kanäle in der Außenmembran bilden und somit letale Auswirkungen auf die Wirtszelle haben. Zusätzlich sollten Messungen an künstlichen Lipid-Membranen eine klare Aussage über die Funktion der potentiellen Porine liefern, aber auch diese Methode erzielte leider nicht die gewünschten Resultate. Es konnte jedoch eine Grundlage für Verbesserungen zukünftiger Experimente geschaffen werden und aussagekräftige Messungen zur Bestimmung der Funktion als Porin scheinen durchführbar und auch viel versprechend.
Weiters wurde die Produktion von Antikörpern als geeignete Methode gewählt, um die Lokalisierung des Porins pc1077 in der Außenmembran von *P. amoebophila* zu zeigen.

In einem zusätzlichen Projekt wurde das Transkriptionsprofil von pc1489 mittels qPCR untersucht. Die daraus resultierenden Ergebnisse entsprachen den Erwartungen, die von Studien der Außenmembrankomponenten von klinischen Chlamydien abgeleitet werden konnten. pc1489 wurde somit dem „late gene“ Cluster zugeordnet, dessen Mitglieder vor allem zu späteren Zeitpunkten des Entwicklungszyklus große Wichtigkeit zugesprochen wird. Dieses Ergebnis unterstützt die Theorie, pc1489 als Schlüsselfaktor im Prozess der Umstrukturierung von RBs zu EBs zu sehen, während dem hohe Stabilität der Außenmembran von größter Bedeutung ist.

Im Rahmen eines dritten Projektes wurde ein neuer Standardantikörper generiert, um mit Immunfluoreszenz Zellpermeabilität zu demonstrieren. Bei der Verwendung von Antikörpern, die gezielt Komponenten der Außenmembran von *P. amoebophila* detektieren sollen, ist der Vergleich zu intrazellulären Signalen essentiell, um signifikante Aussagen machen zu können. Zu diesem Zweck wurde das cytoplasmatische Protein Dnak erfolgreich in *E. coli* überexprimiert und spezifische Antikörper wurden generiert. Die Spezifität dieser Antikörper konnte mittels Immunfluoreszenz visualisiert und durch Western Blot Analysen bestätigt werden. Außerdem wurde der neu generierte Standardantikörper gegen DnaK von *P. amoebophila* erfolgreich für die Detektion homologer Proteine in *Waddlia chondrophila* und *Simkania negevensis* eingesetzt.

Diese Arbeit bietet eine viel versprechende Grundlage, um unser Wissen im Hinblick auf die Außenmembranbestandteile von *P. amoebophila*, ihrer Funktionen und Strukturen und letztendlich ihrer Rolle während des ersten Kontakts von Chlamydien mit ihren Wirtszellen zu vertiefen.

6 List of abbreviations

16S rRNA	small ribosomal subunit RNA
1D	one-dimensional
2D	two-dimensional
3`	three prime end of nucleic acids
5`	five prime end of nucleic acids
%	percentage
°C	degree celcius
λ	wavelength
µ	micro (10^{-6})
Ø	diameter
A.	*Acanthamoeba*
A	adenine
ab	antibody
ACN	acetonitrile
Amp	ampicillin
APS	ammonium persulfate
ARB	software package for phylogenetic analyses (from lat. *arbor*)
ATP	adenosine-5'-triphosphate
bidest.	bidestillatus (double destilled)
BLAST	basic local alignment search tool
bp	base pairs
BSA	bovine serum albumin
c	centi (10^{-2})
C.	*Chlamydia* or *Chlamydophila*
C	cytosine
CA	California
Cam	Chloramphenicol
CBs	crescent bodies
cDNA	complementary DNA
CLSM	confocal laser scanning microscope
COMC	chlamydia outer membrane complex
Corr	correlation coefficient

Cy2	5,5`-di-sulfo.1,1`-di-(X-carbopentynyl)-3,3,3`,3`-tetra-methylindol-Cy2.18-derivative N-hydroxysuccimidester
Cy3	5,5`-di-sulfo.1,1`-di-(X-carbopentynyl)-3,3,3`,3`-tetra-methylindol-Cy3.18-derivative N-hydroxysuccimidester
Cy5	5,5`-di-sulfo.1,1`-di-(X-carbopentynyl)-3,3,3`,3`-tetra-methylindol-Cy5.18-derivative N-hydroxysuccimidester
Da	Dalton, unit of mass
DAPI	4', 6-diamidino-2-phenylindole
ddNTPs	didesoxynucleotides
DDT	dithiothreitol
DEPC	di-ethyl-pyrocarbonate
DIC	differential interference contrast
DNA	desoxyribonucleic acid
DNase	desoxyribonuclease
dNTP	desoxyribonucleotide triphosphate
E.	Escherichia
EB(s)	elementary bodies
EDTA	ethylenediaminetetraacetic acid
e.g.	exempli gratia (lat., "example given")
et al.	et alteri (lat., "and others")
EtBr	ethidium bromide
EtOH	ethanol
EtOHabs.	ethanol absolute
F	forward (used for labelling of primers)
FA	formamide; formaldehyde
Fig.	figure
FITC	fluorescein isothiocyanate
g	gram
G	guanine
GST	glutathion-S-transferase
h	hour(s)
H_2O	water
H_2O_2	hydrogen peroxide
H_2O_{dd}	double distilled and filtered water

HCl	hydrochloric acid
HEPES	(4-(2-hydroxyethyl)-1-piperazineethanesulfonic acid)
h p.i.	hours post infection
HPLC	high performance liquid chromatography
His	histidine
HRP	horseraddish-peroxidase
Hsp	heat shock protein
Hsp60	heat-shock protein 60
i.	induced (by 1mM IPTG)
IF	immunofluorescence
Ig	Immunglobulin
in prep.	in preparation
IPTG	Isopropyl-β-D-thiogalactopyranosid
k	kilo
Kan	kanamycin
KBL	kilobase-ladder (DNA length standard)
KCL	potassium chloride
KH_2PO_4	potassiumdihydrogenphosphate
l	liter
LB	Luria Bertani
LC	liquid chromatography
LPS	lipopolysaccharides
m	milli (10^{-3}), meter
M	molar
MALDI	matrix-assisted laser desorption/ionization
Mg	magnesium
$MgCl_2$*6 H_2O	magnesium chloride hexahydrate
$MgSO_4$*7 H_20	magnesium sulfate heptahydrate
min	minute(s)
MOI	multiplicity of infection
MOMP	major outer membrane protein
mRNA	messenger RNA
MS	mass spectrometry
MS/MS	tandem mass spectrometry

MW	molecular weight
n	nano (10^{-9})
Na_2HPO_4*2 H_2O	disodiumhydrogenphosphate dihydrate
NaH_2PO_4*H_2O	sodiumdihydrogenphosphate monohydrate
NaCl	sodium chloride
NaOH	sodium hydroxide
NCBI	National Center for Biotechnology Information
Neff	*Acanthamoeba castellanii* Neff
Neff/E25	*A. castellanii* Neff asynchronously infected with *P. amoebophila*
n.i.	not induced (by 1mM IPTG)
n.- i.	non-infected
NJ	New Jersey
OD	optical density
o/n	over night
p	pico
P.	*Protochlamydia*
p.a.	pro analyticum (grade of purity)
PAGE	polyacrylamide gel electrophoresis
PAS	Page's amoebic saline
PBS	phosphate buffered saline
PCR	polymerase-chain-reaction
PFA	paraformaldehyde
pgEX	vector pgEX-4T-3
PMP	polymorphic outer membrane protein
pQE	vector pQE-30
PYG	peptone-yeast extract-glucose
qPCR	quantitative polymerase-chain-reaction
r	radius
R	reverse (used for labelling of primers)
RB(s)	reticulate bodies
rcf	relative centrifugal force
RNA	ribonucleic acid
rpm	revolutions per minute
rRNA	ribosomal RNA

RT	room temperature, reverse transcriptase
S	Siemens
sec	seconds
SD	standard deviation
SDS	sodium dodecyl sulfate
sp.	species
SPG	sucrose-phosphate-glutamate
T	thymine
Ta	annealing temperature
tab.	table
TAE	Tris-acetate-EDTA
Taq	thermostable DNA-polymerase from *Thermus aquaticus*
TB	Terrific Broth
TCA	tricarboxylic acid cycle
TEMED	N,N,N´,N´-tetramethylethane-1,2-diamine
Tm	melting temperature
TOF	time-of-flight mass analyzer
Tris	trishydroxymethylaminomethane
TSY	trypticase soy broth with yeast extract
u	unit
UK	United Kingdom
USA	United States of America
UV	ultraviolet
UWE	University of Washington environmental isolate
V	volt
Vol.	volume(s)
v/v	volume to volume
vs.	versus
WA	Washington
WI	Wisconsin
w/v	weight to volume
w/w	weight per weight
x	times

7 References

Abdelrahman, Y. M. and Belland, R. J. (2005). The chlamydial developmental cycle. *FEMS Microbiol Rev* **29**(5): 949-59.

Aistleitner, K. (2009). Characterization of a novel porin from Protochlamydia amoebophila

Alam, M., Ho, S., et al. (2002). Heterologous expression, purification, and characterization of human triacylglycerol hydrolase. *Protein Expr Purif* **24**(1): 33-42.

Altschul, S. F., Gish, W., et al. (1990). Basic local alignment search tool. *J Mol Biol* **215**(3): 403-10.

Amann, R., Springer, N., et al. (1997). Obligate intracellular bacterial parasites of acanthamoebae related to Chlamydia spp. *Appl Environ Microbiol* **63**(1): 115-21.

Amberger, A., Maczek, C., et al. (1997). Co-expression of ICAM-1, VCAM-1, ELAM-1 and Hsp60 in human arterial and venous endothelial cells in response to cytokines and oxidized low-density lipoproteins. *Cell Stress Chaperones* **2**(2): 94-103.

Baehr, W., Zhang, Y. X., et al. (1988). Mapping antigenic domains expressed by Chlamydia trachomatis major outer membrane protein genes. *Proc Natl Acad Sci U S A* **85**(11): 4000-4.

Baneyx, F. (1999). Recombinant protein expression in Escherichia coli. *Curr Opin Biotechnol* **10**(5): 411-21.

Baneyx, F. and Mujacic, M. (2004). Recombinant protein folding and misfolding in Escherichia coli. *Nat Biotechnol* **22**(11): 1399-408.

Bannwarth, M. and Schulz, G. E. (2003). The expression of outer membrane proteins for crystallization. *Biochim Biophys Acta* **1610**(1): 37-45.

Barker, J. and Brown, M. R. (1994). Trojan horses of the microbial world: protozoa and the survival of bacterial pathogens in the environment. *Microbiology* **140 (Pt 6)**: 1253-9.

Barker, W. C., Garavelli, J. S., et al. (1998). The PIR-International Protein Sequence Database. *Nucleic Acids Res* **26**(1): 27-32.

Baud, D., Thomas, V., et al. (2007). Waddlia chondrophila, a potential agent of human fetal death. *Emerg Infect Dis* **13**(8): 1239-43.

Bavoil, P., Ohlin, A., et al. (1984). Role of disulfide bonding in outer membrane structure and permeability in Chlamydia trachomatis. *Infect Immun* **44**(2): 479-85.

Beatty, W. L., Byrne, G. I., et al. (1994). Repeated and persistent infection with Chlamydia and the development of chronic inflammation and disease. *Trends Microbiol* **2**(3): 94-8.

Bedson, S. P., J. O. W. Bland (1932). A morphological study of psittacosis virus, with the description of a developmental cycle. *Br. J. Exp. Pathol.* **13**: 461-466.

Belland, R. J., Ouellette, S. P., et al. (2004). Chlamydia pneumoniae and atherosclerosis. *Cell Microbiol* **6**(2): 117-27.

Belland, R. J., Zhong, G., et al. (2003). Genomic transcriptional profiling of the developmental cycle of Chlamydia trachomatis. *Proc Natl Acad Sci U S A* **100**(14): 8478-83.

Benz, R. (2004). Bacterial and Eukaryotic Porins. Weinheim, WILEY-CH Verlag GmbH & Co. KGaA.

Benz, R., Schmid, A., et al. (1988). Characterization of the nucleoside-binding site inside the Tsx channel of Escherichia coli outer membrane. Reconstitution experiments with lipid bilayer membranes. *Eur J Biochem* **176**(3): 699-705.

Blattner, F. R., Plunkett, G., 3rd, et al. (1997). The complete genome sequence of Escherichia coli K-12. *Science* **277**(5331): 1453-62.

Brandts, J. F. and Hunt, L. (1967). The thermodynamics of protein denaturation. 3. The denaturation of ribonuclease in water and in aqueous urea and aqueous ethanol mixtures. *J Am Chem Soc* **89**(19): 4826-38.

Brunham, R. C. and Peeling, R. W. (1994). Chlamydia trachomatis antigens: role in immunity and pathogenesis. *Infect Agents Dis* **3**(5): 218-33.

Bujard, H., Gentz, R., et al. (1987). A T5 promoter-based transcription-translation system for the analysis of proteins in vitro and in vivo. *Methods Enzymol* **155**: 416-33.

Bukau, B. and Horwich, A. L. (1998). The Hsp70 and Hsp60 chaperone machines. *Cell* **92**(3): 351-66.

Bullock, W. O., Fernandez, J. M. and Short, J. M. (1987). XL1-Blue: a high efficiency plasmid transforming recA Escherichia coli strain with b-galactosidase selection. *Biotechniques 5(4)*: 376-378.

Caldwell, H. D., Kromhout, J., et al. (1981). Purification and partial characterization of the major outer membrane protein of Chlamydia trachomatis. *Infect Immun* **31**(3): 1161-76.

Chua, P. K., Corkill, J. E., et al. (2005). Isolation of Waddlia malaysiensis, a novel intracellular bacterium, from fruit bat (Eonycteris spelaea). *Emerg Infect Dis* **11**(2): 271-7.

Collingro, A., Toenshoff, E. R., et al. (2005). 'Candidatus Protochlamydia amoebophila', an endosymbiont of Acanthamoeba spp. *Int J Syst Evol Microbiol* **55**(Pt 5): 1863-6.

Corsaro, D. and Greub, G. (2006). Pathogenic potential of novel Chlamydiae and diagnostic approaches to infections due to these obligate intracellular bacteria. *Clin Microbiol Rev* **19**(2): 283-97.

Corsaro, D., Thomas, V., et al. (2007). 'Candidatus Rhabdochlamydia crassificans', an intracellular bacterial pathogen of the cockroach Blatta orientalis (Insecta: Blattodea). *Syst Appl Microbiol* **30**(3): 221-8.

Corsaro, D., Venditti, D., et al. (2002). New parachlamydial 16S rDNA phylotypes detected in human clinical samples. *Res Microbiol* **153**(9): 563-7.

de Bary, A. (1879). Die Erscheinung der Symbiose. Strassburg, Austria, Verlag von Karl J. Trubner.

Douglas, A. L. and Hatch, T. P. (2000). Expression of the transcripts of the sigma factors and putative sigma factor regulators of Chlamydia trachomatis L2. *Gene* **247**(1-2): 209-14.

Draghi, A., 2nd, Popov, V. L., et al. (2004). Characterization of "Candidatus piscichlamydia salmonis" (order Chlamydiales), a chlamydia-like bacterium associated with epitheliocystis in farmed Atlantic salmon (Salmo salar). *J Clin Microbiol* **42**(11): 5286-97.

Drew, D., Froderberg, L., et al. (2003). Assembly and overexpression of membrane proteins in Escherichia coli. *Biochim Biophys Acta* **1610**(1): 3-10.

Dumon-Seignovert, L., Cariot, G., et al. (2004). The toxicity of recombinant proteins in Escherichia coli: a comparison of overexpression in BL21(DE3), C41(DE3), and C43(DE3). *Protein Expr Purif* **37**(1): 203-6.

Edwards, A. M., Arrowsmith, C. H., et al. (2000). Protein production: feeding the crystallographers and NMR spectroscopists. *Nat Struct Biol* **7 Suppl**: 970-2.

Everett, K. D., Bush, R. M., et al. (1999). Emended description of the order Chlamydiales, proposal of Parachlamydiaceae fam. nov. and Simkaniaceae fam. nov., each containing one monotypic genus, revised taxonomy of the family Chlamydiaceae, including a new genus and five new species, and standards for the identification of organisms. *Int J Syst Bacteriol* **49 Pt 2**: 415-40.

Everett, K. D. and Hatch, T. P. (1995). Architecture of the cell envelope of Chlamydia psittaci 6BC. *J Bacteriol* **177**(4): 877-82.

Fadel, S. and Eley, A. (2007). Chlamydia trachomatis OmcB protein is a surface-exposed glycosaminoglycan-dependent adhesin. *J Med Microbiol* **56**(Pt 1): 15-22.

Farabaugh, P. J., Schmeissner, U., et al. (1978). Genetic studies of the lac repressor. VII. On the molecular nature of spontaneous hotspots in the lacI gene of Escherichia coli. *J Mol Biol* **126**(4): 847-57.

Filip, C., Fletcher, G., et al. (1973). Solubilization of the cytoplasmic membrane of Escherichia coli by the ionic detergent sodium-lauryl sarcosinate. *J Bacteriol* **115**(3): 717-22.

Findlay, H. E., McClafferty, H., et al. (2005). Surface expression, single-channel analysis and membrane topology of recombinant Chlamydia trachomatis Major Outer Membrane Protein. *BMC Microbiol* **5**: 5.

Fourel, D., Mizushima, S., et al. (1992). Dynamics of the exposure of epitopes on OmpF, an outer membrane protein of Escherichia coli. *Eur J Biochem* **206**(1): 109-14.

Fritsche, T. R., Gautom, R. K., et al. (1993). Occurrence of bacterial endosymbionts in Acanthamoeba spp. isolated from corneal and environmental specimens and contact lenses. *J Clin Microbiol* **31**(5): 1122-6.

Fritsche, T. R., Horn, M., et al. (2000). Phylogenetic diversity among geographically dispersed Chlamydiales endosymbionts recovered from clinical and environmental isolates of Acanthamoeba spp. *Appl Environ Microbiol* **66**(6): 2613-9.

Fritsche, T. R., Sobek, D., et al. (1998). Enhancement of in vitro cytopathogenicity by Acanthamoeba spp. following acquisition of bacterial endosymbionts. *FEMS Microbiol Lett* **166**(2): 231-6.

Gasteiger, E., Gattiker, A., et al. (2003). ExPASy: The proteomics server for in-depth protein knowledge and analysis. *Nucleic Acids Res* **31**(13): 3784-8.

Gomes, J. P., Hsia, R. C., et al. (2005). Immunoreactivity and differential developmental expression of known and putative Chlamydia trachomatis membrane proteins for biologically variant serovars representing distinct disease groups. *Microbes Infect* **7**(3): 410-20.

Gomes, J. P., Nunes, A., et al. (2006). Polymorphisms in the nine polymorphic membrane proteins of Chlamydia trachomatis across all serovars: evidence for serovar Da recombination and correlation with tissue tropism. *J Bacteriol* **188**(1): 275-86.

Graslund, S., Nordlund, P., et al. (2008). Protein production and purification. *Nat Methods* **5**(2): 135-46.

Greub, G., Mege, J. L., et al. (2003). Parachlamydia acanthamoebae enters and multiplies within human macrophages and induces their apoptosis [corrected]. *Infect Immun* **71**(10): 5979-85.

Greub, G. and Raoult, D. (2002). Parachlamydiaceae: potential emerging pathogens. *Emerg Infect Dis* **8**(6): 625-30.

Grodberg, J. and Dunn, J. J. (1988). ompT encodes the Escherichia coli outer membrane protease that cleaves T7 RNA polymerase during purification. *J Bacteriol* **170**(3): 1245-53.

Haider, S. (2004). Phylogenie und Expression der GroEL-Chaperone eines Chlamydien-ähnlichen Symbionten frei lebender Amöben

Haider, S., Collingro, A., et al. (2008). Chlamydia-like bacteria in respiratory samples of community-acquired pneumonia patients. *FEMS Microbiol Lett* **281**(2): 198-202.

Harb, O. S., Gao, L. Y., et al. (2000). From protozoa to mammalian cells: a new paradigm in the life cycle of intracellular bacterial pathogens. *Environ Microbiol* **2**(3): 251-65.

Hatch, T. P. (1996). Disulfide cross-linked envelope proteins: the functional equivalent of peptidoglycan in chlamydiae? *J Bacteriol* **178**(1): 1-5.

Hatch, T. P., Allan, I., et al. (1984). Structural and polypeptide differences between envelopes of infective and reproductive life cycle forms of Chlamydia spp. *J Bacteriol* **157**(1): 13-20.

Hatch, T. P., Miceli, M., et al. (1986). Synthesis of disulfide-bonded outer membrane proteins during the developmental cycle of Chlamydia psittaci and Chlamydia trachomatis. *J Bacteriol* **165**(2): 379-85.

Hatch, T. P., Vance, D. W., Jr., et al. (1981). Identification of a major envelope protein in Chlamydia spp. *J Bacteriol* **146**(1): 426-9.

Heinz, E. (2004). Untersuchung zu Membranproteinen eines Chlamydien-ähnlichen Symbionten frei lebender Amöben

Heinz, E. (2008). The chlamydial inclusion membrane and cell envelope as key features for host adaption: A genomic, proteomic and evolutionary analysis of the amoeba symbiont Protochlamydia amoebophila

Henderson, I. R. and Lam, A. C. (2001). Polymorphic proteins of Chlamydia spp.--autotransporters beyond the Proteobacteria. *Trends Microbiol* **9**(12): 573-8.

Hendrick, J. P. and Hartl, F. U. (1993). Molecular chaperone functions of heat-shock proteins. *Annu Rev Biochem* **62**: 349-84.

Hogan, R. J., Mathews, S. A., et al. (2004). Chlamydial persistence: beyond the biphasic paradigm. *Infect Immun* **72**(4): 1843-55.

Horn, M. (2008). Chlamydiae as symbionts in eukaryotes. *Annu Rev Microbiol* **62**: 113-31.

Horn, M., Collingro, A., et al. (2004). Illuminating the evolutionary history of chlamydiae. *Science* **304**(5671): 728-30.

Horn, M. and Wagner, M. (2001). Evidence for additional genus-level diversity of Chlamydiales in the environment. *FEMS Microbiol Lett* **204**(1): 71-4.

Horn, M. and Wagner, M. (2004). Bacterial endosymbionts of free-living amoebae. *J Eukaryot Microbiol* **51**(5): 509-14.

Horn, M., Wagner, M., et al. (2000). Neochlamydia hartmannellae gen. nov., sp. nov. (Parachlamydiaceae), an endoparasite of the amoeba Hartmannella vermiformis. *Microbiology* **146 (Pt 5)**: 1231-9.

Huang, J. and Gogarten, J. P. (2007). Did an ancient chlamydial endosymbiosis facilitate the establishment of primary plastids? *Genome Biol* **8**(6): R99.

Hughes, E. S., Shaw, K. M., et al. (2001). Mutagenesis and functional reconstitution of chlamydial major outer membrane proteins: VS4 domains are not required for pore formation but modify channel function. *Infect Immun* **69**(3): 1671-8.

Hunten, P., Costa-Riu, N., et al. (2005). Identification and characterization of PorH, a new cell wall channel of Corynebacterium glutamicum. *Biochim Biophys Acta* **1715**(1): 25-36.

Hybiske, K. and Stephens, R. S. (2007). Mechanisms of host cell exit by the intracellular bacterium Chlamydia. *Proc Natl Acad Sci U S A* **104**(27): 11430-5.

Iost, I., Guillerez, J., et al. (1992). Bacteriophage T7 RNA polymerase travels far ahead of ribosomes in vivo. *J Bacteriol* **174**(2): 619-22.

Ishizaka, K., Okudaira, H., et al. (1975). Immunogenic properties of modified antigen E. II. Ability of urea-denatured antigen and alpha-polypeptide chain to prime T cells specific for antigen E. *J Immunol* **114**(1 Pt 1): 110-5.

Israelsson, O. (2007). Chlamydial symbionts in the enigmatic Xenoturbella (Deuterostomia). *J Invertebr Pathol* **96**(3): 213-20.

Jorgensen, I. and Valdivia, R. H. (2008). Pmp-like proteins Pls1 and Pls2 are secreted into the lumen of the Chlamydia trachomatis inclusion. *Infect Immun* **76**(9): 3940-50.

Kahane, S., Kimmel, N., et al. (2002). The growth cycle of Simkania negevensis. *Microbiology* **148**(Pt 3): 735-42.

Kalman, S., Mitchell, W., et al. (1999). Comparative genomes of Chlamydia pneumoniae and C. trachomatis. *Nat Genet* **21**(4): 385-9.

Kane, J. F. (1995). Effects of rare codon clusters on high-level expression of heterologous proteins in Escherichia coli. *Curr Opin Biotechnol* **6**(5): 494-500.

Karlsen, M., Nylund, A., et al. (2008). Characterization of 'Candidatus Clavochlamydia salmonicola': an intracellular bacterium infecting salmonid fish. *Environ Microbiol* **10**(1): 208-18.

Karunakaran, K. P., Noguchi, Y., et al. (2003). Molecular analysis of the multiple GroEL proteins of Chlamydiae. *J Bacteriol* **185**(6): 1958-66.

Klebba, P. E., Benson, S. A., et al. (1990). Determinants of OmpF porin antigenicity and structure. *J Biol Chem* **265**(12): 6800-10.

Koehler, J. E., Birkelund, S., et al. (1992). Overexpression and surface localization of the Chlamydia trachomatis major outer membrane protein in Escherichia coli. *Mol Microbiol* **6**(9): 1087-94.

König, L. (2008). Insights into the developmental cycle of Protochlamydia amoebophila UWE25, an endosymbiont of free-living amoebae

Korepanova, A., Douglas, C., et al. (2001). N-terminal extension changes the folding mechanism of the FK506-binding protein. *Protein Sci* **10**(9): 1905-10.

Korepanova, A., Gao, F. P., et al. (2005). Cloning and expression of multiple integral membrane proteins from Mycobacterium tuberculosis in Escherichia coli. *Protein Sci* **14**(1): 148-58.

Kostanjsek, R., Strus, J., et al. (2004). 'Candidatus Rhabdochlamydia porcellionis', an intracellular bacterium from the hepatopancreas of the terrestrial isopod Porcellio scaber (Crustacea: Isopoda). *Int J Syst Evol Microbiol* **54**(Pt 2): 543-9.

Kubo, A. and Stephens, R. S. (2000). Characterization and functional analysis of PorB, a Chlamydia porin and neutralizing target. *Mol Microbiol* **38**(4): 772-80.

Lane, D. J. (1991). Nucleic acid techniques in bacterial systematics. New York, NY, John Wiley and Sons.

LaVerda, D., Kalayoglu, M. V., et al. (1999). Chlamydial heat shock proteins and disease pathology: new paradigms for old problems? *Infect Dis Obstet Gynecol* **7**(1-2): 64-71.

Lindquist, S. and Craig, E. A. (1988). The heat-shock proteins. *Annu Rev Genet* **22**: 631-77.

Mabey, D. and Fraser-Hurt, N. (2003). Trachoma. *Clin Evid*(10): 777-88.

Makrides, S. C. (1996). Strategies for achieving high-level expression of genes in Escherichia coli. *Microbiol Rev* **60**(3): 512-38.

Maurer, A. P., Mehlitz, A., et al. (2007). Gene expression profiles of Chlamydophila pneumoniae during the developmental cycle and iron depletion-mediated persistence. *PLoS Pathog* **3**(6): e83.

McCoy, A. J. and Maurelli, A. T. (2006). Building the invisible wall: updating the chlamydial peptidoglycan anomaly. *Trends Microbiol* **14**(2): 70-7.

Miller, E. M. and Nickoloff, J. A. (1995). Escherichia coli electrotransformation. *Methods Mol Biol* **47**: 105-13.

Miroux, B. and Walker, J. E. (1996). Over-production of proteins in Escherichia coli: mutant hosts that allow synthesis of some membrane proteins and globular proteins at high levels. *J Mol Biol* **260**(3): 289-98.

Mizuno, T., Chou, M. Y., et al. (1983). A comparative study on the genes for three porins of the Escherichia coli outer membrane. DNA sequence of the osmoregulated ompC gene. *J Biol Chem* **258**(11): 6932-40.

Moelleken, K. and Hegemann, J. H. (2008). The Chlamydia outer membrane protein OmcB is required for adhesion and exhibits biovar-specific differences in glycosaminoglycan binding. *Mol Microbiol* **67**(2): 403-19.

Moustafa, A., Reyes-Prieto, A., et al. (2008). Chlamydiae has contributed at least 55 genes to Plantae with predominantly plastid functions. *PLoS One* **3**(5): e2205.

Mygind, P., Christiansen, G., et al. (1998). Topological analysis of Chlamydia trachomatis L2 outer membrane protein 2. *J Bacteriol* **180**(21): 5784-7.

Neff, R. J. (1957). Purification, axenic cultivation, and description of a soil amoeba, Acanthamoeba sp. *Protozool.* **4**: 176-182.

Newhall, W. J. t. (1987). Biosynthesis and disulfide cross-linking of outer membrane components during the growth cycle of Chlamydia trachomatis. *Infect Immun* **55**(1): 162-8.

Nielsen, H., Engelbrecht, J., et al. (1997). A neural network method for identification of prokaryotic and eukaryotic signal peptides and prediction of their cleavage sites. *Int J Neural Syst* **8**(5-6): 581-99.

Nikaido, H. (2003). Molecular basis of bacterial outer membrane permeability revisited. *Microbiol Mol Biol Rev* **67**(4): 593-656.

Pal, S., Theodor, I., et al. (1997). Immunization with an acellular vaccine consisting of the outer membrane complex of Chlamydia trachomatis induces protection against a genital challenge. *Infect Immun* **65**(8): 3361-9.

Pan, P., Wu, E., et al. (1999). [Relation between Chlamydia pneumoniae infection and acute attack of asthma]. *Hunan Yi Ke Da Xue Xue Bao* **24**(2): 209-10.

Peipert, J. F. (2003). Clinical practice. Genital chlamydial infections. *N Engl J Med* **349**(25): 2424-30.

Pickett, M. A., Ward, M. E., et al. (1988). High-level expression and epitope localization of the major outer membrane protein of Chlamydia trachomatis serovar L1. *Mol Microbiol* **2**(5): 681-5.

Porath, J. (1992). Immobilized metal ion affinity chromatography. *Protein Expr Purif* **3**(4): 263-81.

Prilipov, A., Phale, P. S., et al. (1998). Coupling site-directed mutagenesis with high-level expression: large scale production of mutant porins from E. coli. *FEMS Microbiol Lett* **163**(1): 65-72.

Read, T. D., Brunham, R. C., et al. (2000). Genome sequences of Chlamydia trachomatis MoPn and Chlamydia pneumoniae AR39. *Nucleic Acids Res* **28**(6): 1397-406.

Read, T. D., Myers, G. S., et al. (2003). Genome sequence of Chlamydophila caviae (Chlamydia psittaci GPIC): examining the role of niche-specific genes in the evolution of the Chlamydiaceae. *Nucleic Acids Res* **31**(8): 2134-47.

Rogl, H., Kosemund, K., et al. (1998). Refolding of Escherichia coli produced membrane protein inclusion bodies immobilised by nickel chelating chromatography. *FEBS Lett* **432**(1-2): 21-6.

Rozen, S. and Skaletsky, H. (2000). Primer3 on the WWW for general users and for biologist programmers. *Methods Mol Biol* **132**: 365-86.

Ruhl, S., Casson, N., et al. (2009). Evidence for Parachlamydia in bovine abortion. *Vet Microbiol* **135**(1-2): 169-74.

Rurangirwa, F. R., Dilbeck, P. M., et al. (1999). Analysis of the 16S rRNA gene of micro-organism WSU 86-1044 from an aborted bovine foetus reveals that it is a member of the order Chlamydiales: proposal of Waddliaceae fam. nov., Waddlia chondrophila gen. nov., sp. nov. *Int J Syst Bacteriol* **49 Pt 2**: 577-81.

Schmid, B., Kromer, M., et al. (1996). Expression of porin from Rhodopseudomonas blastica in Escherichia coli inclusion bodies and folding into exact native structure. *FEBS Lett* **381**(1-2): 111-4.

Scholtz, J. M. (1995). Conformational stability of HPr: the histidine-containing phosphocarrier protein from Bacillus subtilis. *Protein Sci* **4**(1): 35-43.

Scidmore-Carlson, M. and Hackstadt, T. (2000). Chlamydia internalization and intracellular fate. *Subcell Biochem* **33**: 459-78.

Shin, S., Lu, G., et al. (2005). Escherichia coli outer membrane protein A adheres to human brain microvascular endothelial cells. *Biochem Biophys Res Commun* **330**(4): 1199-204.

Shirai, M., Hirakawa, H., et al. (2000). Comparison of whole genome sequences of Chlamydia pneumoniae J138 from Japan and CWL029 from USA. *Nucleic Acids Res* **28**(12): 2311-4.

Singh, S. M. and Panda, A. K. (2005). Solubilization and refolding of bacterial inclusion body proteins. *J Biosci Bioeng* **99**(4): 303-10.

Smith, D. B. and Johnson, K. S. (1988). Single-step purification of polypeptides expressed in Escherichia coli as fusions with glutathione S-transferase. *Gene* **67**(1): 31-40.

Stephens, R. S., Kalman, S., et al. (1998). Genome sequence of an obligate intracellular pathogen of humans: Chlamydia trachomatis. *Science* **282**(5389): 754-9.

Stephens, R. S., Koshiyama, K., et al. (2001). Heparin-binding outer membrane protein of chlamydiae. *Mol Microbiol* **40**(3): 691-9.

Stephens, R. S., Sanchez-Pescador, R., et al. (1987). Diversity of Chlamydia trachomatis major outer membrane protein genes. *J Bacteriol* **169**(9): 3879-85.

Stephens, R. S., Wagar, E. A., et al. (1988). High-resolution mapping of serovar-specific and common antigenic determinants of the major outer membrane protein of Chlamydia trachomatis. *J Exp Med* **167**(3): 817-31.

Stewart, E. J., Aslund, F., et al. (1998). Disulfide bond formation in the Escherichia coli cytoplasm: an in vivo role reversal for the thioredoxins. *EMBO J* **17**(19): 5543-50.

Stothard, D. R., Toth, G. A., et al. (2003). Polymorphic membrane protein H has evolved in parallel with the three disease-causing groups of Chlamydia trachomatis. *Infect Immun* **71**(3): 1200-8.

Stothard, P. (2000). The sequence manipulation suite: JavaScript programs for analyzing and formatting protein and DNA sequences. *Biotechniques* **28**(6): 1102, 1104.

Strauch, K. L. and Beckwith, J. (1988). An Escherichia coli mutation preventing degradation of abnormal periplasmic proteins. *Proc Natl Acad Sci U S A* **85**(5): 1576-80.

Studier, F. W. and Moffatt, B. A. (1986). Use of bacteriophage T7 RNA polymerase to direct selective high-level expression of cloned genes. *J Mol Biol* **189**(1): 113-30.

Sugimura, K. and Higashi, N. (1988). A novel outer-membrane-associated protease in Escherichia coli. *J Bacteriol* **170**(8): 3650-4.

Sun, G., Pal, S., et al. (2007). Structural and functional analyses of the major outer membrane protein of Chlamydia trachomatis. *J Bacteriol* **189**(17): 6222-35.

Swietnicki, W. (2006). Folding aggregated proteins into functionally active forms. *Curr Opin Biotechnol* **17**(4): 367-72.

Tan, T. W., Herring, A. J., et al. (1990). Protection of sheep against Chlamydia psittaci infection with a subcellular vaccine containing the major outer membrane protein. *Infect Immun* **58**(9): 3101-8.

Taylor, H. R., Maclean, I. W., et al. (1990). Chlamydial heat shock proteins and trachoma. *Infect Immun* **58**(9): 3061-3.

Terpe, K. (2003). Overview of tag protein fusions: from molecular and biochemical fundamentals to commercial systems. *Appl Microbiol Biotechnol* **60**(5): 523-33.

Thao, M. L., Baumann, L., et al. (2003). Phylogenetic evidence for two new insect-associated Chlamydia of the family Simkaniaceae. *Curr Microbiol* **47**(1): 46-50.

Thomas, V., Casson, N., et al. (2006). Criblamydia sequanensis, a new intracellular Chlamydiales isolated from Seine river water using amoebal co-culture. *Environ Microbiol* **8**(12): 2125-35.

Todd, W. J. and Storz, J. (1975). Ultrastructural cytochemical evidence for the activation of lysosomes in the cytocidal effect of Chlamydia psittaci. *Infect Immun* **12**(3): 638-46.

Tudor, J. J. and Karp, M. A. (1994). Translocation of an outer membrane protein into prey cytoplasmic membranes by bdellovibrios. *J Bacteriol* **176**(4): 948-52.

Uchiyama, T., Kawano, H., et al. (2006). The major outer membrane protein rOmpB of spotted fever group rickettsiae functions in the rickettsial adherence to and invasion of Vero cells. *Microbes Infect* **8**(3): 801-9.

Untergasser, A., Nijveen, H., et al. (2007). Primer3Plus, an enhanced web interface to Primer3. *Nucleic Acids Res* **35**(Web Server issue): W71-4.

Vincentelli, R., Bignon, C., et al. (2003). Medium-scale structural genomics: strategies for protein expression and crystallization. *Acc Chem Res* **36**(3): 165-72.

Wagner, S., Baars, L., et al. (2007). Consequences of membrane protein overexpression in Escherichia coli. *Mol Cell Proteomics* **6**(9): 1527-50.

Wagner, S., Bader, M. L., et al. (2006). Rationalizing membrane protein overexpression. *Trends Biotechnol* **24**(8): 364-71.

Wang, S. P., Kuo, C. C., et al. (1985). Immunotyping of Chlamydia trachomatis with monoclonal antibodies. *J Infect Dis* **152**(4): 791-800.

Waugh, D. S. (2005). Making the most of affinity tags. *Trends Biotechnol* **23**(6): 316-20.

Wehrl, W., Brinkmann, V., et al. (2004). From the inside out--processing of the Chlamydial autotransporter PmpD and its role in bacterial adhesion and activation of human host cells. *Mol Microbiol* **51**(2): 319-34.

Welte, W., Nestel, U., et al. (1995). Structure and function of the porin channel. *Kidney Int* **48**(4): 930-40.

Wick, G., Kleindienst, R., et al. (1995). Role of heat shock protein 65/60 in the pathogenesis of atherosclerosis. *Int Arch Allergy Immunol* **107**(1-3): 130-1.

Wilkinson, D. L. and Harrison, R. G. (1991). Predicting the solubility of recombinant proteins in Escherichia coli. *Biotechnology (N Y)* **9**(5): 443-8.

Wyllie, S., Ashley, R. H., et al. (1998). The major outer membrane protein of Chlamydia psittaci functions as a porin-like ion channel. *Infect Immun* **66**(11): 5202-7.

Yuan, Y., Lyng, K., et al. (1992). Monoclonal antibodies define genus-specific, species-specific, and cross-reactive epitopes of the chlamydial 60-kilodalton heat shock protein (hsp60): specific immunodetection and purification of chlamydial hsp60. *Infect Immun* **60**(6): 2288-96.

Yuan, Y., Zhang, Y. X., et al. (1989). Nucleotide and deduced amino acid sequences for the four variable domains of the major outer membrane proteins of the 15 Chlamydia trachomatis serovars. *Infect Immun* **57**(4): 1040-9.

8 Acknowledgments

This diploma thesis was conducted from May 2009 till January 2010 at the Department of Microbial Ecology (DOME) of the Vienna Ecology Center (University of Vienna) under the leadership of Prof. Dr. Michael Wagner.

The last year of doing my diploma thesis stands out because I got to know exceptional personalities, showing me scientific life in an inspiring and motivating way. I want to thank Matthias Horn for giving me the opportunity to write my diploma thesis as a member of his group, for all his support and encouragement; also Michael Wagner for being the creative head of an outstanding research group and awaking my interests in microbial ecology.

My special thanks go to Karin for being the most enthusiastic, motivating, sympathetic and patient advisor I could imagine. Thanks for all your support, our discussions, your competent help and, of course, great and funny times in- and outside the lab. And I want to thank the whole DOME crew and especially my L2-lab colleagues, for answering my tons of questions, providing a supportive and pleasant environment and also for the great times outside the lab.

Sincere thanks to my mum and dad for supporting me financially and, even more important, my ideas and me, as the person that I am; my sister for trusting in me and having great laughs together; my grandma for lively discussions during Sunday lunch times and her never ending interest in the things I am doing; my flat mate Magi, Ari and all my friends for being patient in times I was too busy for any social events; and Faris, never say never.

9 Curriculum vitae

Alexandra Hörmann

Personal data

Date of birth	April 27th, 1984
Place of birth	Oberpullendorf, Austria
Nationality	Austrian

Education

1990-1994	Volksschule Mühlfeld, 2620 Neunkirchen, Austria
1994-2002	Bundesgymnasium/Bundesrealgymnasium Neunkirchen, 2620 Neunkirchen, Austria
2002-2004	Kolleg für Kultur- und Kongressmanagement, 2500 Baden, Austria
2004-2006	Studies in biology at the University of Vienna
Since 2006	Branch of study: microbiology/genetics, diploma thesis at the Department of Microbial Ecology (2009), University of Vienna